Mechanistic Study on the Antitumor Potential of the Endocannabinoid Reuptake Inhibitor OMDM-2

Dissertation

zur

Erlangung des Doktorgrades (Dr. rer. nat.)

der

Mathematisch-Naturwissenschaftlichen Fakultät

der

Rheinischen Friedrich-Wilhelms-Universität Bonn

vorgelegt von

Ramy Mohammed Ahmed Ammar

aus

Kairo, Ägypten

Bonn, 2014

Angefertigt mit Genehmigung der Mathematisch-Naturwissenschaftlichen Fakultät der Rheinischen Friedrich-Wilhelms-Universität Bonn

1. Gutachter: **PD. Dr. Gudrun Ulrich-Merzenich**
Universitätsklinikum Bonn
Medizinische Klinik III
Zentrum für Innere Medizin
Gebäude 334, Labore UG 65/69
Sigmund-Freud-Straße 25
53127 Bonn, Germany

2. Gutachter: **Prof. Dr. Ulrich Jaehde**
Pharmazeutisches Institut
Universität Bonn
Klinische Pharmazie
An der Immenburg 4
D-53121 Bonn, Germany

Tag der Promotion: 17. Oktober 2014
Erscheinungsjahr: 2014

Index

Abbreviations

2-AG	2-Arachidonoylglycerol (5Z,8Z,11Z,14Z)-5,8,11,14-Eicosatetraenoic acid, 2-hydroxy-1-(hydroxymethyl) ethyl ester
5-FU	5-Fluorouracil
Δ^9-THC	Delta-9-tetrahydrocannabinol
AA-5-HT	N-arachidonoyl-5-hydroxytryptamine
ActR	Activin receptor
AEA	Anandamide or Arachidonoylethanolamine N-(2-Hydroxyethyl)-5Z,8Z,11Z,14Z eicosatetraenamide
AKT	Protein kinase B
ALK	Activin receptor-like kinase
AM-251	N-(piperidin-1-yl)-5-(4-iodophenyl)-1-(2,4-dichlorophenyl) -4-methyl-1Hpyrazole-3-carboxamide
AM-404	N-(4-hydroxyphenyl) arachidonylamide
AMHR	anti-Müllerian hormone receptor
Bcr-Abl	Breakpoint cluster region/Abelson oncogene
bFGF	basic fibroblast growth factor
BMPRII	Bone morphpogenic protein receptor
B-Raf	Rapidly accelerated fibrosarcoma-B, oncogenic protein
BSA	Bovine serum albumine
CB-1	Cannabinoid receptor 1
CB-2	Cannabinoid receptor 2
CBD	Cannabidiol

CD-105	Endoglin receptor
CI	Combination Index
CXCR4	Chemokine receptor 4
DAB	3,3´-diaminobenzidine
DMSO	Dimethyl sulfoxide
DRI	Dose Reduction Index
EAC	Ehrlich Ascites Carcinoma
EDTA	Ethylenediaminetetraacetic acid
EGF	Epidermal growth factor
EMT	Epithelial mesenchymal transition
ERK	Extracellular regulated kinase
FAAH	Fatty acid amide hydrolase
FAST-1	Forkhead activin signal transducer
FBS	Fetal bovine serum
FGF	Fibroblast growth factor
GBM	Glioblastoma multiforme
GPCR	G protein coupled receptor
H_2O_2	Hydrogen peroxide
Hb	Hemoglobin
HDAC	Histone deacetylase
HER	Human epidermal growth factor receptor
HIF	Hypoxia inducible factor
HRB	Horseradish peroxidase

HU-210	{-}-11-OH-D-9-tetrahydrocannabinol dimethylheptyl
i.d.	intra-dermal
i.p.	intra-peritoneal
iv	intra-venous
IGF-1	Insulin-like growth factor
IL-1β	Interleukin-1 beta
ILS	Increase life span
JAK2	Janus kinase 2
JNK	Jun N-terminal Kinase
JWH-133	(3-(1'1'Dimethylbutyl)-1-deoxy-Δ^8-tetrahydrocannabinol
LAP	Latency associated protein
LTBP	Latent transforming growth factor binding protein
LY109514	Nabilone or Cesamet (6aR,10aR)-1-hydroxy-6,6-dimethyl-3-(2-methyloctan-2-yl)-6H,6aH,7H,8H,9H,10H,10aH-benzo[c]isochromen-9-one
MAPK	Mitogen activated protein kinase
MCF-7	Michigan Cancer Foundation-7, Human breast cancer cell line
MEK	Mitogen activated protein kinase kinase /extracellular signal regulated kinase kinase
MGL	Monoacylglycerol liapase
MST	Mean survival time
mTOR	Mammalian target of Rapamycin
mTORC1	Mammalian target of Rapamycin complex 1
MVD	Microvessel density

NF-κB	Nuclear factor-kappaB
NIDA 41020	N-(Piperidin-1-yl)-5-(4-methoxyphenyl)-1-(2,4-dichlorophenyl)-4-methyl-1*H*-pyrazole-3-carboxamide
OMDM-2	(S)-N-oleoyl-(1'-hydroxybenzyl)-2'-ethanolamine
PBS	Phosphate buffer saline
PCD	Programmed cell death
PD-ECGF	Placental derived endothelial cell growth factor
PDGFR	Platelet derived growth factor receptor
PI3K	Phosphatidylinositol-3-kinase
PPAR	Peroxisome proliferator activated receptor
Raf	Rapidly accelerated fibrosarcoma
RANKL	Receptor activator of nuclear factor kappa B ligand
Ras	Rat sarcoma
RB	Retinoblastoma
RBC	Red blood cells
R-Met	(R)-(+)-Methanandamide
RTK	Receptor tyrosine kinase
RTV	Relative tumor volume
s.c	Subcutaneous
SDS	Sodium Dodecyl Sulfate Polyacrylamide
SR141716A	N-Piperidino-5-(4-chlorophenyl)-1-(2,4-dichlorophenyl)-4-methylpyrazole-3-carboxamide

SR144528	N-[(1S)-endo-1,3,3-Trimethylbicyclo[2.2.1]heptan-2-yl]-5-(4-chloro-3-methylphenyl)-1-(4-methoxybenzyl)-pyrazole-3-carboxamide
Src	Sarcoma oncoprotein
T.V	Tumor volume
TBS	Tris-buffered saline
TBST	Tris-buffered saline+Tween
TEMED	N,N,N´,N´-Tetramethylethylenediamine
TGDT	Tumor growth delay time
TGF-β	Transforming growth factor beta
TGT	Tumor growth time
TNF-α	Tumor necrosis factor alpha
TRAIL	Tumor necrosis factor-related apoptosis-inducing ligand
TRIS	2-amino-2-hydroxymethyl-1,3-propanediol
TRPV1	Transient receptor potential vanilloid 1
U-87	Human primary glioblastoma cell line
UCM-707	N-(3-furylmethyl)eicosa-5,8,11,14-tetraenamide
URB-597	[3-(3-carbamoylphenyl)phenyl] N-cyclohexylcarbamate
VDM-11	(5Z,8Z,11Z,14Z)-N-(4-Hydroxy-2-methylphenyl)-5,8,11,14-eicosatetraenamide
VEGF	Vascular endothelial growth factor
VPF	Vascular permeability Factor = Vascular endothelial growth factor
WBC	White blood cells
WIN-55,212-2	[(4,5-dihydro-2-methyl-4(4-morpholinylmethyl)-1-(1-naphthalenyl-carbonyl)-6H-pyrrolo[3,2,1ij]quinolin-6-one

List of Tables

List of Figures

1. Introduction

1.1 Cancer

The hallmarks of cancer comprise six biological capabilities acquired during the multistep development of human tumors ***(Hanahan and Weinberg, 2000)***. The hallmarks constitute an organizing principle for rationalizing the complexities of neoplastic disease **(Figure I)**. They include sustaining proliferative signaling, evading growth suppressors, resisting cell death, enabling replicative immortality, inducing angiogenesis, and activating invasion and metastasis. Underlying these lineaments are genome instability, which generates the genetic diversity that expedites their acquisition, and inflammation, which fosters multiple hallmark functions ***(Hanahan and Weinberg, 2011)***.

Conceptual progress in the last decade has added two emerging lineaments of potential generality to this list: **reprogramming of energy metabolism** and **evading immune destruction** ***(Pisanti et al., 2013)***. In addition to cancer cells, tumors exhibit another dimension of complexity: they contain a repertoire of recruited, ostensibly normal cells that contribute to the acquisition of cancer traits by creating the tumor microenvironment ***(Hanahan and Weinberg, 2011)***. Recognition of the widespread applicability of these concepts will increasingly affect the development of new means to treat human cancer.

Now the importance of lipid mediators in cancer progression is raised after the addition of reprogramming of energy metabolism, occurs in tumor cells, to the list of hallmarks ***(Hanahan and Weinberg, 2011)***. Besides switching from oxidative to glycolytic metabolism, tumor cells require anabolic processes to augment the synthesis of proteins, nucleic acids, and lipids. Whereas most tissues besides the liver, adipose tissue, and breast acquire fatty acids primarily from dietary sources, tumor cells increase de novo fatty acid synthesis to produce membrane building blocks (phosphoglycerides, sterols, and sphingolipids), to store energy (triacylglycerides), and to contribute to energy homeostasis ***(Santos and Schulze, 2012)***. In addition, lipid moieties are necessary to generate lipid messengers, such as sphingolipids, lysolipids, and arachidonic-acid-derived endocannabinoids, to modulate important cellular

processes from proliferation and apoptosis to neoplastic transformation, tumor growth, and progression. Therefore, better knowledge of the physiological contribution or deregulation of these signaling systems in tumor growth and progression, especially in terms of mechanistic insights into the signal transduction components involved, could lead to the disclosure of novel therapeutic targets and tools like the endocannabinoid system ***(Pisanti et al., 2013)***.

The 2014 World Cancer Report, produced by the WHO's specialized cancer agency, predicts the rise of cancer cases from an estimated 14 million in 2012 to 22 million annually within two decades. Over the same period, cancer deaths are tipped to rise from 8.2 million a year to 13 million annually.

Breast cancer is the leading cause of female cancer-related mortality, with more than 458000 deaths estimated worldwide in 2008 ***(Ferlay et al., 2010)***. The incidence of breast cancer varies worldwide, with rates in North America and North and West Europe higher than those in South America and South Europe, with the lowest rates in Africa and Asia ***(Ferlay et al., 2010)***. Although incidence remains much lower in Arab populations compared with those from Europe and the USA, rates are increasing steadily ***(El Saghir et al., 2007)***. Although the rates of mortality have declined mainly due to adjuvant systemic therapy and earlier detection by palpation and mammograms, certain breast tumors remain resistant to conventional therapies ***(Chouchane et al., 2013)***. In addition, current treatments have side effects that substantially affect the patients' quality of life ***(DeSantis et al., 2011)***. It is therefore obvious that new therapeutic strategies are needed for the management of this condition.

Brain tumors are the second and fifth leading causes of cancer-related deaths in males and females ages 20 to 39, respectively ***(Jemal et al., 2009)***. Among the various brain tumors which affect humans, glioblastoma are the most common (1/50,000 persons/year), malign (mortality near 100%) and fastest evolving (life expectation of weeks/months after diagnosis). Nowadays treatment of glioblastoma is generally ineffective or merely palliative, and implies such therapies as surgery, radiotherapy, chemotherapy and immunotherapy ***(Torres et al., 2011)***. Additionally gene therapy is

beginning to be used as an experimental treatment for glioblastomas, although so far it has produced few positive results ***(Parolaro and Massi, 2008)***. The unlikelihood of success of these therapeutic approaches can be further complicated by factors such as the rapid growth, great heterogeneity, high level of infiltration and an extreme resistance to chemotherapy shown by glioblastomas ***(Torres et al., 2011)***. It would therefore be highly desirable to develop novel therapeutic alternatives for the treatment of brain tumors.

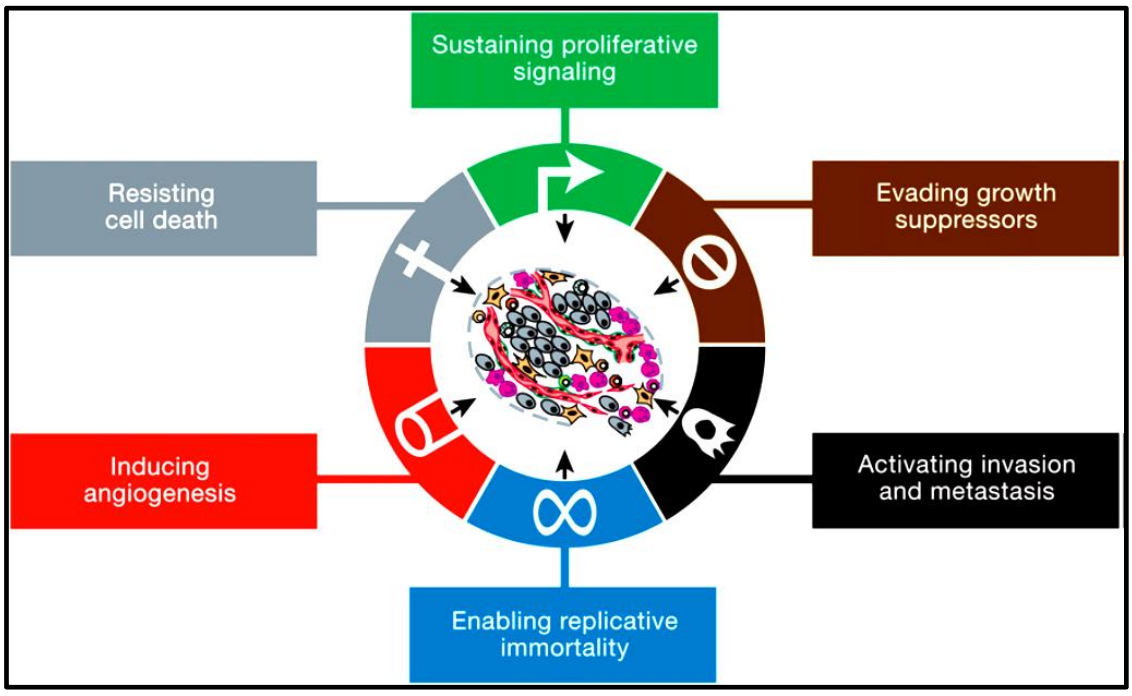

Figure I. The hallmarks of cancer (Adopted from ***Hanahan and Weinberg, 2000***)

1.2 Role of angiogenesis in cancer

1.2.1 Introduction

The generation of new capillaries from pre-existing blood vessels is defined as angiogenesis ***(Folkman, 1971)***. Angiogenesis process takes place physiologically during embryogenesis and in the adult, for example in the female reproductive system and wound healing. Additionally angiogenesis occurs in pathological conditions such as cancer, macular degeneration, psoriasis and rheumatoid arthritis ***(Klagsbrun and Moses, 1999)***.

Angiogenesis and tumor progression are closely linked as tumor cells depend on angiogenesis to safeguard their oxygen and nutrients supply for their growth and expansion. Indeed several studies on tumor development showed that an alteration in the blood supply can noticeably affect the tumor growth and its metastasis **(*Lutsenko et al, 2003)***.

The growth of a tumor is fed initially by nearby blood vessels. Once a certain tumor size is reached (1-2 mm in diameter), these blood vessels are no longer sufficient and new blood vessels are required to continue growth ***(Folkman, 1972)***. The ability of a tumor to induce the formation of new vasculature has been termed the "angiogenic switch" and can occur at different stages of the tumor progression pathway depending on the type of tumor and the environment ***(Bergers and Benjamin, 2003)*** **(Figure II)**. Acquisition of the angiogenic phenotype can result from genetic changes or local environmental changes that lead to the activation of endothelial cells.

One way for a tumor to activate endothelial cells is through the secretion of pro-angiogenic growth factors, which then bind to receptors on nearby dormant endothelial cells that line the interior of vessels. The growth factors can also act on more distant cells recruiting bone marrow derived precursor endothelial cells and circulating endothelial cells to migrate to the tumor vasculature ***(Bergers and Benjamin, 2003; Carmeliet, 2003)***. The pro-angiogenic growth factors may be overexpressed because of genetic alterations of oncogenes and tumor suppressors, or in response to the reduced availability of oxygen (hypoxia).

Tumor cell expression of many of the angiogenic factors, including vascular endothelial growth factor (VEGF), is regulated by hypoxia through the transcription factor hypoxia inducible factor (HIF) ***(Pugh and Ratcliffe, 2003)***. As the tumor cells proliferate, oxygen becomes depleted and a hypoxic microenvironment occurs within the tumor. HIF is degraded in the presence of oxygen, and therefore formation of hypoxic conditions leads to HIF activation and transcription of target genes. The strongest activation of HIF results from hypoxia, but several other factors can contribute to the increased expression and activity of HIF, including growth factors and cytokines such as tumor necrosis factor-α (TNF-α) ***(Hellwig-Bürgel et al., 1999)***, interleukin-1β (IL-1β) ***(Stiehl et al., 2002)*** epidermal growth factor (EGF) ***(Zhong et al., 2000; Jiang et al., 2001*)** and insulin-like growth factor-1 (IGF-1) ***(Fukuda et al., 2002)*** which lead to increased cell signaling and activity of endothelial cells. Along similar lines, oncogenes that trigger increased expression of growth factors and overactive signaling pathways can increase HIF expression and activity.

1.2.2 Vascular endothelial growth factor (VEGF)

VEGF is also known as vascular permeability factor (VPF) because it was initially recognized for its ability to increase the microvascular permeability ***(Dvorak et al., 1999)***. It was initially identified in 1983 as a tumor derived factor capable of increasing vascular permeability ***(Senger et al., 1983)***.

VEGF is essential for normal vessel development in the embryo, where it promotes the differentiation, proliferation and survival of endothelial cells and expansion of the vascular tree. Beside its function during embryogenesis, VEGF also plays a crucial role in angiogenesis in the adult. VEGF was detected in the ovary during corpus luteum formation ***(Ferrara et al., 1998)*** and in the uterus during growth of endometrial vessels and at the side of embryo implantation. Also, high VEGF levels were detected during the proliferative phase of wound healing ***(Nissen et al., 1998)***. VEGF is equally detectable in areas where endothelial cells are quiescent, such as heart, lung, and brain, pointing to the role of VEGF as a survival factor ***(Veikkola and Alitlo, 1999)***. Finally,

VEGF is thought to play a role in several human cancers, diabetic retinopathy, rheumatoid arthritis, and atherosclerosis ***(Inoue et al., 1998)***.

In addition to the hypoxia, several cytokines, growth factors and their receptors play a significant role as VEGF-gene transcription regulators. These include the EGF and its receptor EGFR; the IGF and its receptor IGFR; the fibroblast growth factor (FGF), both acidic and basic isoforms; transforming growth factor (TGF), both alpha and beta isoforms; TNF-α; placental derived endothelial cell growth factor (PD-ECGF); and angiopoietin and prostaglandins. Many oncogenes and tumor suppressor genes have also been reported to influence angiogenesis by direct or indirect up-regulation of VEGF ***(Vogelstein and Kinzler, 2004)***.

The angiogenic effects of VEGF ligands are mediated by their binding to different receptors. The main VEGF receptors are VEGFR-1, VEGFR-2, and VEGFR-3. VEGFR-2 activation is considered most closely associated with signals for proliferation, migration, permeability and tube formation ***(Millauer et al., 1994)***, while activation of VEGFR-1 is more closely associated with monocyte migration ***(Zhu and Witte, 1999)***. Although VEGFR-2 is highly expressed in vascular endothelial progenitors in early emryogenesis, VEGFR-2 expression declines during later stages of vascular development to become up-regulated under conditions of pathological angiogenesis such as in tumors ***(Matsumoto and Claesson-Welsh, 2001)***.

VEGF is ubiquitously expressed in almost all human tumors studied to date. Higher levels of expression of VEGF/VEGFR have been associated with increased tumor vascularity, rapid growth, invasion, metastasis, and poor clinical prognosis in tumors of the bladder ***(Crew et al., 1997)***, brain ***(Vaquero et al., 2000)***, breast ***(Linderholm et al., 2000)***, colon ***(Tokunaga et al., 1998)***, lung ***(Fontanini et al., 2002)***, ovary ***(Fujimoto et al., 1998)***, neuroblastoma ***(Davidoff et al., 2001)***, and gliomas ***(Millauer et al., 1994)***.

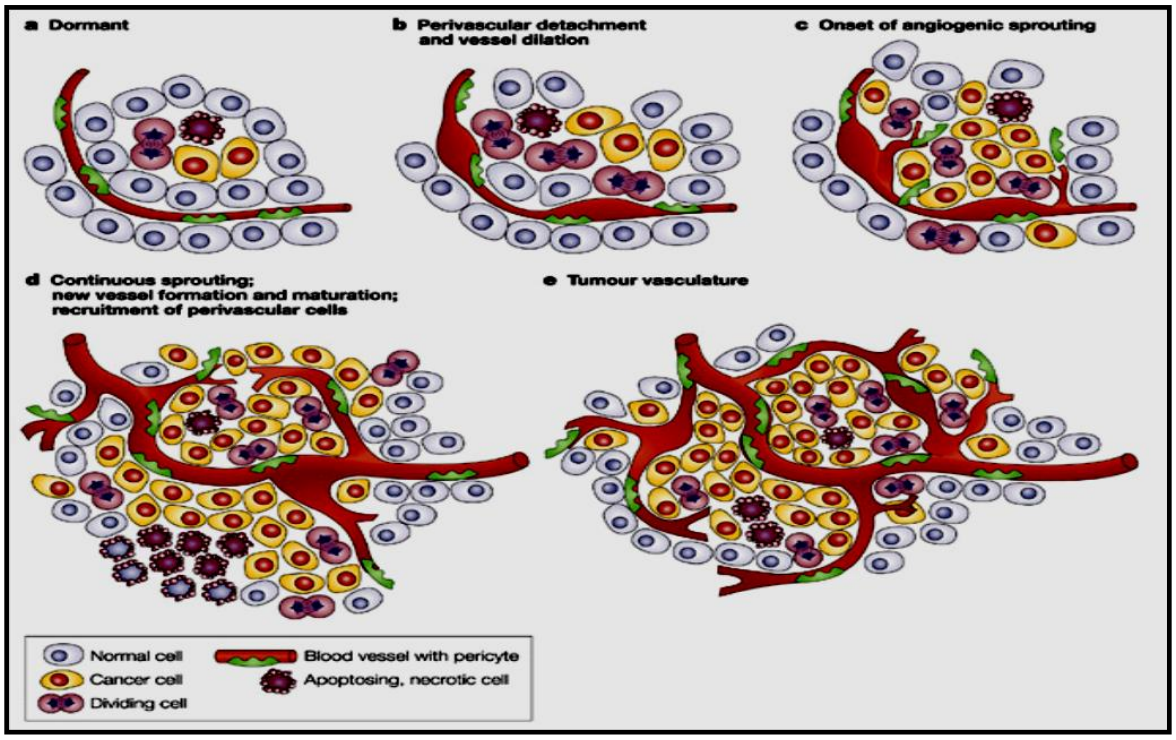

Figure II. The angiogenic switch:
(**a**) Almost all tumors start growing as avascular nodules (dormant) until they reach a steady-state level of proliferating and apoptotic cells. The angiogenic switch starts when tumor needs the oxygen and nutrients in order to grow. (**b**) The switch begins with vessel dilation and perivascular detachment, then (**c**) Angiogenic sprouting starts, (**d**) The new vessels are formed and start to mature; the recruitment of perivascular cells takes place, (**e**) The newly formed blood vessels will specifically feed hypoxic and necrotic areas of the tumor to provide it with essential nutrients and oxygen so the tumor can grow. (Adopted from ***Bergers et al., 2003***)

1.3 Role of transforming growth factor β (TGF-β) in cancer

TGF-β plays a dual and paradoxical role in cancer ***(Katz et al., 2013)***. On one hand it acts as a tumor suppressor during the early phase of carcinogenesis, inhibiting cell growth and inducing apoptosis or differentiation ***(Derynck et al., 2001)***. On the other hand, cancer cells that have lost this inhibitory growth response exploit the ability of TGF-β to modulate processes such as cell invasion, angiogenesis, immune regulation, or interactions between tumor cells and their microenvironment that make them more malignant ***(Derynck et al., 2001)***. The tumor suppressor and tumor promoting effect of TGF-β may be exerted on the tumor cells themselves or indirectly by taking the advantage of the interactions between the tumor and stroma ***(Stover et al., 2007)***.

Some cancer cells evade the tumor suppressor effects of TGF-β by accumulating inactivating mutations in the TGF-β receptors and SMAD proteins ***(Levy and Hill, 2006)***. This is particularly true for subsets of colorectal, pancreatic, ovarian, gastric, and head and neck carcinomas. However, the core components of TGF-β signaling remain intact in majority of tumors (i.e., breast and prostate carcinomas, melanomas, gliomas and hematopoietic neoplasias). Cells within these tumors avoid the tumor suppressor activity of TGF-β by a variety of mechanisms that are not fully understood and which lead to the loss of the TGF-β anti-proliferative response ***(Seoane, 2006)***.

Other alterations that may contribute to the loss of the anti-proliferative response of TGF-β in gliomas are phosphatidylinositol-3-kinase (PI3K) hyperactivation or mutational inactivation of the retinoblastoma (RB) locus ***(Jennings and Pietenpol, 1998)***. However, in many tumors that preserve an intact TGF-β signaling pathway the precise mechanisms leading to the loss of the TGF-β cytostatic response is unknown.

TGF-β_1, which is the most extensively characterized, is secreted as a biologically inactive protein complex consisting of the TGF-β_1 homodimer and the latency associated protein (LAP) which is associated with the latent TGF-β_1 binding protein (LTBP) glycoprotein via a disulfide bond ***(Rifkin, 2005)***. Activated TGF-β ligands initiate their cellular effects by binding to high affinity cell surface receptors, including type I (activin like kinase (ALK) 1-7) and type II TGF-β superfamily receptors (ActR-

II, ActR-IIB, BMPRII, AMHRII, and TβR-II) **(Figure III)**. The type II receptors are constitutively active serine/threonine kinases, with ligand binding resulting in conformational changes that induces recruitment and complex formation with an appropriate type I receptor forming a heteromeric complex **(Figure III)** ***(Samad et al., 2005)***. The type II receptor then phosphorylates the type I receptor in the glycine serine rich domain, activating its serine/threonine kinase activity ***(*De *caestecker, 2004)***. The activated type I receptors mediate their cellular effects through interaction and phosphorylation of SMAD proteins, a family of conserved transcription factors, as summarized in **Figure III**.

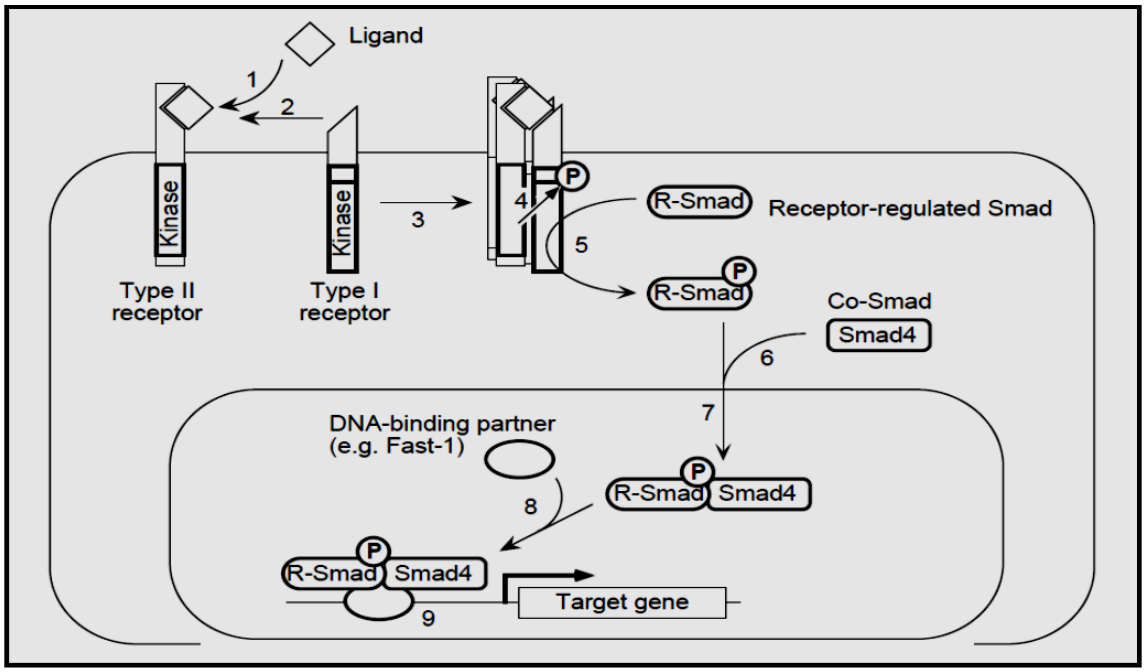

Figure III. The transforming growth factor β (TGF-β) /SMAD pathway:

Binding of a the TGF-β family member to its type II receptor (*1*) in concert with a type I receptor (*2*) leads to formation of a receptor complex (*3*) and phosphorylation of the type I receptor (*4*). Thus activated, the type I receptor subsequently phosphorylates a receptor-regulated SMAD (R-SMAD) (*5*), allowing this protein to associate with SMAD4 (*6*) and move into the nucleus (*7*). In the nucleus, the SMAD complex associates with a DNA-binding partner, such as Fast-1 (*8*), and this complex binds to specific enhancers in targets genes (*9*), activating transcription. (Adopted from ***Massagué, 1998***)

1.4 Role of endoglin in cancer (CD-105)

CD-105 is an auxiliary membrane receptor of TGF-β that interacts with type I and type II TGF-β receptors and modulates TGF-β signaling. Mutations in endoglin are involved in Hereditary Hemorrhagic Telangiectasia type I, a disorder characterized by cutaneous telangiectasias, epistaxis (nosebleeds) and major arteriovenous shunts, mainly in liver and lung ***(Pérez-Gómez et al, 2010)***.

CD-105 is overexpressed in tumor-associated endothelium, which modulates angiogenesis and facilitates metastasis. This finding implies that CD-105 has a role in tumor progression through its effects on the stroma ***(Chakhachiro et al., 2013)***. Expression of CD-105 by malignant cells also has been documented in human sarcoma, metastatic melanoma and breast tumor cells ***(Fonsatti et al., 2001; Postiglione et al., 2005; Oxmann et al., 2008)***. In a recent study, ***Pérez-Gómez et al (2010)*** suggested that changes in CD-105 expression levels in tumor cells contribute to deregulation of TGF-β dependent and TGF-β independent signaling pathways and malignant progression. Based on these preclinical data, antibodies specific for CD-105 have been developed and are currently being used in phase I and II clinical trials ***(Rosen et al., 2012)***.

CD-105 expression is necessary for the activation of ALK1 mediated endothelial cell stimulation. ALK1 activation causes an increase in endothelial cell proliferation and migration as well as transcription of the pro-angiogenic genes including, CD-105 itself ***(Bertolino et al., 2005; Blanco et al., 2005)***. In contrast, ALK5 signaling induces endothelial cell quiescence by inhibiting proliferation and migration and increases expression of maturation-specific genes, such as fibronectin, connexin-37, α_3/β_1 integrin, and plasminogen activator inhibitor-1 ***(Bertolino et al., 2005; Lebrin et al., 2005; Bobik, 2006)***. ALK5 signaling on endothelial cells also promotes the recruitment and differentiation of vascular smooth muscle cells during vessel formation ***(Bertolino et al., 2005)***. ALK5 is the predominant mediator of TGF-β signaling in quiescent endothelial cells, but during angiogenesis, ALK1 is preferentially activated ***(Bertolino et al., 2005; Lebrin et al., 2005)***.

In addition, the complete absence of ALK5 in cells causes a decrease in ALK1 signaling, indicating that the presence of ALK5 is also necessary for signaling via

ALK1 ***(Lebrin et al., 2004)***. TGF-β signaling in the presence of CD-105 causes an activation of ALK1-associated SMAD-1/5 proteins **(Figure IV)** as well as negative regulation of the ALK5-associated SMAD-2/3 proteins ***(Duff et al., 2003; Santibanez et al., 2007)***.

Loss of the inhibitory function of TGF-β_1 has been noted in cells with up-regulated CD-105, causing the tumor cells to be resistant to the inhibitory effects of TGF-β ***(Warrington et al., 2005)***. When CD-105 expression was reduced by an antisense approach, the inhibitory effects of TGF-β on cells proliferation, migration were heightened ***(Li et al., 2000)***. These effects were mediated by ALK5 signaling **(Figure IV)**, emphasizing that CD-105 is a negative regulator of ALK5 activity ***(Lebrin et al., 2005)***. Stable transfection of endothelial cells with small interfering RNA (siRNA) to CD-105 also enhanced the ability of TGF-β to suppress growth and migration ***(Lebrin et al., 2004; Warrington et al., 2005)***. Furthermore, when CD-105 siRNA-transfected cells were irradiated *in-vitro*, they showed a decrease in cell viability, with elevation of p53 (pro-apoptotic) and reduction of bcl-2 (anti-apoptotic) levels compared with mock-transfected cells ***(Warrington et al., 2005)***.

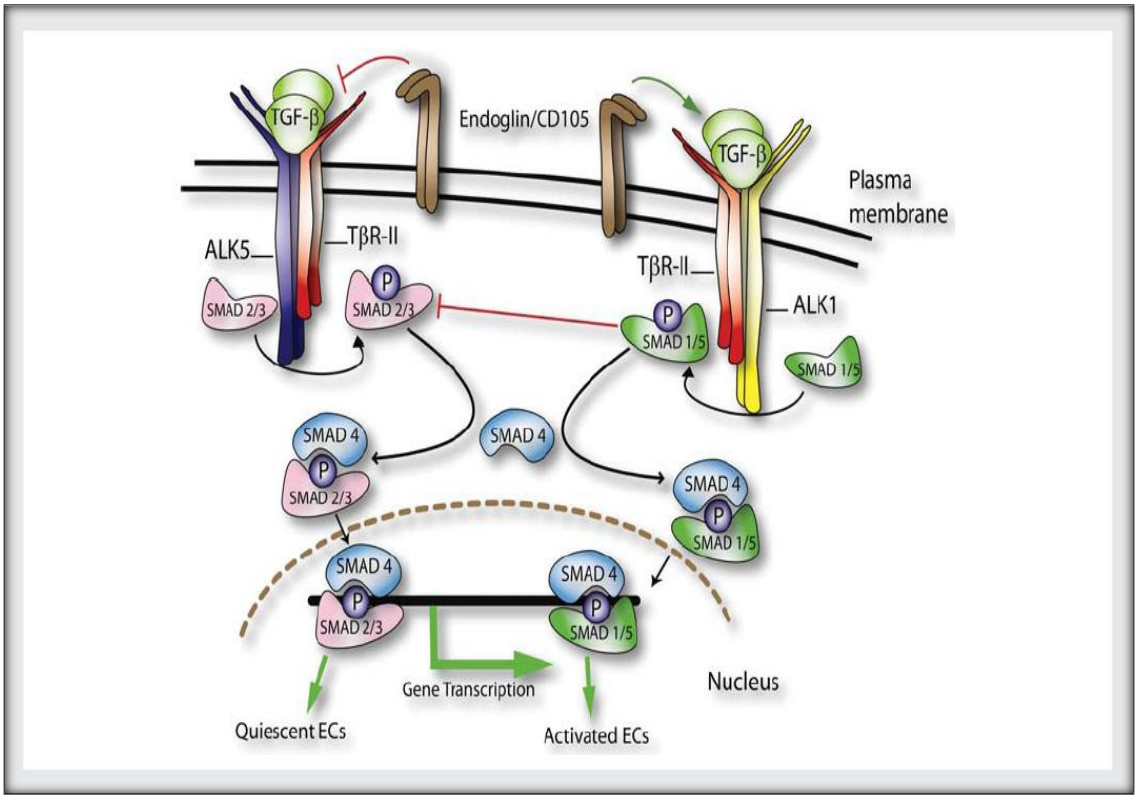

Figure IV. A schematic hypothetical role of CD-105 in TGF-β/ALK-1 and TGF-β/ALK-5 signaling pathways in endothelial cells (ECs):

In endothelial cells, TGF-β can activate two types I receptor pathways with opposite effects: ALK-5 inducing SMAD 2/3 phosphorylation and ALK-1 promoting SMAD 1/5 phosphorylation. CD-105 binds TGF-β by associating with TGF-β signaling receptors type II (TβR-II). This association results in an altered phosphorylation state of TβR-II promoting endothelial cells proliferation via TGF-β/ALK-1 signaling pathway and inducing an indirect inhibition of ALK-5 signaling pathway. Upon activation, phosphorylated SMADs form heteromeric complexes with the common mediator SMAD 4, which in the nucleus act as transcription factor complexes regulating the transcriptional activity of target genes. (Adopted from ***Fonsatti et al., 2010***)

Abbreviations: ALK, activin receptor like kinase (type of TGF-β receptor I); ECs, endothelial cells; TGF-β, transforming growth factor beta; TβR-II, TGF-β receptor II.

1.5 Role of extracellular signal regulated kinases in cancer

The extracellular signal regulated kinases (ERK1/2) are ubiquitous regulators of multiple cellular processes such as proliferation, differentiation, survival, and transformation ***(Deschenes-Simard et al., 2014)***. These kinases are the last components of a signaling module composed of the small GTPase RAS and the protein kinases RAF and MEK1/2 ***(Karnoub and Weinberg, 2008)***. With an overall mutation incidence of up to 30% in human cancer, mutant RAS is among the most common human oncogenes ***(Schubbert et al., 2007)***. RAF mutations are also frequent, particularly in melanoma ***(Maurer et al, 2011)***, but MEK mutations are rare and ERK mutations have never been reported as drivers in human cancers. Nevertheless, current thinking proposes that both RAS and RAF oncogenes promote human cancers by activating the ERK kinases ***(Schubbert et al., 2007)***. Consistent with this idea is the fact that ERK kinases positively regulate the cell cycle by increasing the availability of building blocks for cell growth, by stimulating the cyclin-dependent kinase (CDK)–cyclin complexes required for cell-cycle progression, and by preventing cell death ***(Deschenes-Simard et al., 2014)***. In addition, deregulated nuclear accumulation of activated ERKs (p-ERK) can lead to genomic instability and subsequent tumor progression ***(Duhamel et al., 2012)***. On the other hand, many reports indicate that the ERK kinases may trigger tumor suppressor pathways as well ***(Bric et al., 2009; Deschenes-Simard et al., 2013)*** and that this activity depends on the strength of their activation ***(Deschenes-Simard et al., 2013)***. Hence, the role of ERK kinases in human cancers appears to be context dependent and more complex than originally suspected, reflecting its involvement in both oncogenesis and tumor suppression ***(Deschenes-Simard et al., 2014)***. Clinical studies indicate a variable association between ERK activation and human cancers, consistent with either an oncogenic or a tumor-suppressing role. Consequently, ERK activation in human cancers has been linked to either good or bad prognosis ***(Deschenes-Simard et al., 2014)***. Therefore, it is unclear whether sustained ERK hyperphosphorylation is an obligate prerequisite of cancer initiation or progression despite activated oncogenes upstream of the pathway.

1.6 The endocannabinoid system

1.6.1 Introduction

Cannabinoid refers to a group of chemicals naturally found in the marijuana plant *Cannabis sativa* and includes compounds that are either structurally or pharmacologically similar to Δ^9-tetrahydrocannabinol (THC) or those that bind to the cannabinoid receptors. There are three types of cannabinoids: 1) plant-derived cannabinoids such as THC and cannabidiol occur uniquely in the cannabis plant; 2) endogenous cannabinoids also known as endocannabinoids such as N-arachidonoylethanolamine or anandamide (AEA) and 2-arachidonoylglycerol (2-AG) are produced in the bodies of humans and animals; and 3) synthetic cannabinoids, such as WIN-55, 212-2, JWH-133, and (R)-methanandamide (R-Met), which are developed in a laboratory and bear structural similarities to either natural or endogenous cannabinoids ***(Sarfaraz et al., 2008)***.

The endogenous cannabinoid system consists of the cannabinoid receptors, their endogenous ligands (endocannabinoids) and the proteins responsible for their synthesis and inactivation ***(Bisogno et al., 2005)***. In mammals, the endocannabinoid system has effects on many organ systems and it regulates cardiovascular, nervous, digestive, metabolic, reproductive and immune functions ***(Mackie, 2006; Pacher et al., 2006)***. Studies to date indicate that the endocannabinoid system usually has suppressive effects, exemplified by decreased contractility in the heart, vasorelaxation, neuroprotection in acute and chronic neurological conditions and anti-inflammatory effects ***(Flygare and Sander, 2008)***.

It was earlier thought that endocannabinoids exert their physiologic and behavioral effects via non-specific interaction with cell membranes. In the early 1990s, the two G protein-coupled receptors (GPCR); cannabinoid receptor type-1 (CB-1) ***(Matsuda et al., 1990; Gérard et al., 1991)*** and cannabinoid receptor type-2 (CB-2) ***(Munro et al., 1993)*** were cloned. Based on their predominant expression in the central nervous system and in the peripheral immune system, CB-1 and CB-2 were initially denoted the central and the peripheral cannabinoid receptor, respectively. It later became evident that CB-1 is also found at peripheral nerve terminals and in non-neuronal tissues, e.g.

the pituitary gland, immune cells, vascular endothelium, eye, ileum and reproductive tissues ***(Pertwee, 2005; Bifulco et al., 2006)***, and that CB-2 is expressed also in the central nervous system ***(Van Sickle et al., 2005)***. However, the major role played by CB-1 is the inhibition of the release of neurotransmitters, whereas CB-2 mainly modulates functions of the immune system by regulating cell migration and cytokine release. The cannabinoid receptors participate in the regulation of cell survival ***(Guzmán et al., 2001)***. In this context, signaling via MAPK and PI3K-AKT as well as generation of ceramide have been implicated ***(Guzmán, 2003)***

Endocannabinoids have several characteristics that distinguish them from classical neurotransmitters. According to the traditional view, neurotransmitters are synthesized in presynaptic neurons and stored in vesicles to be released after neural activation and subsequent calcium influx ***(Burnstock, 2009)***. On the contrary, endocannabinoids are synthesized from membrane lipids in postsynaptic neurons after calcium influx that follows neural activation. AEA synthesis primarily depends on the activity of phospholipase D, whereas 2-AG synthesis involves phospholipase C. Also diverging from the classical concept of neurotransmission, endocannabinoids immediately diffuse to the synaptic cleft, instead of being stored in vesicles due to their lipophilic nature ***(Piomelli, 2003; Kano et al., 2009)***. Complementing this picture, CB-1 receptors are mainly located in presynaptic terminals. Activation of CB-1 receptors leads to a decrease in synaptic transmission via a complex set of intracellular signaling cascades. Thus, endocannabinoids act as retrograde messengers, which are synthesized and released on demand following depolarization of the postsynapse to reach presynaptically localized CB-1 receptors, where they restrain the release of neurotransmitters ***(Wilson and Nicoll, 2002)*** **(Figure V)**.

In addition to cannabinoid receptors, the vanilloid receptor type 1 (transient receptor potential vanilloid 1, TRPV1) is well established as a target for AEA, while other receptors, e.g. the peroxisome-proliferator-activated receptor-γ (PPAR-γ, a nuclear receptor) and the GPR55 (G protein-coupled receptor) orphan receptor have also been suggested ***(Pertwee, 2005; Jonsson et al., 2006)***. AEA can also act as a modulator of

other signaling pathways; allosteric sites for AEA are present on muscarinic and glutamate receptors ***(Flygare and Sander, 2008)***.

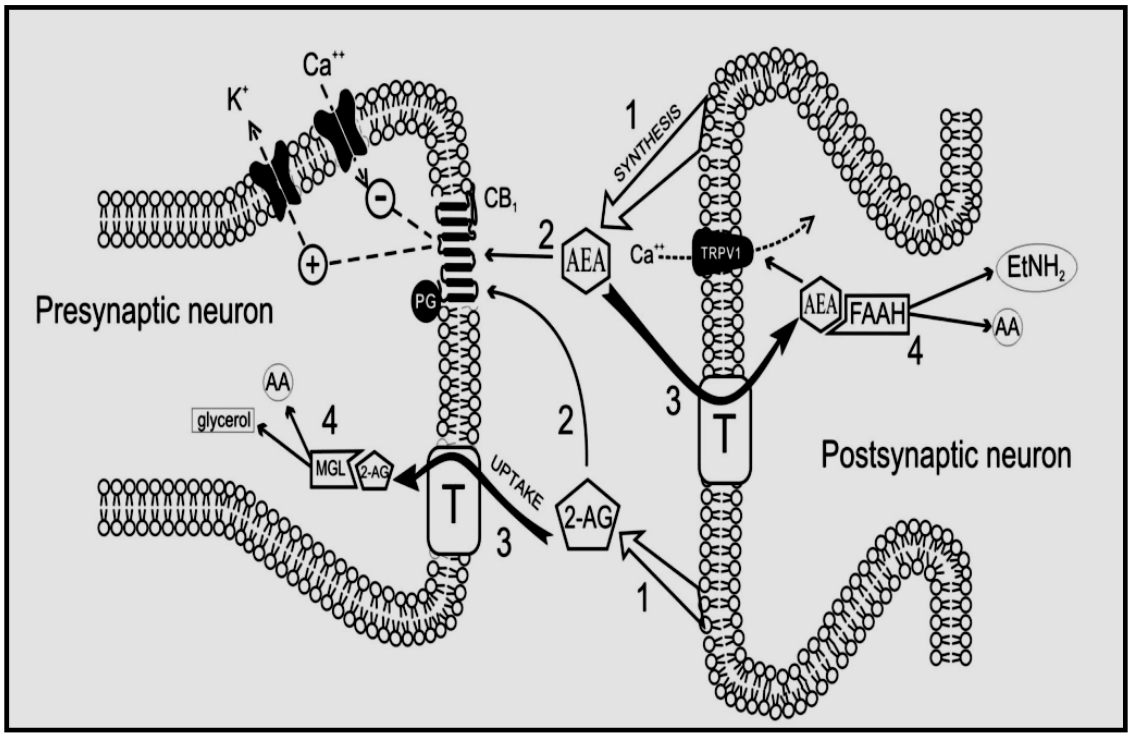

Figure V. Schematic representation of endocannabenoid actions:

Endocannabinids are sythesized in and released from the membrane of postsynaptic neurons on demand after calcium influx (1). They activate presynaptic CB-1 receptors and restrain neural activity (2). AEA and 2-AG are removed from the synaptic cleft by uptake into the post and presynapse respectively (3). Once inside neurons, AEA binds TRPV1 (with consequences opposite to those of CB-1 activation) and undergoes hydrolysis by FAAH, wherease 2-AG is hydrolysed by MGL (4). (Adopted from ***Saito et al., 2010***)

Abbreviations: 2-AG, 2-arachidonoyl glycerol; AA, arachidonic acid; AEA, anadamide; CB-1, cannabinoid receptor type 1; $EtNH_2$, ethanolamine; FAAH, fatty acid amide hydrolase; MGL, monoacyl glycerol lipase; T, transporter; TRPV1, transient receptor potential vanilloid type-1.

1.6.2 Endocannabinoid inactivation

Following release from the cells, AEA and 2-AG can act on molecular targets in an autocrine or paracrine manner, and are subsequently inactivated by cellular re-uptake and hydrolysis. The exact uptake mechanisms responsible for these processes are still unknown. Two possibilities have been proposed in this context: First, endocannabinoids might cross the cell membrane along a concentration gradient in a passive process not governed by any enzyme or transport protein. Second, a protein transporter might exist, which favors the movement of endocannabinoids through the cell membrane ***(Glaser, 2005)***. The later view is supported by experiments showing that the uptake process is saturable, temperature-dependent, and can be inhibited by specific compounds ***(Piomelli, 2003)***. However, an endocannabinoid transporter could not be identified and cloned yet. Once inside cells, endocannabinoids are catabolized by different enzymes.

AEA undergoes hydrolysis by the enzyme fatty acid amide hydrolase (FAAH) ***(Ahn et al., 2008; Ueda et al., 2010)***, an integral membrane protein identified primarily in postsynaptic sites in rodents and primates. FAAH breaks down AEA into arachidonic acid and ethanolamine. 2-AG, in contrast, is hydrolyzed mainly by presynaptically localized monoacylglycerol lipase (MGL) into arachidonic acid and glycerol ***(Dinh et al., 2002, Blankman et al., 2007)*** **(Figure V)**. Interestingly, biological activity of the degradation products has been reported. Ethanolamine has been shown to protect neuroblastoma cells against apoptosis ***(Matas et al., 2007)***, and arachidonic acid can be further metabolized to leukotrienes and prostaglandins, the well-known inflammatory mediators.

1.6.3 Changes in the endocannabinoid system in cancer

Little is currently known about the biological role of the endocannabinoid system in cancer physiopathology ***(Velasco et al., 2012)***. Although there are some exceptions that may be tumor type-specific, both cannabinoid receptors and their endogenous ligands are generally up-regulated in tumor tissue compared with non-tumor tissue ***(Guzmán, 2003; Caffarel et al., 2006; Malfitano et al., 2011)***. Additionally, different studies have associated the expression levels of cannabinoid receptors, endocannabioids and endocannabinoid-metabolizing enzymes with tumor aggressiveness ***(Nomura et al., 2010; Thors et al., 2010; Malfitano et al., 2011)*** which suggest that the endocannabinoid system may be over-activated in cancer and so it may be pro-tumorigenic ***(Guzmán, 2003)***. In support of this, in mouse models of cancer, genetic ablation of CB-1 and CB-2 receptors reduces ultraviolet light-induced skin carcinogen-esis ***(Zheng et al., 2008)***, and CB-2 receptor overexpression enhances predisposition to leukemia following leukemia virus infection ***(Joosten et al., 2002)***.

Conversely, and in line with evidence that the pharmacological activation of cannabinoid receptors reduces tumor growth ***(Guzmán, 2003; Sarfaraz et al., 2008)***, the up-regulation of endocannabinoid-degrading enzymes has been observed in aggressive human tumors and cancer cell lines ***(Nomura et al., 2010; Thors et al., 2010)***, indicating that endocannabinoid signaling can also have a tumor-suppressive role. In support of this, the deletion of CB-1 receptors accelerates intestinal tumor growth in a genetic mouse model of colon cancer ***(Wang et al., 2008)***; increased endocannabinoid levels diminish azoxymethane-induced precancerous lesions in the mouse colon ***(Izzo et al., 2008)***; and a reduction in the expression of the endocannabinoid-degrading enzyme monoacylglycerol lipase reduces tumor growth in xenografted mice ***(Nomura et al., 2010)***.

Elevated levels of endocannabinoids (AEA and 2-AG) have been reported in several types of tumors when compared with their normal counterparts e.g. glioblastoma, meningioma, pituitary adenoma, prostate and colon carcinoma and endometrial sarcoma ***(Pagotto et al., 2001; Schmid et al., 2002; Ligresti et al., 2003; Nithipatikom et al., 2004; Petersen et al., 2005)***.

Both AEA and 2-AG have been shown to be increased in human colorectal adenomatous polyps and carcinomas compared to normal colorectal mucosa ***(Ligresti et al., 2003)***, suggesting that these endocannabinoids increase when passing from normal to transformed mucosa. Similarly, AEA levels were enhanced by 17-fold in glioblastomas whereas meningiomas were characterized by a massively enhanced level of 2-AG ***(Petersen et al., 2005)***. The overall interpretation of these data could be that endocannabinoids act as endogenous tumor suppressors.

1.6.4 Cannabinoids in the treatment of cancer

The therapeutic properties of marijuana have been known for millennia, but the use in the clinic of either plant-derived preparations or pure cannabinoids is still very limited due to their psychotropic side effects ***(Di Marzo, 2008)***. In the context of cancer, only two cannabinoid-based medicines can be prescribed, and for very specific indications to date. Sativex® (nabiximols, an oromucosal spray containing plant extracts enriched in THC and cannabidiol at an approximate 1:1 ratio) has been recently approved in Canada for the treatment of cancer-associated pain ***(Brown et al., 2013)***. In addition, Marinol® and Cesamet® (oral capsules of nabilone – a synthetic THC analog) can be prescribed to prevent nausea and vomiting elicited by standard chemotherapeutic regimes ***(Brown et al., 2013)***. Aside from these palliative actions, recent preclinical evidence suggests that cancer patients might benefit from cannabinoids in an additional manner: since the late 1990s, an important amount of experimental data has shown that these compounds exert anti-tumor effects in different models of cancer, ranging from cell cultures to xenografted and genetically engineered mice ***(Hermanson and Marnett, 2011)***. Interestingly, some – if not all – of these effects have been observed in tumor cells from very different origin, including gliomas, melanomas, carcinomas of the breast, skin, lungs, liver, pancreas, colon, prostate, and lymphomas amongst others, which indicates that cannabinoid anti-tumor action has a general rather than tumor-type specific nature ***(Velasco et al., 2012)***.

The proposed mechanisms for such efficacy are complex and may involve cytotoxic or cytostatic effects, apoptosis induction, anti-metastatic effect accompanied by inhibition of neo-angiogenesis and tumor cell migration ***(Velasco et al., 2012)***. Moreover the

effect, depending on the type of cannabinoid and the target tissue, is CB-1, CB-2 or TRPV1 receptor-dependent or sometimes receptor independent (e.g. lipid rafts, cyclooxygenase, PPAR) ***(Pisanti and Bifulco, 2009)*** **(Figure VI)**. A schematic representation of the major signaling pathways that are implicated in the activation of different cannabinoid receptor subtypes through their agonists and their involvement in these processes is summarized in **Figure VII**.

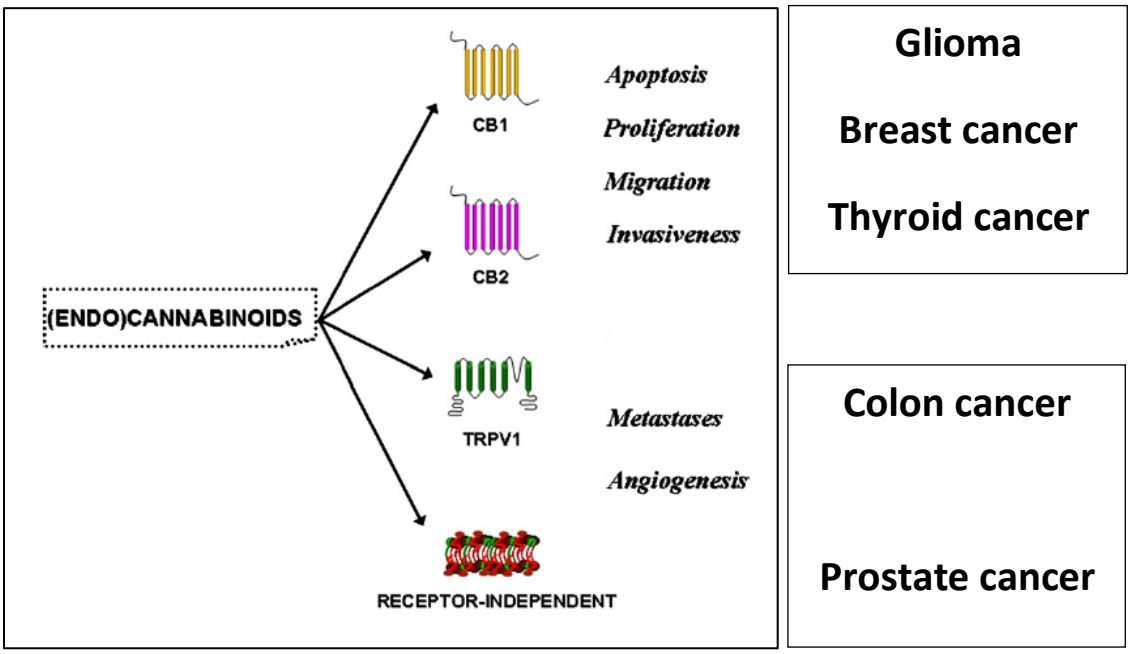

Figure VI. Effects of cannabinoids in cancer (Adopted from ***Pisanti and Bifulco, 2009***).

Abbreviations: CB1, Cannabinoid receptor 1; CB2, Cannabinoid receptor 2; TRPV1; Transient receptor potential vanilloid 1

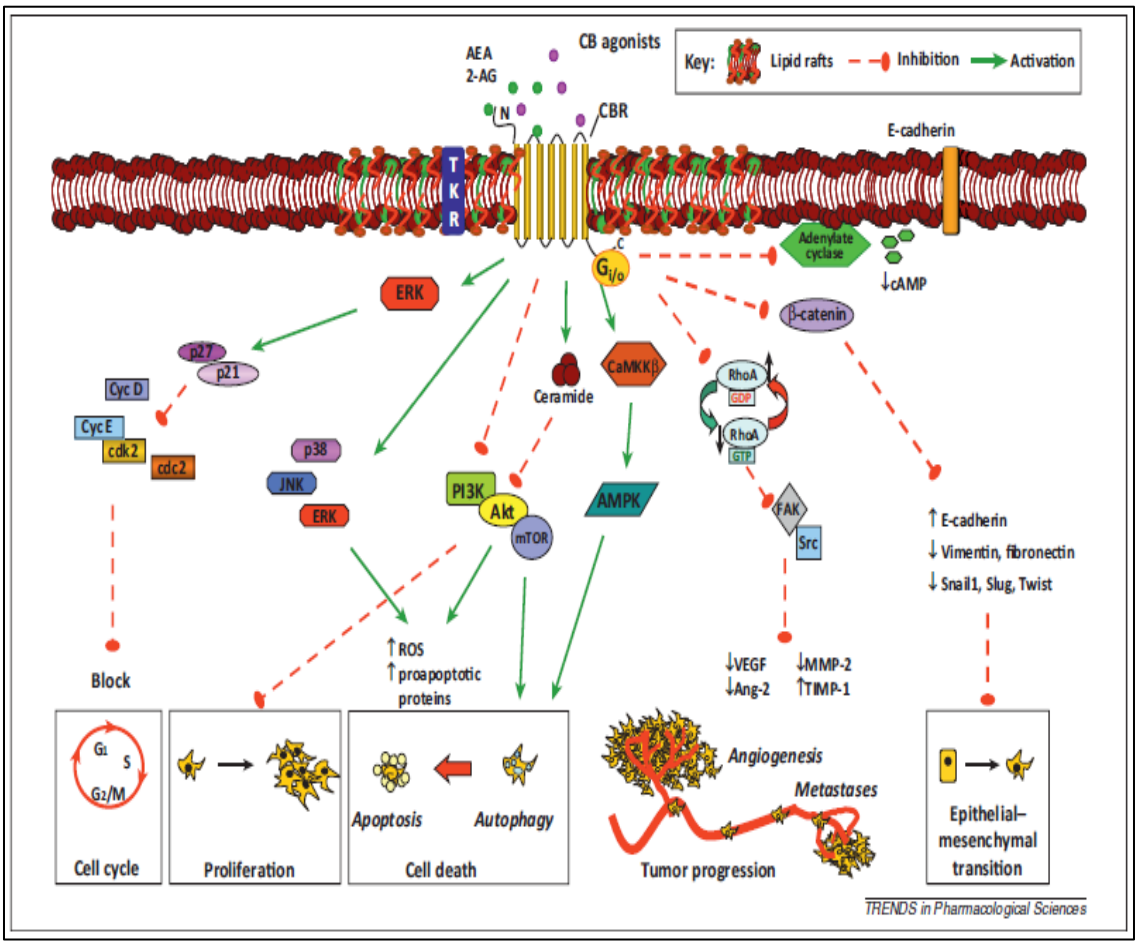

Figure VII. Schematic representation of different mechanisms/signaling pathways through which cannabinoids impact apoptosis, proliferation, angiogenesis and migration: The figure depicts the main signaling cascades elicited downstream of CB receptor activation by endocannabinoids and cannabinoids, which affect all the hallmarks of cancer: inhibition of cell proliferation; cell-cycle arrest; induction of cell death (apoptosis and autophagy); prevention of tumor progression (cancer cell vascular adhesiveness, invasiveness, and metastasis formation); inhibition of angiogenesis in tumor environment; and inhibition of the epithelial–mesenchymal transition. (Adopted from ***Pisanti et al., 2013***)

Abbreviations: AC, adenylyl cyclase; AKT, protein kinase B; AR, androgen receptor; ATP, adenosine triphosphate; Bax, pro-apoptotic protein; Bcl2, antiapoptotic protein; brca1, breast cancer susceptibility gene product; cAMP, cyclic adenosine monophosphate; CB-1, cannabinoid receptor 1; CB-2, cannabinoid receptor 2; Cdc2, p34 cyclin-dependent kinase 1; CDK, cyclin-dependent kinases; EGF, epidermal growth factor; ERK, extracellular regulated kinase; GPR55, G protein-coupled receptor 55; H2O2, hydrogen peroxide; p27/KIP1, cyclin kinase inhibitor; PRL, prolactin receptor; p53, p53 protein; p21ras, p21 ras protein; PI3K, phosphatidyl inositol 3 kinase; PKA, protein kinase A; PKB, protein kinase B; PSA, prostate-specific antigen; Raf-1, protein Raf-1; Trk, high-affinity nerve growth factor receptor; TRPV1, transient receptor potential cation channel V1.

1.6.5 Side effects of direct cannabiniods agonists

The applicability of direct cannabinoid agonists is limited in clinical practice due to their psychoactive effects ***(Di Marzo, 2008)***. Cannabinoid treatment may cause addiction and tolerance, induce sedative effects, and impair learning and memory. In general, low doses tend to induce anxiolytic activity, whereas higher doses may induce opposite effects ***(Moreira et al., 2009; Moreira and Wotjak, 2009)***. The reasons for these differences remain to be determined. They might be attributed to dose-dependent actions upon different brain regions and neural populations ***(Moreira and Wotjak, 2009)***. Moreover, high cannabinoid concentrations may lead to desensitization/ internalization of CB-1 receptors, thus resulting in decreased endocannabinoid signaling. It is tempting to assume that such processes account for the paradoxical effects of cannabis consumption on emotional responses such as episodes of anxiety and panic ***(Saito et al., 2010)***.

As the unwanted psychotropic effects of cannabinoids are mediated largely or entirely by CB-1 receptors in the brain ***(Guzmán, 2003)***; a first possibility would be to use cannabinoids that target CB-2 receptors. Selective CB-2 receptor activation in mice induces regression of gliomas ***(Sánchez et al., 2001)*** and skin carcinomas ***(Casanova et al., 2003)*** and can also inhibit pain ***(Malan et al., 2003)*** in the absence of obvious signs of psychoactivity but its use resulted in immunosuppressive effects typical of plant cannabinoids, which seem to be mediated mostly by the CB-2 receptors ***(Guzmán, 2003)***. Another strategy would be to manipulate the effects of endocannabinoids. Achieving high endocannabinoid levels in the location of the tumors by selectively inhibiting endocannabinoid degradation has proved successful in animal models, as drugs that block anandamide breakdown exert antitumor effects with little psychoactivity ***(Bifulco et al., 2004)***.

1.6.6 Pharmacological manipulation of the endocannabinoid system

1.6.6.1 Attenuation of endocannabinoid signaling

Rimonabant (SR141716A) was the first CB-1 receptor antagonist synthesized ***(Rinaldi-Carmona et al., 1994)***. This drug has provided invaluable insights into the physiology of the endocannabinoid system as well as in the pharmacology of cannabinoids. In the meantime, several other CB-1 antagonists have been developed, including AM-251 ***(Gatley et al., 1996)***. As for the other cannabinoid receptors, selective CB-2 antagonists have also been developed, such as SR144528 ***(Pertwee, 2008)***. In addition, there are also antagonists for TRPV1 receptors, such as capsazepine ***(Di Marzo et al., 2008)***. By specific blockade of CB-1, CB-2 receptors and TRPV1 channels, it is possible to measure cellular, physiological or behavioral consequences of attenuated endocannabinoid signaling.

1.6.6.2 Facilitation of endocannabinoid signaling

Drugs that enhance the endocannabinoid action may provide a more subtle strategy for pharmacological interventions than direct activation of cannabinoid receptors. Given that endocannabinoids are produced and released on-demand, compounds interfering with endocannabinoid uptake and degradation could increase endocannabinoid signaling. Such drugs are expected to induce fewer side effects compared to direct agonists ***(Saito et al., 2010)***.

Two main strategies have emerged for increasing endocannabinoid signaling at the level of their receptors: First, chemical compounds, such as N-arachidonoyl phenolamine (AM-404), VDM-11 or UCM-707, may interfere with the uptake process of the endocannabinoids, thereby increasing the availability of endocannabinoids at CB receptors ***(Beltramo et al., 1997; Giuffrida et al., 2001)***. However, their exact mechanisms of action still remain to be characterized. Moreover, these compounds lack specificity, as they may also interfere with endocannabinoid degradation and TRPV1 channels ***(Piomelli, 2003)***. Second, a very promising strategy for enhancing endocannabinoids signaling is based on the inhibition of their hydrolysis. Specific inhibitors of FAAH and MGL have been developed, which are able to increase the

levels of AEA and 2-AG, respectively. The most prominent inhibitor of FAAH is URB-597, which causes a 5-fold increase in the brain levels of AEA ***(Kathuria et al., 2003)***, thus corroborating findings obtained with genetic deletion of FAAH ***(Cravatt et al., 2001)***. MGL, in turn, is inhibited, among others, by JZL184, which causes an 8-fold increase in 2-AG tissue content ***(Long et al., 2009)***.

1.6.7 Targeting inactivation of endocannabinoids as an anticancer therapy

The major difference between the action of endogenous and exogenous cannabinoids is the on-demand activation of the endocannabinoid system in a temporally and spatially restricted manner ***(Saito et al., 2010)***.

The degradation of endocannabinoids is an active and rapid process. Therefore, blocking the degradation pathway may enhance the anti-proliferative effects of AEA and has beneficial effects in cancer treatment. Indeed, treatment of human breast cancer cells *in-vitro* with palmitoylethanolamide enhanced the anti-proliferative effects of AEA ***(Di Marzo et al., 2001)***. This agent was shown to reduce the expression of FAAH up to 30-40% thereby allowing the accumulation of AEA and increasing its anti-proliferative effects ***(Di Marzo et al., 2001)***. In addition, intra-tumoral administration of VDM-11 or AA-5-HT to athymic mice xenografted with thyroid tumor increased the intra-tumoral levels of AEA and significantly decreased tumor volume ***(Bifulco et al., 2004)***. The anti-proliferative actions of these agents could be only partly inhibited by the pretreatment with the CB-1 receptor antagonist, suggesting that endocannabinoids control tumor growth *in-vivo* by both CB-1 mediated and non CB-1 mediated mechanisms ***(Bifulco et al., 2004)***. Regardless of the molecular mechanism by which AEA and other endocannabinoids regulate tumor growth, inhibitors of their inactivation might be useful for the development of novel anticancer drugs ***(Bifulco et al., 2004)***.

1.6.8 OMDM-2

OMDM-2 is an oleic acid derivative with a modified phenyl head group substitution **(Figure VIII)**. This compound, unlike the widely used AM-404, is inactive as fatty acid amide hydrolase inhibitor and does not activate the vanilloid TRPV1 receptors ***(De Lago et al., 2004)***. Unlike both AM-404 and VDM-11, it is also metabolically stable, and is among the most potent inhibitors ever characterized of AEA cellular uptake by isolated intact cells ***(Ortar et al., 2003)***. Like other similar inhibitors, OMDM-2 is almost inactive as a direct agonist at cannabinoid CB-1 and CB-2 receptors. Therefore its efficacy cannot be explained by the direct activation of these receptors especially when used over the concentration range required for AEA uptake inhibition (3-10 µM) ***(Ortar et al., 2003)***.

OMDM-2 does not show any significant activity on the motor behavior that would render it unique among the AEA uptake inhibitors developed so far ***(De Lago et al., 2004; Nicolussi et al., 2014)***. Finally, this compound does not exhibit drug-reinforcing effects in normal rodents, and hence are not likely to induce dependence ***(Bortolato et al, 2006; Vlachou et al, 2006)***. Thus far, only one report has been explicitly dedicated to the anti-proliferative activity of OMDM-2 in cancer. The drug reduced the viability of C6 glioma cells over a concentration range similar to that required for the inhibition of AEA uptake *in-vitro*, albeit with a longer latency ***(De Lago et al., 2006)***.

Hence, the current study aims at more in-depth evaluation of the *in-vitro* and *in-vivo* antitumor potential of OMDM-2, in addition to investigate the possible mechanisms involved in this activity. This would enhance the credibility of its usefulness in cancer therapy.

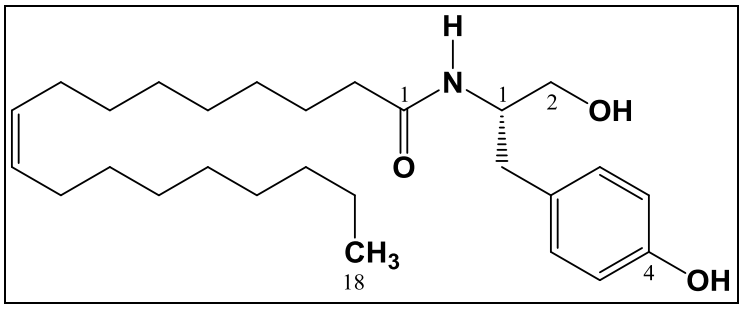

Figure VIII. Structure of OMDM-2.

1.7 Curcumin

Turmeric has been widely used for centuries in indigenous medicine for the treatment of a variety of inflammatory conditions and other diseases ***(Ammon and Wahl, 1991)***. Curcumin is the most active component of turmeric. It is a bis-α, β-unsaturated β diketone and exists in equilibrium with its enol tautomer **(Figure IX)**. The bis-keto form predominates in acidic and neutral aqueous solutions and in the cell membrane whereas the enolate form is found above pH 8 ***(Sharma et al., 2005)***. It exhibits low oral bioavailability in rodents and may undergo intestinal metabolism; absorbed curcumin undergoes rapid first-pass metabolism and excretion in bile. Curcumin is relatively insoluble in water, but dissolves in acetone, dimethylsulphoxide and ethanol.

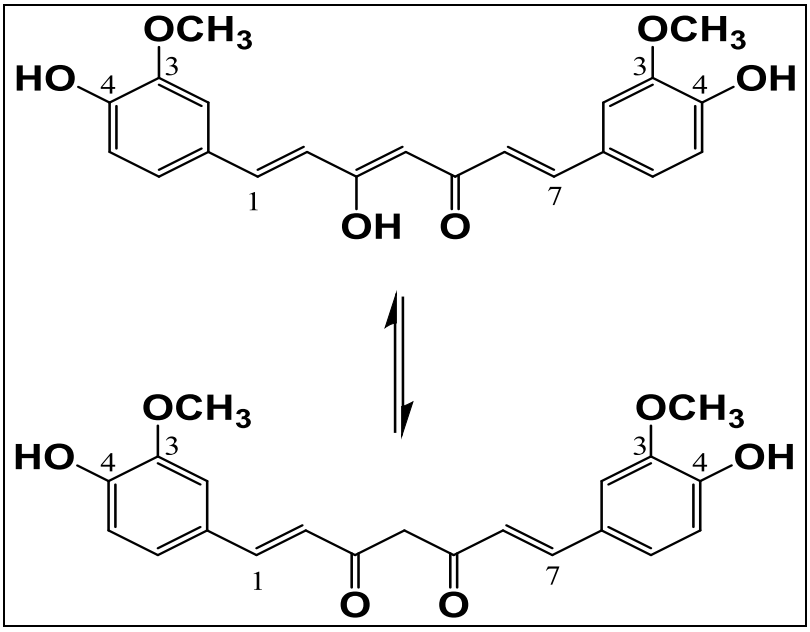

Figure IX. Tautomerism of curcumin under physiological conditions.

Curcumin has been shown to possess wide range of pharmacological activities. Curcumin exhibits strong antioxidant activity comparable to vitamins C and E ***(Mansouri et al., 2012)***. Curcumin with its proven anti-inflammatory properties has been shown to have several therapeutic advantages. It was shown to be a potent scavenger of a variety of reactive oxygen species including superoxide anion radicals, hydroxyl radicals ***(Reddy and Lokesh, 1994)*** and nitrogen dioxide radicals ***(Sreejayan and Rao, 1997)***. It was also shown to inhibit lipid peroxidation in different animal models ***(Reddy and Lokesh, 1992; Sreejayan and Rao, 1994)***.

In addition, Curcumin also possesses anti-viral, anti-fungal, and anti-bacterial activities ***(Maheshwari et al., 2006)***.

Numerous studies have found that curcumin has a dose dependent chemopreventive effect in several animal tumor bioassay systems including colon, duodenal, stomach, esophageal and oral carcinogenesis. It has been shown to reduce tumors induced by benz(a) pyrene and 7, 12 dimethyl benz(a)anthracene, tumor promotion induced by phorbol esters on mouse skin, on carcinogen-induced tumorigenesis in the fore stomach and N-ethyl-N′-nitro-Nnitrosoguanidine- induced duodenal tumors ***(Maheshwari et al., 2006)***.

The molecular bases of the anti-carcinogenic and the chemopreventive effects of curcumin are attributed to its anti-proliferative, anti-angiogenic, and anti-metastatic activities ***(Maheshwari et al., 2006; Hasima and Aggarwal, 2012)***. These activities depend on the ability of curcumin to affect several targets including transcription factors (eg. NF-κB), growth regulators (eg. EGF), inflammatory biomarkers (eg. CXCR4), cellular components, angiogenesis regulators (eg. VEGF), oncoproteins, and protein kinases **(Figure X)**.

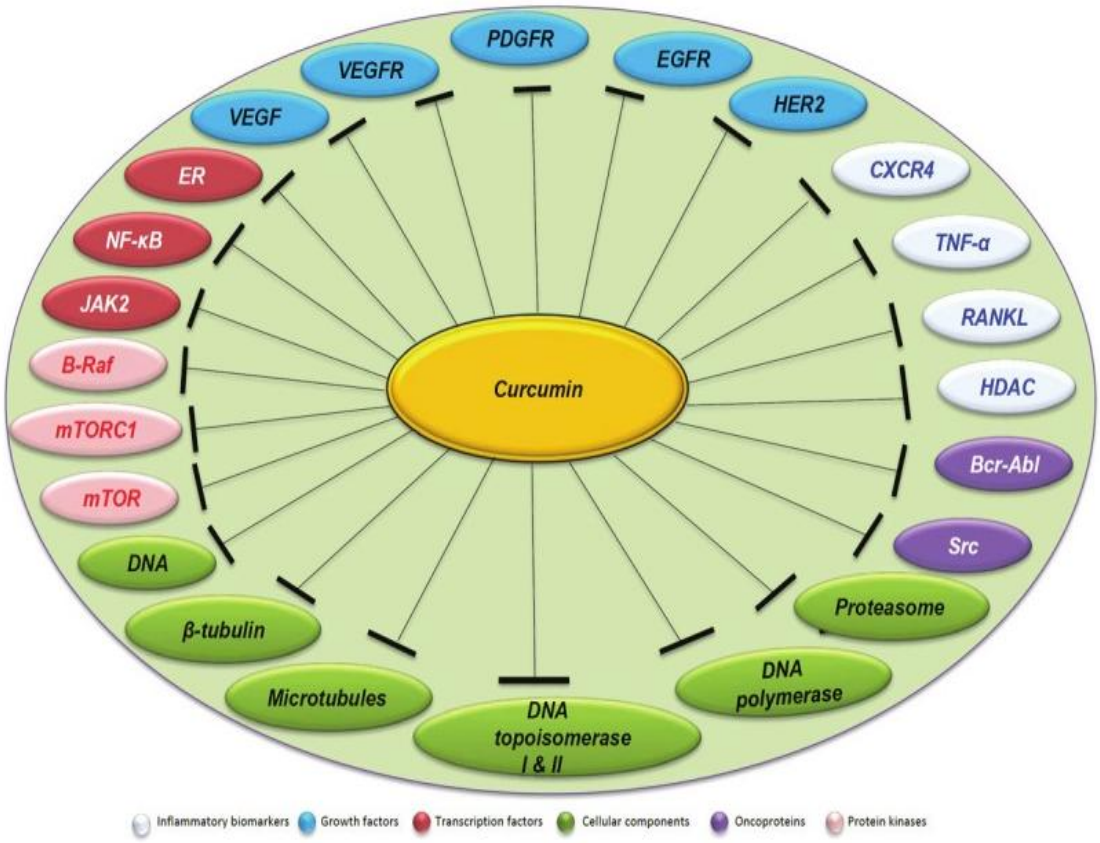

Figure X. Cancer targets and curcumin (Adopted from ***Hasima and Aggarwal, 2012***). (Abbreviations page i)

1.8 Aim of the work

We evaluated the antitumor activity of a systemic administration of OMDM-2 in comparison to the direct cannabinoid agonist, R-methanandamide in Ehrlich ascites carcinoma (EAC) bearing mice using carboplatin as a reference standard. We further investigated underlying mechanism(s) of action of OMDM-2 as an anticancer agent, as well as an optimization strategy by combining OMDM-2 with either the natural product curcumin or benchmark chemotherapeutic agents.

Our strategy depends on the manipulation of the effects of endogenous cannabinoids by using OMDM-2 which enhances the half-life of endogenous cannabinoids by preventing their reuptake and hence degradation. Depending on the "on demand" nature of endogenous cannabinoids, this strategy should lead to an indirect enhancement of the functionality of endocannabinoid receptors only in those tissues and cells in which there is an ongoing synthesis, release, action and degradation of endocannabinoids like in cancer cells. With respect to adverse events, the reuptake inhibitors should be more selective and safer than direct agonists.

Objectives:

I. *In-vivo* evaluation of the antitumor activity of the systemic administration of OMDM-2 in comparison with R-Methanandamide (R-Met) in Ehrlich Ascites Carcinoma (EAC) bearing mice using carboplatin as a reference standard. The following parameters were assessed:

1. Tumor volume and relative tumor volume.
2. Tumor weight (time course).
3. Tumor growth time (TGT) and tumor growth delay time (TGDT).
4. Percentage survival of animals.
5. Mean survival time (MST).
6. Percentage increased life span (%ILS).
7. Hematological parameters.

II. *In-vivo* evaluation of the possible mechanisms of actions involved in this activity:

1. Assessment of the involvement of CB-1 receptor by using the pharmacological inhibitor NIDA 41020.
2. Assessment of the anti-angiogenic activity using Evans blue method and investigation of the involvement of CB-1 receptor in this activity.
3. Evaluation of the time course of serum levels of TGF-β_1 in EAC bearing mice and in the treatment groups.
4. Evaluation of the time course expression of the CD-105 receptor in tumor tissue in EAC bearing mice and in the treating groups.

III. *In-vitro* investigation of the cytotoxic activity of OMDM-2 against 2 different human cell lines MCF-7 (breast cancer cells) and U-87 (glioma cells) using Resazurin based assay.

IV. Investigation of mechanisms involved in the cytotoxic activity of OMDM-2:

1. Assessment of the involvement of the CB-1 and TRPV1 receptors by using their pharmacological inhibitors NIDA 41020 and Capsazepine, respectively.
2. Assessment of the type of cell death by evaluation of single-stranded DNA fragments at different time points (ELISA), DNA laddering (Electrophoresis), and the morphology of the cells.
3. Assessment of the involvement of Caspase-3 by measuring its activity spectrophotometrically at different time points.
4. Investigation of the signal transduction pathway leading to OMDM-2 induced anti-proliferative activity using Western blot analysis.

V. Investigation of the possible optimization of OMDM-2 treatment by combination with curcumin or benchmark chemotherapeutic agents.

2. Materials

2.1 Animals

2.1.1 Ethics statement

All animal experiments were performed within strict adherence to the criteria outlined in the NIH "Guide for Care and Use of Laboratory Animals" (publication #86-23 revised 1985) ***(Louhimies, 2002)*** and the protocol was approved by the Ethical and Animal Care Committee at Sinai University. All efforts were made to ameliorate animal suffering. Animal sacrifice was performed by cervical dislocation.

2.1.2 Mice

Male and female Swiss albino mice (age 5-6 weeks) (weight 20-25 g) were obtained from the Modern Veterinary Office for laboratory animals, Cairo, Egypt and housed under controlled conditions (25±1 °C constant temperature, 55% relative humidity, and 12 hrs dark / light cycles). All animals were allowed to acclimatize under standard animal house conditions (Faculty of Pharmacy, Sinai University) for 1 week before assignment to the experimental protocol. Food and water were allowed *ad libitum* during the study period.

2.2 Tumor cell lines

A- Ehrlich ascites carcinoma

Ehrlich ascites carcinoma (EAC) cell line, used for *in-vivo* studies, was purchased from Tumor Biology Department, National Cancer Institute, Cairo University. EAC is a murine spontaneous breast cancer that served as the original tumor from which an ascites variant was obtained. On intraperitoneal (i.p.) inoculation, an ascites rich in tumor cells was produced. The tumor cell line was maintained in our laboratory by serial i.p. passage into Swiss female albino mice at a 7-10 days interval.

B- Human breast cancer cell line (MCF-7 cells)

Human breast cancer (estrogen receptor positive) MCF-7 cell line, used for *in-vitro* studies, was purchased from the German collection of microorganisms and cell cultures (DSMZ, ACC 115), Germany. The source of MCF-7 cells is the mammary gland, and the disease related to these cells is adenocarcinoma of the breast. The morphology of MCF-7 cells is epithelial and they are adherent in nature. The MCF-7 cell line retains several

characteristics of differentiated mammary epithelium including the ability to process estradiol via cytoplasmic estrogen receptors and the capability of forming domes.

C- Human primary glioblastoma cell line (U-87 MG cells)

Human glioblastoma grade IV cell line, used for *in-vitro* studies, was purchased from the cell line service (CLS). U-87 is a highly malignant anaplastic glioma clone derived from a 44-year-old Caucasian woman. The morphology of U-87 MG cells is epithelial and they are adherent in nature.

2.3 Drugs

- (R)-(+)-Methanandamide (in Tocrisolve^{TM} 100):

  The non-selective direct cannabinoid agonist, R-Methanandamide (R-Met) was purchased from Tocris bioscience, Germany. This product was supplied as an emulsion at a concentration of 10 mg/ml in a soya oil/water (1:4) using the block co-polymer, Pluronic F68 as an emulsifier. R-Met was administered at a dose of 0.5 mg/kg, i.p. every third day, after dilution with distilled water ***(Bifulco et al., 2004)***.

- OMDM-2:

  The endocannabinoid reuptake inhibitor, (S)-N-oleoyl-(1'-hydroxybenzyl)-2'-ethanolamine (OMDM-2) was purchased from Cayman Chemical, Germany. It was supplied as a crystalline powder (Purity > 98%). In the current study, OMDM-2 was administered *in-vivo* at a dose of 5 mg/kg, i.p., every third day, after dissolving in DMSO ***(De Lago et al., 2004; Nicolussi et al., 2014)***. For *in-vitro* studies, the following concentrations were used for MCF-7 cells: 2.5 µM, 5 µM, 10 µM, 20 µM, 40 µM and 80 µM. For U-87 cells, the following concentrations were used: 0.625 µM, 1.25 µM, 2.5 µM, 5 µM, and 10 µM, 20 µM, 40 µM and 80 µM.

- NIDA 41020:

  The CB-1 blocker, NIDA 41020 was purchased from Tocris bioscience, Germany. It was supplied as a white solid powder (Purity > 99%). NIDA 41020 is structurally similar to the widely used CB-1 blocker; rimonabant. In the current study, NIDA 41020 was administered *in-vivo* ***(Bifulco M et al., 2004)*** at a dose of 0.7 mg/kg, i.p.,

every third day, after dissolving in DMSO. For *in-vitro* studies, the following concentration was used, 0.2 µM.

- Capsazepine:

  The TPRV1 blocker, capsazepine was purchased from Sigma Aldrich, Germany. It was supplied as an off-white solid powder (Purity > 98%). Capsazepine is a synthetic analogue of capsaicin. In the current study, capsazepine was used for *in-vitro* experiments after dissolving in DMSO at a concentration 1 µM.

- Carboplatin:

  It was purchased from MP Biomedicals, LLC, France. It was supplied as off-white crystalline powder. Carboplatin was administered at a dose of 5 mg/kg, i.p., every third day, after dissolving in distilled water ***(Chen et al, 2007)***.

- Paclitaxel:

  Semi-synthetic paclitaxel was purchased from Sigma Aldrich, Germany. Its growth inhibitor effect alone or in combination with OMDM-2 was examined in MCF-7 *in-vitro* using the following concentrations: 10 nM, 100 nM, 1 µM, and 10 µM, 100 µM.

- Temozolomide:

  It was purchased from Sigma Aldrich, Germany. Its growth inhibitor effect alone or in combination with OMDM-2 was examined in U-87 glioma cells *in-vitro* using the following concentrations: 50 µM, 100 µM, 200 µM, 300 µM, and 400 µM.

- Curcumin:

  It was purchased from Sigma Aldrich, Germany. It was supplied as yellow powder. Its growth inhibitory effect alone or in combination with OMDM-2 was examined against both MCF-7 and U-87 glioma cells *in-vitro* using the following concentrations: 5 µM, 10 µM, 20 µM, 30 µM, 40 µM, and 80 µM.

2.4 Chemicals and reagents

2.4.1 Chemicals

The sources of the chemicals used in this study are included in the following table:

Table (I): List of chemicals

Chemicals	Source
Acrylamide/bis-Acrylamide solution (30%)	Sigma Aldrich, Germany
Ammonium persulphate	Sigma Aldrich, Germany
Agarose	Sigma Aldrich, Germany
Acetic acid	Sigma Aldrich, Germany
Bovine serum albumin (BSA)	Pierce™, Germany
Dimethyl sulfoxide (DMSO)	Sigma Aldrich, Germany
Ethylenediaminetetraacetic acid sodium salt (EDTA)	Sigma Aldrich, Germany
Evans blue	Sigma, USA
Ethidium bromide	Sigma Aldrich, Germany
Formaldehyde (37%)	Al-Gomhorya Co., Egypt.
Glycerol	Merck, Germany
Glycine	Sigma Aldrich, Germany
Methanol (100%)	Applichem GmbH, Germany
β-Mercaptoethanol	Sigma Aldrich, Germany
Protease inhibitor cocktail	Sigma Aldrich, Germany
Proteinase K	Sigma Aldrich, Germany
RNase	Gentra Purgene, USA
Sodium orthovandate	Sigma Aldrich, Germany
Sodium dodecyl sulfate solution (SDS, 20%)	Biorad, Germany
Sodium desoxycholate	Sigma Aldrich, Germany
Sodium chloride	Sigma Aldrich, Germany
Sodium fluoride (NaF)	Sigma Aldrich, Germany
Sodium pyrophosphate	Sigma Aldrich, Germany
N,N,N´,N´-Tetramethylethylenediamine (TEMED)	Sigma Aldrich, Germany
Tris Base (Trizma)	Sigma Aldrich, Germany
Tris HCl	Sigma Aldrich, Germany

Chemicals	Source
Tween 20	Sigma Aldrich, Germany
Triton X-100	Sigma Aldrich, Germany
Trypan blue	Al-Gomhorya Co., Egypt. & Sigma Aldrich, Germany

2.4.2 Growth mediums

- Roswell Park Memorial Institute – 1640 medium (RPMI-1640):
  It was purchased from Life technologies (Gibco), Germany and used for the growth of MCF-7 cells. It was supplemented with 10% fetal bovine serum gold (FBS), PAA, Germany; 0.1 mM non-essential amino acids, Life technologies (Gibco), Germany; 1 mM sodium pyruvate, Sigma Aldrich, Germany; 10 µg/ml human insulin solution, Sigma Aldrich, Germany, and 1% penicillin/streptomycin (10000 IU/ml each)/fungizone (25 µg/ml), Promocell, Germany.

- Minimum essential medium supplemented with L-glutamine (MEM):
  It was purchased from Life technologies (Gibco), Germany and used for the growth of U-87 MG cells. It was supplemented with 10% FBS, 0.1 mM non-essential amino acids, 1 mM sodium pyruvate, and 1% penicillin/streptomycin (10000IU/ml each)/fungizone (25 µg/ml).

- Freezing media:
  Two different freezing media were prepared for the storage of each cell line. They were prepared as following: 70% medium + 20% FBS + 10% DMSO

2.4.3 Solutions

- Calcium and magnesium free-Dulbecco's phosphate buffered saline (DPBS):
  It was purchased from Life technologies (Gibco), Germany.

- Trypsin EDTA (10x):
  It was purchased from PAA, Germany. 5 ml stock solution were diluted with 45 ml DPBS.

- Western blot solutions

RIPA lysis buffer for protein isolations:

Tris HCl	20 mM
Triton X-100	1%
Glycerol	20 mM
EDTA	2.5 mM
Sodium pyrophosphate	10 mM
NaF	50 mM
SDS	0.1%
Sodium desoxycholate	1%
Protease inhibitor cocktail	1% } Freshly added immediately before lysis
Sodium orthovandate	0.5% }

10% Separation gel buffer (8 ml):

Distilled water	3.2 ml
Acrylamide/Bis-Acrylamide (30%)	2.67 ml
1.5M Tris, pH 8.8	2 ml
SDS (10%)	80 µL
Ammonium persulphate (10%)	80 µL
TEMED	8 µL

6% Stacking gel buffer (5 ml):

Distilled water	2.6 ml
Acrylamide/Bis-Acrylamide (30%)	1 ml
0.5M Tris, pH 6.8	1.25 ml
SDS (10%)	50 µL
Ammonium persulphate (10%)	50 µL
TEMED	5 µL

Protein Sample buffer:

Tris HCl, pH 6.8	50 mM
SDS	2% (w/v)
Glycerol	10% (v/v)
Bromophenol blue	0.0025% (w/v)
1 M DTT	10% (v/v)

Laemmeli gel electrophoresis buffer (Running buffer):

Tris Base	25 mM
SDS	0.5% (w/v)
Glycine	192 mM

Towbin transfer buffer:

Tris HCl	25 mM
Glycine	192 mM
Methanol	20% (v/v)

TBS:

Tris Base	20 mM
NaCl	140 mM

Wash buffer (TBST):

Tris Base	20 mM
NaCl	140 mM
Tween 20	0.1% (v/v)

Blocking solution:

TBS	150 ml
BSA	1%
Tween 20	1% (v/v)

Antibody-Dilution-Buffer:

TBS	20 ml
BSA	1%
Tween 20	0.1% (v/v)

Harsh stripping buffer (100 ml):

Buffer and strip membranes were prepared under a fume-hood

Tris HCl (pH 6.8)	12.5 ml
SDS (10%)	20 ml
Distilled water	67.5 ml

780 µl of β-Mercaptoethanol was added under fume-hood immediately before stripping.

Western blotting luminol reagent (ECL, 32106):

It was purchased from Thermo scientific, Germany. It was used for the detection of horseradish peroxidase (HRP) on immunoblots using the chemiluminescence imaging machine (PEQLAB, Germany).

- DNA gel electrophoresis

DNA lysis buffer (pH 8)

Tris base	100 mM
EDTA	0.5 mM
NaCl	0.2 M
SDS	0.5%

TEA gel electrophoresis buffer

Tris base	40 mM
Acetic acid	20 mM
EDTA	1 mM

5x Sample buffer

Glycerol	50% (v/v)
EDTA	0.002 mM
Bromo phenol blue	0.0025% (w/v)
Xylene cyanol	0.0025% (w/v)

Agarose gel

TAE	50 ml
Agarose	1.5% (w/v)
Ethidium bromide	10 µl

Tris-EDTA buffer (TE buffer, pH 8)

Tris HCl	10 mM
EDTA	1 mM

- EDTA solution:

  EDTA was used as an anticoagulant during blood collection (at a concentration of 29 µg/ml). EDTA was also used for the preparation of citrate-EDTA buffer used in the immunohistochemistry.

- Formaldehyde:

  It was used for the preparation of neutral buffered formalin (3.7%) by dissolving 4 gm monobasic sodium phosphate and 6.5 gm dibasic sodium phosphate in 900 ml distilled water, to them 100 ml of formaldehyde (37%) was added and mixed well. This solution was used as a fixative for animal tissues for further histopathological examinations.

- Trypan blue:

  0.1 gm of trypan blue powder was dissolved in 100 ml saline and was used for the staining of dead cells during the assessment of the number of viable cells ***(Lazarus et al., 1966)***.

- Evans blue:

  1 gm of Evans blue powder was dissolved in 100 ml saline and was used for the angiostatic study ***(Lee et al., 1990)***.

- Bradford solution (6916):

  It was purchased from Sigma Aldrich, Germany. It was used for spectrophotometric measurement of high protein concentrations ranging from 100 µg/ml to1400 µg/ml.

- Micro BCA reagent (23231):

  It was purchased from Thermo scientific, Germany. It was used for spectrophotometric measurement of low protein concentrations ranging from 2 µg/ml to 40 µg/ml.

2.5 Kits

- VEGF immunoassay kit [Quantikine, ELISA]:

  It was purchased from R&D systems® (Clinilab, Egypt). It was used for the quantitative determination of VEGF concentrations in cell culture supernates.

- Mouse TGF-β_1 immunoassay kit [Quantikine, ELISA]:

  It was purchased from R&D systems® (Clinilab, Egypt). It was used for the quantitative determination of mouse TGF-β_1 concentrations in mouse serum.

- *In-vitro* toxicology assay kit, resazurin based (TOX-8):

  It was purchased from Sigma Aldrich, Germany. It was used for fluorometrically determining the cell number as a function of the metabolic activity using the dye resazurin.

- Cell death detection kit [ELISA]:

  It was purchased from Roche, Germany. It was used for the quantification of apoptosis by determination of mono-oligonucleosomes in the cytoplasmic fraction of cell lysate.

- Caspase-3 colorimetric assay kit:

  It was purchased from R&D systems®, Germany. It was used for the determination of the enzymatic activity of the caspase-3 class of proteases in apoptotic cells by colorimetric reaction.

2.6 Antibody

The following antibodies were used for Western blot. The source and the used dilutions are indicated in the following table:

Table (II): List of antibodies

Antibody	Description	Source
	Primary Antibody	
ERK1/2 (H-72): sc-292838	Detects total p44/42 MAP-Kinase Santa Cruz Biotechnology, WB 1:500 dilution	Rabbit
Phospho-ERK1/2 (Thr202/Tyr204)	Detects phospho-p44/42 MAP-Kinase forms, Santa Cruz Biotechnology, WB 1:1000 dilution	Rabbit
AKT	Detects total Akt, Santa Cruz Biotechnology, WB 1:1000 dilution	Rabbit
Phospho-AKT	Detects phospho-Akt, Santa Cruz Biotechnology, WB 1:1000 dilution	Rabbit
	Secondary Antibody	
Goat anti-rabbit IgG-HRP	Raised in goat against whole rabbit IgG conjugated to horse radish peroxidase, Santa Cruz Biotechnology, WB 1:2000 dilution	Goat

3. Methods

3.1 Evaluation of *in-vivo* anti-tumor activity using EAC cells

This experiment was carried out to determine the effect of R-Met or OMDM-2, either alone or in combination with CB-1 blocker pretreatment, on the tumor development and survival of animals using EAC cells implanted as a solid tumor in the right flank of male Swiss albino mice.

Induction of Ehrlich solid tumor

A- EAC cells preparation

1- Ascitic fluid was withdrawn under aseptic conditions from tumor-bearing mice by needle aspiration from peritoneal cavity, 7-10 days after i.p. inoculation of EAC cells.

2- EAC cells were tested for viability and contamination using trypan blue dye exclusion technique ***(Lazarus et al., 1966)*** in which equal volumes of trypan blue dye (0.1%) and the samples were mixed together. 10 µl of this mixture was mounted on a slide and cells were examined microscopically. Trypan blue dye stains dead cells only. Only EAC cells with at least 90% viability were used.

3- Then, EAC cells were suspended in normal saline so that each 100 µl contains $2.5x10^6$ EAC cells. Cells were counted under the microscope using *Neubauer* hemocytometer.

B- Induction of solid tumor

Each mouse was inoculated s.c in the right flank (after shaving this area) with 100 µl EAC suspension (2.5×10^6 cells).

3.1.1 Measurement of tumor volume (T.V)

Tumor volume was measured using digital vernier caliber (Mitutoyo, Japan), starting seven days after tumor cells inoculation (when the tumor becomes palpable), every third day throughout the experiment. Relative tumor volume (RTV) and tumor growth time (TGT) were calculated.

- **The tumor volume** was calculated after seven days using the following formula:
  Tumor Volume (mm^3) = $0.5X^2$ Y

  Where X, and Y are the minor and major axes, respectively ***(Attia and Weiss, 1966)***.

- **Relative tumor volume** was calculated by dividing the mean tumor volumes of the treated groups by the mean tumor volumes of the control group ***(Chen et al., 2008)***.

- **Tumor growth time (TGT)** was calculated as the average days required by the tumor to reach double, triple, or quadruple the initial tumor volume ***(Attia and Weiss, 1966)***.

3.1.2 Determination of mean survival time (MST) and increase in the life span (%)

Animals were monitored and mortality was recorded daily along the study period (89 days, when last animal died) to calculate percentage survival of animals, mean survival time (MST), and percentage increased life span among all animals.

- **Percentage survival of animals:** mice were followed daily and percentage survival was calculated in each group as:
  (Number of living animals / initial total number of animals) × 100

- **Mean survival time (MST)**: (sum of survival days of all mice in each group) / (total number of mice).

- **Percentage increased life span (%ILS)** was calculated using the following formula:

  %ILS= [(mean survival time of treated group / mean survival time of control group)-1] × 100

An enhancement of life span by 25% or more was considered as effective antitumor response ***(Mazumdar et al., 1997)***.

3.2 Angiostatic activity (vascular permeability)

The objective of this study was to assess the angiostatic activities of treatments on EAC-bearing male Swiss albino mice according to the method of ***lee et al (1990)***.

Each mouse was inoculated intradermally (i.d.) at 2 sites bilaterally on the lower ventral side (after shaving this area) with 100 µl EAC suspension ($2.5x10^6$ cells) on each site.

The treatments were initiated 24 hours after tumor inoculation and given for a single dose. The degree of angiogenesis was assessed by measuring the tumor vascular volume on day 3 as described:

1. On day 3, each mouse was injected intravenously (iv) with 0.25 ml (1% w/v) Evans blue through the tail vein.
2. Two minutes after dye injection, each mouse was sacrificed by cervical dislocation and the implantation sites were punched out.
3. Each two skin discs were pooled up in 2 ml standard solution (mentioned below) and kept at room temperature for 24 hrs with occasional shaking.
4. Following centrifugation, at 4000 rpm for 5 minutes, the absorbance of the supernatant was measured at 620 nm using spectrophotometer (Metertech, Model: Σ960, METERTECHNIC).

Preparation of the standard solution:

1. Two normal mice were injected iv, through the tail vein; with 0.25 ml of 1% (w/v) Evans blue.
2. Two minutes thereafter, the blood was withdrawn from orbital sinus under light ether anesthesia using heparinized microcapillaries and layered on a solution of sodium sulfate (0.5%)/acetone (2/3 v/v) at a concentration of 2 µl blood/ml.
3. The suspension was kept at 4˚C for 24 hours.
4. The supernatant (the standard solution) was then separated by centrifugation at 4000 rpm for 5 minutes and stored at 4˚C until use.

The results were expressed as percentage of angiogenesis which was calculated according to the following formula:

$$\% \text{ Ang.} = [(A-B)/(C-B)] \times 100$$

Where A, B and C represent the optical density measured at 620 nm derived from the treated tumor tissue, background, and control tumor tissue, respectively.

3.3 Assay of serum TGF-β_1 concentration using ELISA

3.3.1 Principle

This assay employs the quantitative sandwich enzyme immunoassay technique. A monoclonal antibody specific for mouse TGF-β_1 has been pre-coated onto a microplate. Standards, control or samples were pipetted into the wells and any TGF-β_1 present was bound by the immobilized antibody. After washing away any unbound substances, an enzyme-linked polyclonal antibody specific for mouse TGF-β_1 was added to the wells to sandwich TGF-β_1 immobilized during the first incubation. Following a wash to remove any unbound antibody-enzyme reagent, a substrate solution is added to the wells and color develops in proportion to the amount of TGF-β_1 bound in the initial step. The color development is stopped and the intensity of the color is measured, the sample values are then read off the standard curve.

3.3.2 Preparation of samples

The blood was withdrawn from the orbital sinus under light ether anesthesia. After clotting for 2 hours at room temperature, samples were centrifuged at 2000 X g (Universal 32R, Germany) for 20 min as recommended by the manufacturer. The separated sera were used for estimation of TGF-β_1. Serum samples required 60-fold dilution into Calibrator Diluent RD5-53.

3.3.3 Reagents

- Mouse TGF-β_1 Microplate: 96 well polystyrene microplate (12 strips of 8 wells) coated with a monoclonal antibody specific for mouse TGF-β_1.
- Mouse TGF-β_1 Conjugate: 12.5 ml/vial of a polyclonal antibody against mouse TGF-β_1 conjugated to horseradish peroxidase with preservatives.

- Mouse TGF-β_1 Standard: 4 ng/vial of recombinant mouse TGF-β_1 in a buffered protein base with preservatives; lyophilized.
- Mouse TGF-β_1 Control: Recombinant mouse TGF-β_1 in a buffered protein base with preservatives; lyophilized.
- Assay Diluent RD1-73: 12.5 ml/vial of a buffered solution with preservatives.
- Calibrator Diluent RD5-53: 21 ml/vial of a 4-fold concentrated buffered protein solution with preservatives.
- Wash Buffer Concentrate: 50 ml/vial of a 25-fold concentrated solution of buffered surfactant with preservatives.
- Color Reagent A: 12.5 ml/vial of stabilized hydrogen peroxide.
- Color Reagent B: 12.5 ml/vial of stabilized chromogen (tetramethylbenzidine).
- Stop Solution: 23 ml/vial of a diluted hydrochloric acid solution.
- Plate Covers: Adhesive strips.

Additional reagents required for sample activation

- Hydrochloric acid.
- Sodium hydroxide.
- HEPES, free acid (M.W. 238.3)

Sample Activation

10 µl of HCl (1 N) were added to 40 µl of serum, and mixed well. The sample was incubated for 10 minutes at room temperature, and then neutralized by adding 8 µl of NaOH (1.2 N)/0.5M HEPES, mix well. Prior to the assay, the activated sample was diluted with Calibrator Diluent 60-fold dilution.

3.3.4 Assay procedure

All reagents and samples were brought to room temperature before use.

1. All reagents, standard dilutions, and activated samples were prepared.

2. 50 µl of assay diluent RD1-73 were added to each well.

3. 50 µl of standard, control, or activated sample were added per well. The plate was gently tapped for one minute, and then covered with the adhesive strip provided and incubated for 2 hours at room temperature.

4. Each well was aspirated and washed three times with the washing buffer. After the last wash, any remaining wash buffer was removed by aspirating or decanting. The plate was inverted and blotted against clean paper towels.

5. 100 µl of mouse TGF-B_1 conjugate were added to each well, covered with a new adhesive strip, and incubated for 2 hours at room temperature.

6. The aspiration/wash was repeated as in step 4.

7. 100 µl of substrate solution were added to each well, and incubated for 30 minutes at room temperature and protected from light.

8. 100 µl of stop solution were added to each well. The plate was gently tapped to ensure thorough mixing.

The optical density of each well was determined within 30 minutes, using a microplate reader (Metertech, Model: Σ960, METERTECHNIC.) set to 450 nm. Correction wavelength was set to 570 nm.

3.3.5 Calculation of results

A standard curve was constructed by plotting the mean absorbance for each standard on the Y-axis against the concentration on the X- axis and the best fit curve was drawn through the points on the graph. Because serum samples have been diluted prior to the assay, their measured concentrations were multiplied by 60.

Intra-assay Precision

Our data: Standard deviation: 2.6-8.2, coefficient of variation (%): 4.5-6.5.

Manufacturer: Standard deviation: 2.3-17.3, coefficient of variation (%): 1.9-2.9.

Recovery (%)

Manufacturer: 105-112.

3.4 Immunohistochemical analysis for intra-tumoral CD-105

For immunohistochemical evaluation of CD-105, each mouse was inoculated i.d. at 2 sites bilaterally on the lower ventral side (after shaving this area) with 100 µl EAC suspension ($2.5x10^6$ cells) on each site.

3.4.1 Preparation of tissue specimens

After cervical dislocation, tumor discs were taken out and fixed in 3.7% neutral buffered formalin up to 24 hrs for assessment of intra-tumoral expression of CD-105 receptor. After fixation, processing was completed using an automatic tissue processor. Tissues were dehydrated using graded alcohols, cleared with xylene, and infiltrated with paraffin wax. The tissues were subsequently embedded with paraffin wax in molds. Tissue blocks were stored at 4-25ºC on completion of embedding. Sectioned tissues were collected on clean glass slides.

CD-105 evaluation was performed using 4 µm paraffin-embedded sections applying streptavidin-biotin-peroxidase method. Endogenous peroxidase activity was quenched by incubating the specimen for 10 minutes with 3% hydrogen peroxide. The specimens were then incubated with mouse monoclonal anti-CD-105 in the humidity chamber at 4ºC overnight. After conjugation with streptavidin-biotin-peroxidase complex, coloring was performed with 3,3´-diaminobenzidine (DAB) substrate-Chromogen and Mayer Hematoxylin was used for counter staining.

3.4.2 Reagents

- **Peroxidase block:** 3% hydrogen peroxide in water.
- **Biotinylated link:** Biotin labeled affinity isolated goat anti-rabbit and goat anti-mouse immunoglobulins in phosphate buffered saline (PBS), containing stabilizing protein and 0.015 M sodium azide.
- **Streptavidin-HRP:** Streptavidin conjugated to horseradish peroxidase in PBS containing stabilizing protein and anti-microbial agents.
- **DAB substrate buffer:** Imidazole-HCL buffer pH 7.5 containing hydrogen peroxide and an anti-microbial agent.
- **DAB chromogen:** 3,3´-diaminobenzidine in chromogen solution.

3.4.3 Antigen retrieval

Antigen retrieval was performed by using Triology (Cell Marque, CA-USA. Catalog no. 920p-06) which is a product that combines the three pretreatment steps: de-paraffinization, rehydration and antigen unmasking. Using this product enhances standardization of the pretreatment procedure, thereby producing more consistent and more reliable results.

Slides were placed in a Koplin's jar filled with 200 ml of triology working solution and the jar was securely positioned in the autoclave. The temperature of autoclave was adjusted to 120^{o}C and maintained for 15 min after which pressure was released and the Koplin's jar was removed to allow slides to cool for 30 min. Sections were then rinsed in PBS and were stained according to the staining protocol mentioned in the following section.

3.4.4 Staining Protocol

STEP 1 PEROXIDASE BLOCK

- Excess liquid was tapped off using gauze pad, carefully wiped around the specimen to remove any remaining liquid and to keep reagents within the prescribed area.
- Enough hydrogen peroxide was applied to cover specimen.
- Incubated for 10 minutes.
- Rinsed gently with buffer solution from a wash bottle and placed in fresh buffer bath.

STEP 2 BACKGROUND STAINING BLOCK

- Broad spectrum LAB-SA detection kit from Invitrogen (Catalog no. 85-9043) was used to visualize any antigen-antibody reaction in the tissues.
- Background staining was blocked by putting on each slide 3 drops of 10% goat non immune serum blocker supplied with the aforementioned kit.
- Incubated in a humidity chamber for 10 min.
- Without washing, excess serum was drained from each slide

STEP 3 PRIMARY ANTIBODY

- Enough of the ready to use mouse monoclonal anti-endoglin antibody (Thermo scientific, USA, Catalog no. MS-1290-PCS) was applied to cover specimen.
- Incubated overnight at 4ºC.
- Slides were rinsed gently with buffer solution from a wash bottle and placed in fresh buffer bath.

STEP 4 BIOTINYLATED LINK

- Excess liquid was immediately tapped off and slides were wiped as mentioned before.
- Enough drops from link antibody were applied to cover specimen.
- Incubated for 20 minutes.
- Slides were rinsed as mentioned in step 2.

STEP 5 STREPTAVIDIN-HRP

- Slides were wiped as mentioned before.
- Enough drops of the streptavidin reagent were applied to cover specimen.
- Incubated for 20 minutes.
- Slides were rinsed as mentioned before.

STEP 6 SUBSTRATE-CHROMOGEN SOLUTION

- DAB substrate-chromogen solutions were removed from refrigerated (2-8^{o}C) storage.
- DAB was prepared by adding 20 µL of the DAB chromogen per 1 ml of substrate buffer.
- Slides were wiped as mentioned before.
- Enough of the DAB substrate-chromogen solution was applied to cover specimen.
- Slides were incubated for 5 minutes.
- Rinsed gently with distilled water from a wash bottle. DAB substrate-chromogen waste was collected in a hazardous materials container for proper disposal.

STEP 7 MAYER'S HEMATOXYLIN COUNTERSTAIN

- Slides were immersed in a bath of Mayer's hematoxylin.
- Incubated for 2-5 minutes, depending on the strength of hematoxylin used.
- Slides were rinsed in a bath of distilled or deionized water for 2-5 minutes.

STEP 8 MOUNTING

- Specimens were mounted and cover slipped with DPX mounting medium.

3.4.5 Evaluation of endoglin receptor (CD-105) expression

The expression of tissue CD-105 was determined by the presence of brown stained cells in the EAC tissue according to ***Bock et al (2011)***. For the evaluation of the CD-105 expression, positive controls which had been prepared from invasive ductal breast carcinoma ***(Bancher-Todesca et al., 1997)*** were used. Those specimens were kindly donated by the Tumor Biology Department, National Cancer Institute, Cairo University. Negative control sections were prepared from the experimental tissue blocks not treated with the primary antibody. CD-105 staining was assessed blindly by evaluating the intensity of staining. The staining was classified according to a four-grade scale ***(Bock et al., 2011)***: **0** absence of immune-staining or faint staining of few cells; **1** weak staining in most of the cells; **2** diffuse staining present in groups of cells; and **3** significant staining in most of the cells. The grade **0** and grade **1** expression of CD-105 were categorized as the low expression group, grade **2** and grade **3** as the high expression group.

3.4.6 Image analysis

Sections on hot spots were examined with conventional microscope (Olympus CX20) at 250x original magnification connected to camera and computer. All the stained sections were examined by image analyzer computer system using the ImageJ software (NIH, version v1.45e, USA) capable of performing high speed digital image processing for the purpose of tissue measurements. Image J software (NIH, version v1.45e, USA) was calibrated and the image was opened on the computer screen for pre-analysis adjustments. For immunostaining intensity, global calibration was performed with values obtained

between 0 and 2.6 micron/pixel. Before calibration, pixel values are in gray level units in the range of 0-255. After calibration, pixel values are in OD.

3.5 Tumors weight

The effect of the treatments on tumors weight of EAC cells implanted as a solid tumor on the lower ventral side of Swiss albino mice was evaluated. At the end of the experiment, all tumors, 2-discs/animal, were punched out, weighed immediately, and the average weight was calculated. All tumors were then kept in 3.7% neutral buffered formalin for histological evaluation.

3.6 Hematological studies

On the 14^{th} day post-inoculation, the blood was withdrawn from the orbital sinus under light ether anesthesia and was collected on heparinized test tubes. The total and differential white blood cells (WBC), red blood cells (RBC), and the hemoglobin (Hb) content, were determined.

***In-vitro* study**

3.7 Cell culture methods

3.7.1 Thawing of cells

Cells were thawed in a 37°C water bath as quickly as possible. In order to minimize the toxic effect of the DMSO, 9 ml of fresh growth medium were added drop by drop to the cells suspended in 1 ml of freezing media. Thereafter, cells were pelleted by centrifugation at 1,200 rpm for 10 minutes. The cell pellet was re-suspended in the appropriate cell culture medium and seeded depending upon the desired cell density in tissue culture flasks and cultivated under standard conditions.

3.7.2 Common cell culture methods

The cells were grown in plastic 75 cm^2 treated tissue culture flasks with vent Cap (BD Falcon, Germany). The flasks were kept in a standard tissue culture incubator (37°C, 95% relative humidity, and 5% CO2) and examined daily by a phase-contrast microscopy (Olympus CK2, Japan). The culture medium was changed twice weekly. Antibiotic mixtures of penicillin and streptomycin (Pen/Strep/fungizone) were used to protect cells from bacterial and fungal contamination.

3.7.3 Passage of mammalian cells

Almost confluent (80-90%) grown cells were passage into a new culture flask. First the medium was removed and cells were washed twice with 10 ml PBS. Approximately 5 ml of a trypsin/EDTA solution were added and the flask was incubated at 37°C for 3-5 min to dislodge the cells. Trypsinization was inhibited by addition of 5 ml serum containing growth medium. Cells were mixed well by pipetting up and down using 10 ml plastic pipette (Greiner bio-one, Germany) and transferred into a Falcon tube. The cells were pelleted by centrifugation (1200 rpm, 10 min.), re-suspended in growth medium and seeded at suitable density (splitting ratio 1:3 for MCF-7 and 1:5 for U-87).

3.7.4 Freezing and storage of cells

A 75 cm^2 confluent culture flask was passaged as mentioned above. Cells were re-suspended in 1 ml cold freezing medium supplied with 10% DMSO and 20% FBS then transferred with a sterile 1 ml pipette into cryotubes (Nunc, Germany). The cells were

stored for 2-3 hrs at -20°C, then overnight at -80°C prior to liquid nitrogen long term storage.

3.7.5 Cell counting

The cell number was determined using a Neubauer modified cell chamber. The cells were diluted with trypan blue and their numbers per ml were calculated by determining the average number of cells in the 4 large squares and multiplying by 10^4 and the dilution factor.

3.8 Cell proliferation assay

3.8.1 Principle

The cell viability was evaluated by using the resazurin dye. The resazurin method is simple, accurate and reproducible. The key component is the oxido-reduction indicator dye resazurin. Solutions of resazurin, prepared in balanced salt solutions without phenol red, are dark blue in color. Bioreduction of the dye by viable cells reduces the amount of its oxidized form [blue] and concomitantly increases the amount of its fluorescent intermediate [pink], indicating the degree of cytotoxicity caused by the test material. The amount of dye conversion in solution is measured fluorometrically in our study.

3.8.2 Procedure

At the end of the stimulation period with the tested drugs, the media were aspirated and 100 µl of resazurin dye (10% (v/v) in growth media without phenol red) were added to each well for 4 hrs. The cell viability was determined by measuring the fluorescence at 535/590 nm (excitation/emission) using FLUOstar multi-plate reader (BMG Labtech, Germany).

3.8.3 Calculation of results

Fluorescence values from vehicle-treated cells were considered as 100% of proliferation. The concentration at which the growth of cells was inhibited to 50% of the control (IC_{50}) was obtained from this dose-response curve.

3.9 VEGF assay

3.9.1 Principle

This assay employs the quantitative sandwich enzyme immunoassay technique. A monoclonal antibody specific for human VEGF has been pre-coated onto a microplate. Standards or samples were pipetted into the wells and any VEGF present was bounded by the immobilized antibody. After washing away any unbound substances, an enzyme-linked polyclonal antibody specific for VEGF was added to the wells. Following a wash to remove any unbound antibody-enzyme reagent, a substrate solution was added to the wells and color developed in proportion to the amount of VEGF bound in the initial step. The color development was stopped and the intensity of the color is measured.

3.9.2 Preparation of samples

The VEGF concentrations secreted by cells in the supernatants of the experimental group and the untreated control were quantified by collecting the cultured supernatant. The collected supernatant was centrifuged at 12,000 rpm for 15 minutes to remove cell debris. The clear supernatant was transferred to a new tube and then ELISA was performed according to the manufacturer's instructions.

3.9.3 Reagents

- VEGF Microplate: 96 well polystyrene microplate (12 strips of 8 wells) coated with a mouse monoclonal antibody against VEGF.
- VEGF Standard: 2000 pg/vial of recombinant VEGF in a buffered protein base with preservatives; lyophilized.
- VEGF Conjugate: 21 ml/vial of a polyclonal antibody against VEGF conjugated to horseradish peroxidase with preservatives.
- Assay Diluent RD1W: 11 ml/vial of a buffered protein base with preservatives.
- Calibrator Diluent RD5K: 21 ml/vial of a buffered protein base with preservatives.
- Wash Buffer Concentrate: 21 ml/vial of a 25-fold concentrated solution of buffered surfactant with preservatives.
- Color Reagent A: 12 ml/vial of stabilized hydrogen peroxide.
- Color Reagent B: 12 ml/vial of stabilized chromogen (tetramethylbenzidine).

- Stop Solution: 6 ml/vial of sulfuric acid.
- Plate Covers: Adhesive strips.

3.9.4 Assay procedure

All reagents and samples were brought to room temperature before use.

1- All reagents, standard dilutions, and activated samples were prepared.

2- 50 µL of assay diluent RD1W were added to each well.

3- 200 µL of standard, control, or sample were added per well. The plate was gently tapped for one minute, and then covered with the adhesive strip provided and incubated for 2 hrs at room temperature.

4- Each well was aspirated and washed with the washing buffer (400 µl), repeating the process for three times. After the last wash, any remaining wash buffer was removed by aspirating or decanting. The plate was inverted and blotted against clean paper towels.

5- 200 µL of VEGF conjugate were added to each well. The plate was covered with a new adhesive strip and incubated for 2 hrs at room temperature.

6- The aspiration/wash was repeated as in step 4.

7- 200 µL of substrate solution were added to each well and incubated for 20 minutes at room temperature and protected from light.

8- 50 µL of stop solution were added to each well. The plate was gently tapped to ensure thorough mixing.

The optical density of each well was determined within 30 minutes, using a microplate reader (Metertech, Model: Σ960) set to 450 nm.

3.9.5 Calculation of results

A standard curve was constructed by plotting the mean absorbance for each standard on the Y-axis against the concentration on the X- axis and the best fit curve was drawn through the points on the graph.

Intra-assay Precision

Our data: Standard deviation: 0.4-3, coefficient of variation (%): 8-10.

Manufacturer: Standard deviation: 1.9-18.4, coefficient of variation (%): 3.5-6.5.

Recovery (%)

Manufacturer: 95-111.

3.10 Apoptosis assay

3.10.1 Principle

The assay is based on the quantitative sandwich enzyme immunoassay principle using mouse monoclonal antibodies directed against DNA and histones. This allows the specific determination of mono- and oligonucleosomes in the cytoplasmic fraction of cell lysates.

1. Anti-histone antibody is adsorptively fixed on the wall of the microplate module, and nonspecific binding sites on the wall are saturated by treatment with blocking solution.
2. The nucleosomes contained in the sample bind via their histone component to the immobilized anti-histone antibody.
3. Anti-DNA-peroxidase reacts with the DNA part of the nucleosome. After removal of unbound peroxidase (POD) conjugate, the amount of peroxidase retained in the immunocomplex is photometrically determined with ABTS as the substrate.

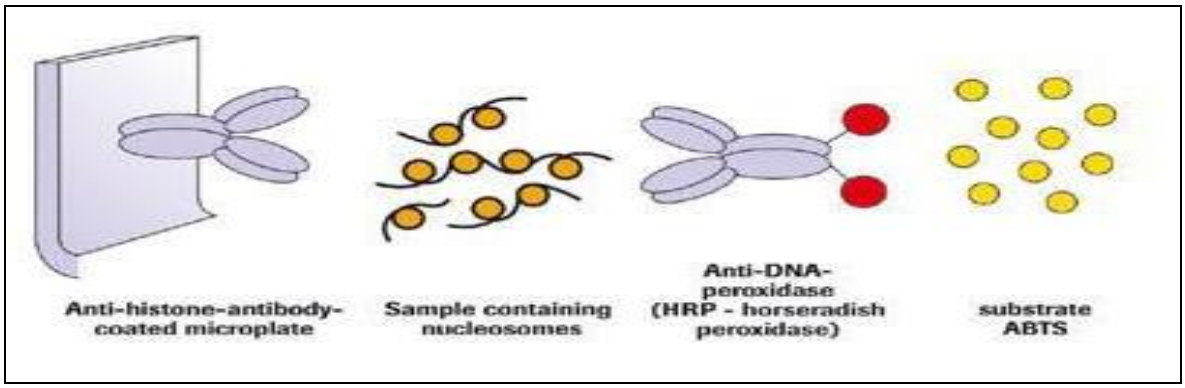

Figure XI: Schematic showing the principle of the Cell Death Detection ELISA (Taken from Roche catalog 11544675001).

3.10.2 Preparation of samples

The floating and adherent cells were pelleted by centrifugation of the 96-well plate at 200 X g for 10 minutes. The supernatant was gently removed and was discarded while the cell pellet was re-suspended with 200 µl incubation buffer and incubated for 30 minutes to lyse the cells. The lysate was centrifuged at 2000 X g for 10 minutes. The supernatant was transferred to clean Eppendorf tube.

3.10.3 Reagents

- Microplate: 12 microplate modules (8 wells, each) and frame.
- Anti-histone antibody: lyophilized vial.
- Anti-DNA-POD: lyophilized vial.
- Coating buffer: 2 ml, 10x conc.
- Washing buffer: 40 ml, 10x conc.
- Incubation buffer: 100 ml, ready-to-use-solution.
- Substrate buffer: 15 ml, ready-to-use-solution.
- ABTS substrate tablet: 3 x 5 mg tablets.

3.10.4 Assay procedure

All reagents and samples were brought to room temperature before use.

1- All reagents and samples were prepared.

2- 100 µL of coating solution were added to each well. The plate was covered with the adhesive strip provided and incubated over night at 2-8^{o}C.

3- Coating solution was removed by tapping.

4- 200 µL of incubation buffer were added to each well. The plate was covered with a new adhesive strip and incubated for 30 minutes at room temperature.

5- Each well was aspirated and washed with 250 µl washing solution, repeating the process three times.

6- 100 µL of sample solution were added to each well. The plate was covered with a new adhesive strip and incubated for 90 minutes at room temperature.

7- The aspiration/wash was repeated as in step 5.

8- 100 µL of conjugate solution were added to each well. The plate was covered with a new adhesive strip and incubated for 90 minutes at room temperature.

9- The aspiration/wash was repeated as in step 5.

10-100 µL of substrate solution were added to each well and incubated on plate shaker at 250 rpm for 20 minutes.

The optical density of each well was determined within 30 minutes, using a microplate reader FLUOstar (BMG Labtech, Germany) set to 405 nm.

3.10.5 Calculation of results

[(mU of the sample) – (mU of the background sample)] / (mU of the negative control sample)

mU: absorbance[10^{-3}], Background sample: samples without cells, Negative control sample: samples contain viable untreated cells.

The values were normalized with protein contents in each sample using a micro BCA protein assay kit.

Intra-assay Precision

Standard deviation: 0.06-0.557, coefficient of variation (%): 1.3-7.

3.11 Assay of caspase-3 activity

3.11.1 Principle

The treated cells were lysed to collect their intracellular contents. The cell lysate was tested for protease activity by the addition of a caspase-specific peptide that is conjugated to the color reporter molecule p-nitroaniline (pNA). The cleavage of the peptide by the caspase releases the chromophore pNA, which can be quantitated spectrophotometrically at a wavelength of 405 nm. The level of caspase enzymatic activity in the cell lysate is directly proportional to the color reaction.

3.11.2 Preparation of samples

After the end of the incubation period with drugs, the floating and adherent cells were centrifuged at 1200 rpm for 10 minutes. The supernatant was gently removed and was discarded while the cell pellet was lysed by the addition of the 25 µl cold lysis buffer per $1x10^6$ cells. The cell lysate was incubated on ice for 10 minutes and then was centrifuged at 10,000 rpm for 1 minute. The supernatant was transferred to a new tube and was kept on ice. Protein estimation was performed using Bradford assay and 150 µg of protein was aliquoted from each sample and used for the assay.

3.11.3 Reagents

- DEVD-pNA Substrate: 500 µL of 4 mM DEVD substrate peptide conjugated to p-nitroaniline.
- Lysis Buffer: 100 mL.
- Reaction Buffer: 4 x 2.0 mL vials of 2X Reaction Buffer.
- DTT: 400 µL of a 1 M solution of dithiothreitol.
- Dilution Buffer: 100 mL.

3.11.4 Assay procedure

The assay was done using 96-well flat bottom microplate:

1- 50 µL of distilled water (blank) or samples were added per well.

2- 50 µL of reaction buffer were added to each well.

3- 5 µL of caspase-3 colorimetric substrate (DEVD-pNA) were added to each well. The plate was incubated at 37^{o}C for 2 hours.

The optical density of each well was determined within 30 minutes, using a microplate reader FLUOstar (BMG Labtech, Germany) set to 405 nm.

3.11.5 Calculation of results

Caspase-3 activity was expressed as the change of activity (fold increase) compared to the control.

Intra-assay Precision

Standard deviation: 0.01-0.24, coefficient of variation (%): 1.3-7.

3.12 DNA isolation and electrophoresis

3.12.1 DNA precipitation in ethanol

Floating and adherent cells were pelleted by centrifugation at 1,200 rpm/ 10 min and lysed with 150 µl DNA lysis buffer at 37^{o}C for 1 hr in the presence of proteinase K (0.1 mg/ml). Then 0.1 mg/ml of RNase were added to the lysates and incubated for 1 hr at 55^{o}C. Ethanol precipitation was used for the purification of DNA. DNA was precipitated by adding 2 volumes of cold 100% ethanol and 2 M of sodium acetate. DNA was washed with cold 70% ethanol and dried for 10 min at room temperature. DNA was dissolved in 200 µl of TE-8 buffer and analyzed on a 1.5% agarose gel stained with ethidium bromide.

3.12.2 Agarose gel electrophoresis

Agarose gel electrophoresis was used to resolve DNA constructs. Agarose gels were casted in TAE Buffer. DNA samples (100 ng) were diluted in 5x loading dye (Fermentase, Germany) before loading on agarose gels. Gels were run at 80 V in TAE buffer. The run was documented using the Chemi Doc system (BQLAB, Germany).

3.13 Protein biochemical and Western blot methods

3.13.1 Protein isolation and separation

Floating and adherent cells were pelleted by centrifugation at 1,200 rpm/ 10 min/ 4°C and lysed with 100 µl RIPA lysis buffer on ice for 10 min in the presence of protease inhibitor cocktail (10 µl/ml) and sodium orthovandate (5 µl/ml). The lysates were cleared by centrifugation at 14,000 rpm/ 10 min/ 4°C. Protein estimation was performed using Bradford assay and 30 µg of protein were aliquoted from each sample and kept on ice. The samples were then boiled (95^{o} C) for 5 min with loading dye. The proteins were separated under reducing conditions in a 10% SDS polyacrylamide minigel.

3.13.2 Estimation of protein concentration (Bradford method)

Samples were diluted appropriately and the Bradford reagent was used to analyze the protein concentrations in duplicates. Different concentrations of BSA were used to construct the standard curve.

3.13.3 Estimation of protein concentration (BCA method)

Samples were diluted appropriately and the BCA kit was used to analyze the protein concentrations in duplicates. Different concentrations of BSA were used to construct the standard curve.

3.13.4 Immunoblotting

After electrophoresis, proteins from a polyacrylamide gel were transferred according to the manufacturer's instructions to a nitrocellulose membrane (8.5 cm x 13.5 cm) (Biorad, Germany) using the Trans-Blot turbo machine (BioRad, Germany). The membranes were blocked by incubation with the blocking solution for 3 hrs at room temperature. The blot was then incubated with appropriately diluted primary antibody solution overnight at 4°C. After the incubation period, the blots were washed 6 times each for 5 min with TBST and later incubated with appropriate secondary antibody conjugated to HRP for 1 hr. The blots were again washed with TBST and then the chemiluminescent peroxidase substrate was used to visualize protein bands. Signals were measured and analyzed using an ECL imager (BQLAB, Germany).

3.13.5 Preparation of Nitrocellulose for re-probing ("Stripping")

The blots were stripped to remove primary and secondary antibodies. The blots were then re-probed with different antibodies.

Procedure

1. The membrane was added to a small plastic box which has a tight lid.
2. The Harsh stripping buffer was added to cover the membrane (~10 ml).
3. The membrane was incubated at 60°C for 30 minutes with some agitation.
4. The membrane was washed with distilled water for 2 times each 5 minutes.
5. Traces of β-mercaptoethanol will damage the antibodies. The membrane was washed extensively for 4 times each 5 minutes with TBST then, washed for another 4 times each 5 minutes with TBS.
6. The membrane was blocked using the blocking solution (3% BSA) and the procedure was repeated as described under the immunoblotting section (page 62).

4. Experimental design [Study design]

The goals of the present study were achieved by carrying out eleven different sets of experiments:

4.1 *In-vivo* antitumor activity and the involvement of CB-1 receptor

Seventy male Swiss albino mice were used in this experiment. Each mouse was inoculated s.c. in the right flank with $2.5x10^6$ EAC cells in 100 µl saline. The animals were randomly divided into seven groups each consisting of 7-10 animals, non-responders were excluded, as follows:

1. **Group I**: received DMSO (i.p.) and served as an **EAC control group**.
2. **Group II**: received R-Met (i.p.) at a dose of 0.5 mg/kg.
3. **Group III**: received OMDM-2 (i.p.) at a dose of 5 mg/kg.
4. **Group IV**: received NIDA 41020 (i.p.) at a dose of 0.7 mg/kg.
5. **Group V**: pretreated with NIDA 41020 (i.p.) at a dose of 0.7 mg/kg (30 minutes) followed by R-Met (i.p.) at a dose of 0.5 mg/kg.
6. **Group VI**: pretreated with NIDA 41020 (i.p.) at a dose of 0.7 mg/kg (30 minutes) followed by OMDM-2 (i.p.) at a dose of 5 mg/kg.
7. **Group VII**: received carboplatin (i.p.) at a dose of 5 mg/kg and serve as a **reference group**.

All the treatments were given every third day starting from day 7 after tumor inoculation (when the tumor becomes palpable) for 6 doses. **Table (III)** summarizes the treatment regimen of the different groups.

Table (III): Summary of the *in-vivo* treatment regimen

Group	Treatment	Dose
I	EAC control	DMSO (100 µl)
II	R-Methanandamide	0.5 mg/kg
III	OMDM-2	5 mg/kg
IV	CB-1 Ant. (NIDA 41020)	0.7 mg/kg
V	CB-1 Ant. + R-Methanandamide	0.7 mg/kg + 0.5 mg/kg
VI	CB-1 Ant. + OMDM-2	0.7 mg/kg + 5 mg/kg
VII	Carboplatin	5 mg/kg

Tumor volume was measured using digital Vernier caliber every third day throughout the experiment starting from the 7^{th} day post-inoculation (when the tumor become palpable). Relative tumor volume (RTV) and tumor growth time (TGT) time were calculated.

Animals were monitored and mortality was recorded daily along the study period to calculate percentage survival of animals, mean survival time (MST), and the increased in the life span (%) among all animals.

4.2 *In-vivo* anti-angiogenic activity and the involvement of CB-1 receptor

Seventy male Swiss albino mice were used. Each mouse was inoculated i.d. at 2 sites bilaterally on the lower ventral side (after shaving this area) with 100 µl EAC suspension ($2.5x10^6$ cells) on each site.

Animals were randomly divided into seven groups (as mentioned in page 63) each consisting of 10 animals. The treatment was initiated 24 hours after tumor inoculation. Animals were given the drug regimens, mentioned under the antitumor experiment section, for a single time. The degree of angiogenesis was assessed by measuring the tumor vascular volume on day 3 as described in page 44 using Evans blue.

4.3 Time course effects on tumor weights, TGF-β_1/CD-105 system and hematological parameters.

In this experiment one hundred and forty seven mice were used. Each mouse was inoculated i.d. at 2 sites bilaterally on the lower ventral side (after shaving this area) with 100 µl EAC suspension ($2.5x10^6$ cells) on each site. Then, animals were randomly divided into seven groups (as mentioned before), 21 mice each. The treatment was initiated 24 hours after tumor inoculation. Animals were given the drug regimens, mentioned under the antitumor experiment section, every third day.

The 21 mice in each group were further subdivided into three subgroups A, B, and C, seven mice each. These subgroups were sacrificed on days 7, 14, and 21, respectively. Blood samples were collected through the orbital sinus, under light ether anesthesia, for the determination of serum TGF-β_1 levels. After cervical dislocation, tumor discs were taken out and weighed then, fixed in 3.7% neutral buffered formalin for the assessment of the intra-tumoral expression of CD-105 receptor. The tumor weight, serum concentrations of TGF-β_1 and expression of CD-105 receptor were evaluated as a time course on days 7, 14, and 21.

In order to determine the influence of treatments on the hematological status of EAC-bearing mice, a comparison was made among the treated groups on the 14^{th} day after inoculation. Blood was drawn from each mouse by the retro-orbital plexus method. The total, differential WBC, RBC, and Hb levels were determined.

Two separate groups, each consisting of six mice served as **Normal control group** were used in the evaluation of serum TGF-β_1 levels and in the hematological studies.

The Pearson's equation was used for the determination of correlation coefficient between serum concentrations of TGF-β_1 and tumor weights.

4.4 *In-vitro* anti-proliferative activity and the involvement of CB-1 and TRPV1 receptors

Two different cell lines were used in this experiment, MCF-7 and U-87 cells. The cells were seeded in flat bottom 96-well plate (Greiner bio-one, Germany) at a concentration of $5x10^3$ cells/well in 100 µl growth medium supplemented with 10% FBS. Previous reports indicated that the presence of serum (i.e., FBS) affect the experimental outcomes of using cannabinoids in *in-vitro* models ***(Greenhough et al., 2007)***. Therefore, after 24 hrs of cell attachment in serum-containing medium, cells were serum starved for 24 hrs (starvation period). Thereafter cells were incubated with the treatment(s) for 24 hrs in serum free medium. Control cells were treated with the solvent control DMSO (0.5%). **Table (IV)** summarizes the treatment protocol for each cell line.

The dehydrogenase activity was fluorometrically determined by measuring the reduction of resazurin (blue, non-fluorescent) to resorufin (pink, highly fluorescent) as described in page 54. Each drug concentration was examined in duplicates in five independent experiments.

Table (IV): Summary of the *in-vitro* treatment regimen

Treatment	MCF-7	U-87
OMDM-2	2.5, 5, 10, 20, 40, 80 µM	0.625, 1.25, 2.5, 5, 10, 20, 40, 80 µM
NIDA41020	0.2 µM*	0.2 µM*
Capsazepine	1 µM*	1 µM*
Curcumin	5, 10, 20, 30, 40, 80 µM	5, 10, 20, 30, 40, 80 µM
Temozolomide	----------	50, 100, 200, 300, 400 µM
Paclitaxel	10, 100, 1000, 10000, 100000 nM	----------

* pre-incubated for 30 minutes before the addition of OMDM-2

4.5 Effect of OMDM-2 on VEGF level

The MCF-7 cells were seeded in 6-well plate at a concentration of $1x10^5$ cells/well in 1 ml of growth medium supplemented with 10% FBS. The cells were incubated at 37^oC in a humidified incubator with 5% CO_2 for 24 hrs. After washing twice with PBS, the cells were exposed to the IC_{50} of OMDM-2 and incubated for 24 hrs. After the end of the stimulation period, the culture supernatant of each sample was transferred to 1.5 ml Eppendorf tube. The cellular debris were pelleted by centrifugation (12000 rpm, 15 min), the resultant clear supernatant was used for estimation of VEGF level as discussed before (page 55).

4.6 Role of apoptosis in the anti-proliferative activity of OMDM-2

The cells were seeded in 96-well plate at a concentration of $2x10^4$ cells/well in 100 µl of growth medium supplemented with 10% FBS. The cells were allowed to attach by incubation at 37^oC in a humidified incubator with 5% CO_2 for a period of 24 hr. Then, the growth medium was removed and replaced by 100 µl/well fresh serum-free medium after washing twice with PBS. After 24 hrs, the medium was aspirated and the cells were treated with 3 different concentrations of OMDM-2 which had been selected based on the results of the cell viability experiments. After the end of the stimulation periods (8, 12, 24 hrs), floating and adherent cells were pelleted by centrifugation (200 X g, 10 min) and the resultant pellet was used for the estimation of apoptosis as discussed before (page 57).

4.7 Role of caspase-3 in the anti-proliferative activity of OMDM-2

U-87 cells were seeded in 35x10 mm dish (DB Falcon, Germany) at a concentration of $1x10^6$ cells in 1 ml of growth medium supplemented with 10% FBS. The cells were allowed to attach by incubation at 37^oC in a humidified incubator with 5% CO_2 for a period of 24 hrs. Then, the growth medium was removed and replaced by 1 ml of fresh serum-free medium after washing twice with PBS. After 24 hrs the medium was aspirated and the cells were treated with 3 different concentrations of OMDM-2 which had been selected based on the results of the cell viability experiments. At the end of the stimulation periods (8, 12, 24 hrs), the floating cells in the media of each sample were transferred to 1.5 ml Eppendorf tube. The attached cells were detached using 500 µl trypsin for 5 min. The detached cells were transferred to the Eppendorf tube corresponding to each sample.

Cells were pelleted by centrifugation (1200 rpm, 10 min) the resultant pellet used for estimation of the activity of caspase-3 as discussed before (page 59).

4.8 Apoptosis-DNA ladder assay (DNA laddering)

U-87 cells were seeded in 35x10 mm dish at a concentration of $0.5x10^6$ cells in 1 ml of growth medium supplemented with 10% FBS. The cells were allowed to attach by incubation at 37°C in a humidified incubator with 5% CO_2 for a period of 24 hr. Then, the growth medium was removed and replaced by 1 ml of fresh serum-free medium after washing twice with PBS. After 24 hrs the medium was aspirated and the cells were treated with 20 µM of OMDM-2. At the end of the stimulation periods (8, 12, 24 hrs), the floating cells in the media of each sample were transferred to 1.5 ml Eppendorf tube. The attached cells were scrapped using 500 µl cold PBS. The detached cells were transferred to the Eppendorf tube corresponding to each sample. Cells were pelleted by centrifugation (1200 rpm, 10 min) the resultant pellet used for estimation of DNA fragmentation as discussed before (page 61). Two positive controls were used, H_2O_2 32 µM (incubated for 24 hrs followed by 3 cycles of freeze-thaw lysis) as a positive control for necrosis while paclitaxel 500 nM (incubated for 72 hrs) represents a positive control for apoptosis.

4.9 Effect of OMDM-2 on morphology of cells

After exposure to different concentrations of OMDM-2 for 24 hrs, the cells were observed under an inverted microscope from Olympus (Olympus CK2, Japan). Pictures were taken with a Coolpix camera from Nikon (Germany).

4.10 Signal cascade pathways induced by OMDM-2 using Western blot analysis

The cells (MCF-7 or U-87) were seeded in 35x10 mm dish at a concentration of $1x10^6$ cells in 1 ml of growth medium supplemented with 10% FBS. The cells were allowed to attach by incubation at 37°C in a humidified incubator with 5% CO_2 for a period of 24 hrs. Then, the growth medium was removed and replaced by 1 ml of fresh serum-free medium after washing twice with PBS. After 24 hrs the medium was aspirated and the cells were treated with 3 different concentrations of OMDM-2 which had been selected based on the results of the cell viability experiments. At the end of the stimulation period, the floating and adherent cells were collected and centrifuged at 1200 rpm/ 10 min/ 4°C. The resultant pellet used for protein separation as discussed before (page 61). 30 µg of proteins were

analyzed for the total and the phosphorylated extracellular regulated kinase (ERK1/2), and AKT using Western blot technique.

4.11 New chemotherapeutic cocktails (combination study)

Resazurin assay as described before (page 54) was used to evaluate the inhibitory efficacy of different combination of drugs. To demonstrate whether there are synergistic, additive or antagonistic effects, cells were treated with different ratios of drugs for each combination as shown in **Table (V)**. The isobole analyses, the combination index (CI) and the dose reduction index (DRI) were used to evaluate each combination ***(Chou and Talalay 1983; Menéndez et al., 2001, Barrio et al., 2013)***.

4.11.1 Isobol analysis

The drug concentration of single or combined regimens that produced a 50% or 70% inhibitory effects were used as coordinates to construct isobolograms. The diagonal straight line connecting the IC_{50} or IC_{70} of single drugs represents the theoretical line of additivity for a continuum of different fixed dose ratios. When the combination is synergistic, the isobol (the line joining the points that represent the combination with the same 50% or 70% inhibitory effect, including the equally effective concentrations of single drugs used alone) is a concave curve, and antagonistic combination yields a convex curve.

4.11.2 Combination index (CI)

The CI was calculated by the CompuSyn software based on the Chou-Talalay equation, which takes into account both potency (Dm or IC50) and the shape of the dose-effect curve. Briefly, CI < 1, CI = 1, and CI > 1 indicate synergism, additive effect and antagonism, respectively.

4.11.3 Dose reduction index (DRI)

Representing the measure of how much the dose of each drug in a combination may be reduced at a given effect level compared with the doses of each drug alone.

Table (V): Summary of combinations ratios

Combinations	Combination ratio	
	MCF-7	**U-87**
OMDM-2:Curcumin	1:8, 1:4, 1:2, 1:1, 2:1, 4:1	1:32,1:16, 1:8, 1:4, 1:2, 1:1, 2:1, 4:1
OMDM-2: Paclitaxel	4:1, 20:1, 100:1, 500:1, 2500:1	----------
OMDM-2:Temozolomide	----------	1:320, 1:160, 1:80, 1:40, 1:20, 1:10, 1:5, 1:2.5

4.12 Data analysis and statistics

Data were expressed as mean ± standard error of the mean (S.E). Statistical analysis was performed using SPSS software, version 16. Data were analyzed for significant differences in tumor volume, relative tumor volume, TGT, tumor weights, MST, serum levels of TGF-β_1, and hematological parameters by using one-way analysis of variance (ANOVA), followed by Bonferroni post-hoc test for multiple comparisons.

Immunohistochemistry for CD-105 was analyzed using Chi-square test. For the survival time of animals, Kaplan-Meier curves were established for each group, and survival was compared using Log rank test. For *in-vitro* studies, data were analyzed for statistical significance by using t-test.

5. Results

5.1 Antitumor activity

The antitumor effects of the systemic administration of R-Met or OMDM-2 either alone or combined with CB-1 blocker pretreatment, NIDA 41020, were determined by assessing the changes in **tumor volume**, **relative tumor volume** (RTV), **tumor growth time** (TGT). The antitumor effect of carboplatin was determined as a reference standard.

5.1.1 Effect on solid tumor volume

The mice treated with vehicle (DMSO) alone developed subcutaneous tumors, the size of which was around 700 mm^3 at the end of the experiment (i.e. 25 days).
The administration of either R-Met or OMDM-2, every third day for 6 doses starting from day 7 post-inoculation, were able to significantly reduce the solid tumor volume as compared to the EAC control group ***(Figures 1, 2)***. Similarly, the treatment with the reference standard, carboplatin, showed a significant antitumor activity ***(Figures 1, 2)***. On the other hand, the treatment with CB-1 blocker (0.7 mg/kg, i.p.), NIDA 41020, *per se* did not affect the tumor volume compared to the control group ***(Figures 1, 2)***.

Meanwhile, the pretreatment with NIDA 41020 significantly antagonized the antitumor activity of R-Met ***(Figure 1)***, an effect that was not observed in OMDM-2 treated group, where OMDM-2 maintained its antitumor potential ***(Figure 2)***.

5.1.2 Effect on relative tumor volume

The systemic administration of OMDM-2 (5 mg/kg, i.p.) or R-Met (0.5 mg/kg, i.p.) resulted in a significant decrement in the relative tumor volume by 38% and 28%, respectively at the end of the experiment compared to the untreated control group ***(Figure 1, 2)***. The treatment with the CB-1 blocker (0.7 mg/kg, i.p.), NIDA 41020, *per se* did not affect the RTV compared to EAC control group.

NIDA 41020 pretreatment significantly antagonized the reducing effect of R-Met on RTV ***(Figure 1)***. While the pretreatment with NIDA 41020 did not antagonize the reducing effect of OMDM-2 on RTV; where OMDM-2 maintained its antitumor potential and reduced the tumor volume by 31% as efficaciously as carboplatin ***(Figure 2)***.

5.1.3 Effect on tumor growth time (TGT)

The administration of either R-Met (0.5 mg/kg, i.p.) or carboplatin (5 mg/kg, i.p.) significantly prolonged ***(Table 1)*** the TGT required to reach three folds the initial tumor volume by 43% and 40%, respectively ***(Figure 3)***. They also were able to inhibit the size of tumor to reach four folds the initial tumor volume.

OMDM-2 (5 mg/kg, i.p.) administration significantly prolonged the TGT required to double the initial tumor volume from the seventh day post inoculation by 122% ***(Table 1 & Figure 3)***. Successfully, the tumor size of OMDM-2-treated mice did not reach three folds the initial volume and consequently four folds.

The pretreatment with NIDA 4120 (CB-1 blocker) significantly antagonized the prolongation effect of R-Met on the tumor growth tripling and quadrupling times and also antagonized the prolongation effect of OMDM-2 on the tumor growth tripling time ***(Table 1 & Figure 3)***.

Tumor growth doubling time of OMDM-2 group pretreated with NIDA 41020 tended to be prolonged by about 50% as compared to EAC control group; however this prolongation was not statistically significant. On the other hand, NIDA 41020 was unable to antagonize the effect of OMDM-2 on tumor growth quadrupling time ***(Table 1 & Figure 3)***.

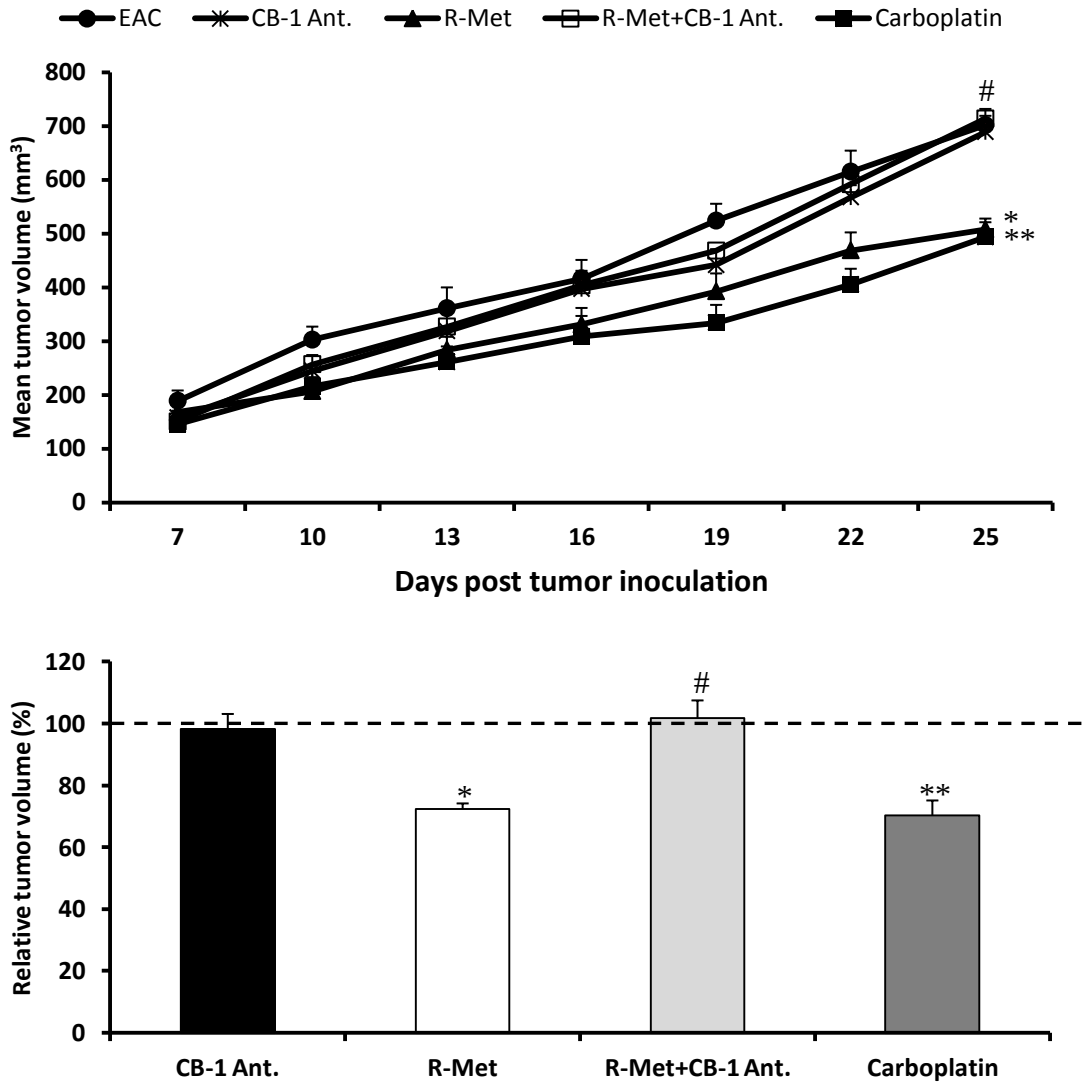

Figure (1): Effect of the systemic administration of R-Met and/or CB-1 antagonist on the solid tumor volume in EAC-bearing mice.

Effect of i.p injection of R-Methanandamide (0.5 mg/kg) either alone or in combination with CB-1 antagonist, NIDA 4120, pretreatment (0.7 mg/kg) on Ehrlich solid tumor volume [upper panel] and on relative tumor volume {(V/Vcontrol) x100} [lower panel]. Mice were inoculated s.c in the right flank with Ehrlich ascites carcinoma cells ($2.5x10^6$ cells/mouse). On day 7 post-inoculation mice bearing solid Ehrlich carcinoma were injected with the drugs every third day for six doses till day 21. The changes in the total volume (mm^3) were determined on day 7 until day 25, and the results were compared with the EAC-bearing mice. Values are expressed as mean ± S.E for *n*=7-10 mice [upper panel]. Values are expressed as mean tumor volumes of treated groups relative to mean tumor volume of EAC-bearing mice (control group) [lower panel]. All the data were analyzed using ANOVA followed by Bonferroni post-hoc test for multiple comparisons of means.

* Significantly different from EAC control group at $p \leq 0.05$. ** Significantly different from EAC control group at $p \leq 0.01$. # Significantly different from the individual corresponding treatment (i.e. without CB-1 antagonist) at $p \leq 0.05$.

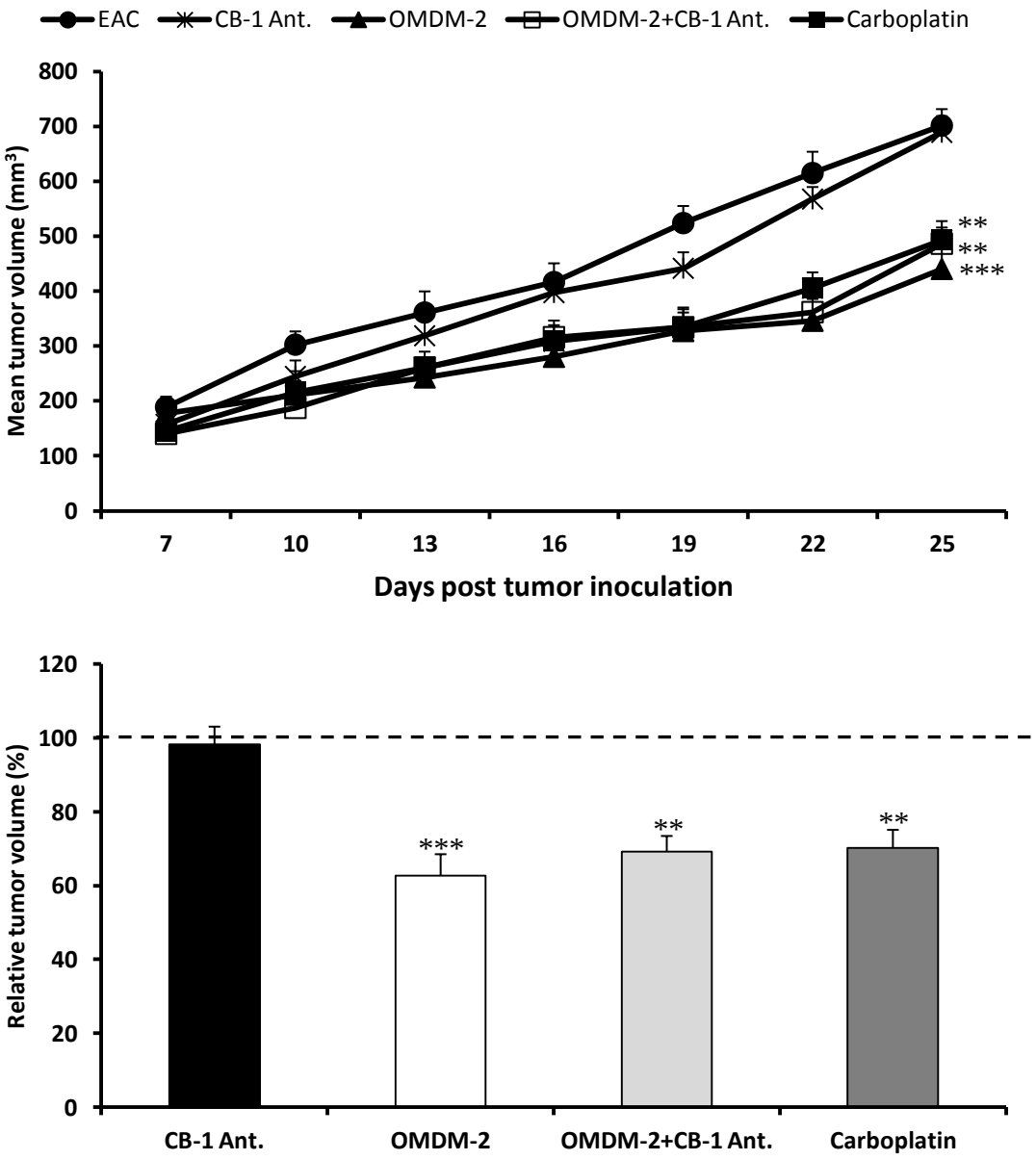

Figure (2): Effect of the systemic administration of OMDM-2 and/or CB-1 antagonist on the solid tumor volume in EAC-bearing mice.

Effect of i.p injection of OMDM-2 (5 mg/kg) either alone or in combination with NIDA 4120 (CB-1 antagonist) pretreatment (0.7 mg/kg) on Ehrlich solid tumor volume [upper panel] and on relative tumor volume {(V/Vcontrol) x100} [lower panel]. Mice were inoculated s.c in the right flank with Ehrlich ascites carcinoma cells ($2.5x10^6$ cells/mouse). On day 7 post-inoculation mice bearing solid Ehrlich carcinoma were injected with the drugs every third day for six doses till day 21. The changes in the total volume (mm^3) were determined on day 7 until day 25, and the results were compared with the EAC-bearing mice. Values are expressed as mean ± S.E for *n*=7-10 mice [upper panel]. Values are expressed as mean tumor volumes of treated groups relative to mean tumor volume of EAC-bearing mice (control group) [lower panel]. All the data were analyzed using ANOVA followed by Bonferroni post-hoc test for multiple comparisons of means. ** Significantly different from EAC control group at $p \leq 0.01$. *** Significantly different from EAC control group at $p \leq 0.001$.

Table (1): Effect of the systemic administration of R-Met or OMDM-2 with/without CB-1 blocker pretreatment on the tumor growth time (TGT) in EAC-bearing mice

Group	Tumor growth time (TGT) (Days)		
	Tumor doubling time	Tumor tripling time	Tumor quadrupling time
EAC-Control	6.3±0.7	12.1±0.9	15.9±0.8
R-Met	9±1.2	17.3±0.7*	----------
OMDM-2	14±1.4**	----------	----------
CB-1 Antagonist	6.5±1.2	12±1.3	16.5±0.4
R-Met+ CB-1 Ant.	6±1.6	10.3±1.6#	15±1.3
OMDM-2+CB-1 Ant.	9.5±2.2	12.5±1.3	----------
Carboplatin	10.5±1.7	17.2±0.5*	----------

TGT is the tumor growth time (days; mean ± S.E) required to reach 2-(doubling), 3-(tripling), or 4-(quadrupling) folds the initial tumor volume. All data were analyzed using ANOVA followed by Bonferroni post-hoc test for multiple comparisons of means. * Significantly different from EAC control group at $p \leq 0.05$. ** Significantly different from EAC control group at $p \leq 0.01$.

Significantly different from individual corresponding treatment (i.e. without CB-1 antagonist) at $p \leq 0.05$.

---------- Means didn't reach the required tumor volume.

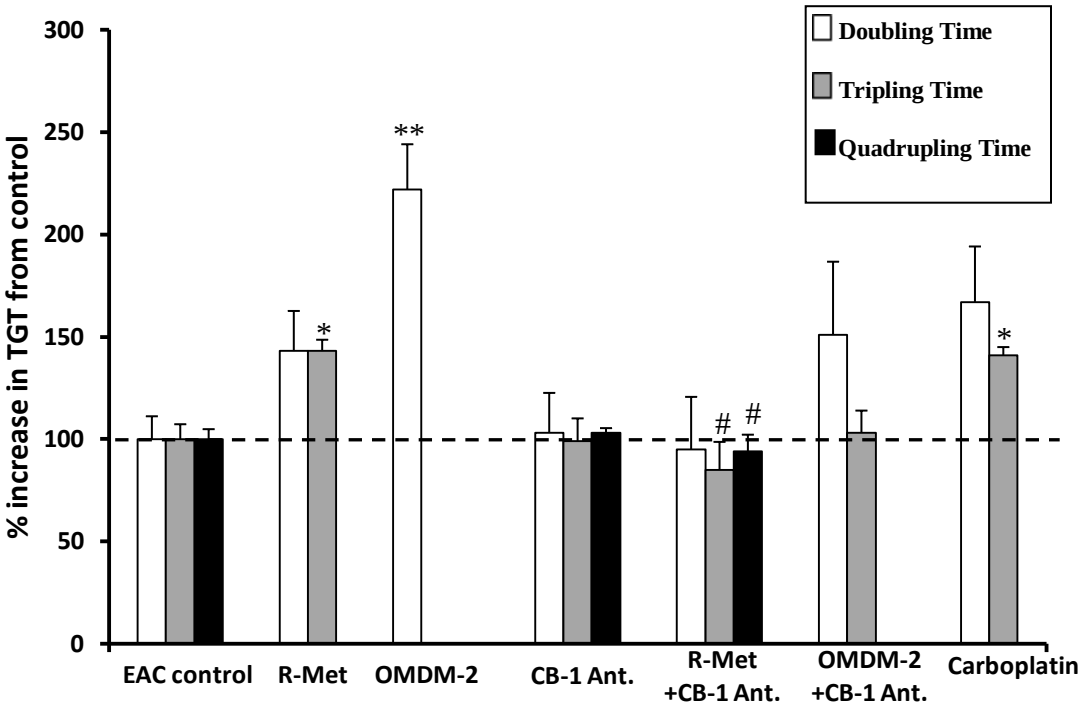

Figure (3): Effect of the systemic administration of R-Met or OMDM-2 with/without CB-1 blocker pretreatment on the percentage of increase in tumor growth time (TGT).

Effect of i.p injection of R-Methanandamide (0.5 mg/kg) or OMDM-2 (5 mg/kg) either alone or in combination with NIDA 4120 (CB-1 antagonist) pretreatment (0.7 mg/kg) on the percentage increase in tumor growth time (TGT) from control to reach double, triple, or quadruple the initial tumor volume in EAC bearing Swiss albino mice. Mice were inoculated s.c in the right flank with Ehrlich ascites carcinoma cells ($2.5x10^6$ cells/mouse). On day 7 post-inoculation mice bearing solid Ehrlich carcinoma were injected with the drugs every third day for six doses till day 21. Values are expressed as percentage from EAC control. All data were analyzed using ANOVA followed by Bonferroni post-hoc test for multiple comparisons of means. * Significantly different from EAC control group at $p \leq 0.05$. ** Significantly different from EAC control group at $p \leq 0.05$. # Significantly different from individual corresponding treatment (i.e. without CB-1 antagonist) at $p \leq 0.05$.

5.2 Survival study

5.2.1 Effect on survival of animals (%)

The change in percent survival of animals was recorded daily for a period of 89 days (when the last animal died) following tumor inoculation. On day 37, there was a 50% survival in the EAC control group; whereas R-Met, OMDM-2 in addition to OMDM-2 group pretreated with NIDA 41020 (CB-1 blocker) showed 100% survival, while both R-Met group pretreated with NIDA 41020 and carboplatin showed 71% survival ***(Table 2 & Figure 4)***. The control EAC-bearing mice showed zero% survival after 56 days of the tumor inoculation. On the same day, a 45% survival was noted in R-Met and OMDM-2 treated groups ***(Table 2 & Figure 4)***. While both OMDM-2 and R-Met groups pretreated with NIDA 41020 maintained 70% and 30% survival, respectively ***(Table 2 & Figure 4)***. Also, on the same day (i.e. day 56) carboplatin showed only 15% survival of animals.

5.2.2 Effect on mean survival time (MST)

The mean survival time (MST) in the EAC-control group was 37.2±4.3 days. OMDM-2 succeeded to significantly increase MST to reach 59.11±4.9. On the other hand, R-Met or carboplatin tended to increase MST to reach 52±3.9 and 50±7.2, respectively but this increment did not reach statistical significance ***(Table 3)***.

OMDM-2 group pretreated with NIDA 41020 showed a significant increment in MST to reach 59.4±2.5, while NIDA 41020 pretreatment counteracted the effect of R-Met on the prolongation of survival time ***(Table 3)***.

5.2.3 Effect on life span (%ILS)

Parallel to the results of MST, R-Met, OMDM-2, and carboplatin were able to enhance the life span of EAC-bearing mice by more than 25% compared to EAC-control group. Also, OMDM-2 group pretreated with NIDA 41020 showed a significant enhancement in the life span of animals. Groups treated with the OMDM-2 either alone or its combination with NIDA 41020 pretreatment showed the highest %ILS, 59.5, and 60.5%, respectively ***(Table 3)***.

Table (2): Number of survived animals in all treatment groups

Time (Days)	EAC	R-Met	OMDM-2	CB-1 Ant.	R-Met + CB-1 Ant.	OMDM-2 +CB-1 Ant.	Carboplatin
1	10	9	9	7	7	7	7
15	10	9	9	7	6	7	7
18	10	9	9	7	5	7	7
20	9	9	9	7	5	7	7
22	8	9	9	7	5	7	7
23	7	9	9	7	5	7	7
25	6	9	9	7	5	7	7
30	6	9	9	7	5	7	6
32	6	9	9	6	5	7	6
37	5	9	9	6	5	7	5
38	5	7	9	6	5	7	5
39	5	7	9	5	5	7	5
40	5	7	8	5	5	7	5
42	5	6	8	4	5	7	4
43	4	5	8	4	5	7	4
44	4	5	8	4	4	7	4
46	3	5	7	4	3	7	3
48	2	5	6	3	3	6	3
51	2	5	6	2	3	5	3
52	1	5	6	0	2	5	2
53	1	5	6		2	5	1
55	1	4	4		2	5	1
56	0	4	4		2	5	1
58		3	4		2	5	1
61		2	4		2	3	1
62		2	2		1	3	1
63		2	2		0	2	1
64		2	2			1	1
66		0	2			1	1
67			2			0	1
82			0				1
89							0

Starting number of animals in each group was 7-10. Number of animals survived daily was recorded in all groups. Experiment was extended to day 89 when the last animal died. The highlighted lines indicate 50% and 0% survival of EAC control.

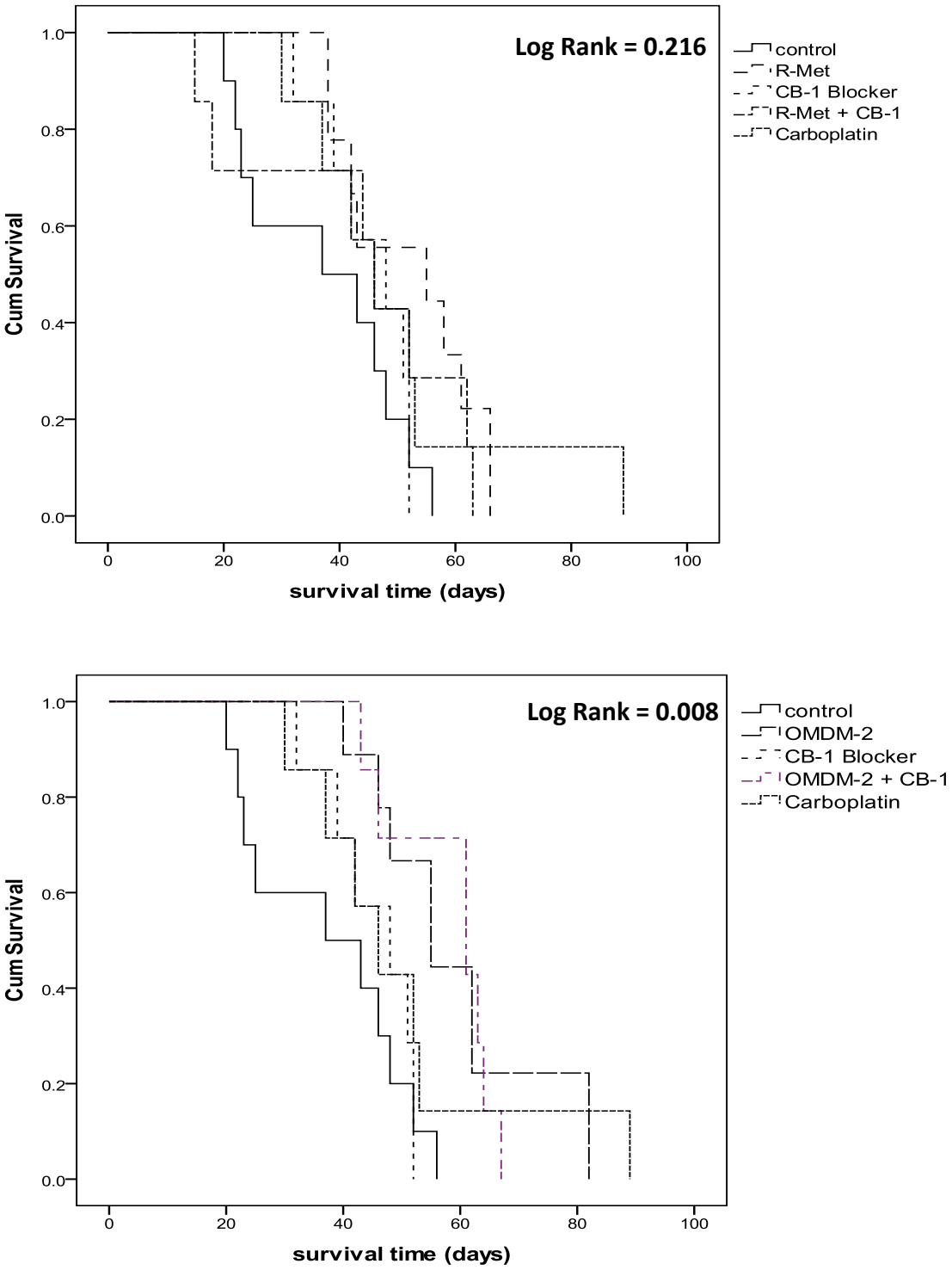

Figure (4): Effect of R-Met (0.5mg/kg, i.p), upper panel; or OMDM-2 (5mg/kg, i.p), lower panel, alone and in combination with CB-1 blocker (0.7mg/kg, i.p) on cumulative survival of EAC-bearing mice.

Cumulative survival of animals = number of living animals/initial total number of animals. Experiment was extended to day 89 when the last animal died in all groups. Survival curves were constructed according to the Kaplan-Meier method and statistical significance was determined using Log rank test.

Table (3): Effect of systemic administration of R-Met or OMDM-2 with/without CB-1 blocker pretreatment on mean survival time (MST)

Group	MST (days)	%ILS
EAC-Control	37±4.3	
R-Met	52±3.9	40.5•
OMDM-2	59±4.9*	59.5•
CB-1 Antagonist	45±2.9	21.6
R-Met+ CB-1 Ant.	43±7.3	16.2
OMDM-2+CB-1 Ant.	59.4±2.5*	60.5•
Carboplatin	50±7.2	35.1•

MST (mean survival time) = sum of survival days of all mice in each group/total number of mice in this group. ILS (increase in life span) = [(MST of treated group/MST of control group)-1]. 7-10 mice were used in each group. Values are expressed as mean ± S.E All data were analyzed using ANOVA followed by Bonferroni post-hoc test for multiple comparisons of means. * Significantly different from EAC control group at $p \leq 0.05$. • ILS > 25%.

5.3 Angiostatic activity (vascular permeability)

In this experiment, the anti-angiogenic effects of R-Met or OMDM-2 either alone or in combination with NIDA 41020 (CB-1 blocker) pretreatment were investigated. The degree of angiogenesis was assessed by measuring the tumor vascular volume using Evans blue; the percentage of angiogenesis was calculated as previously explained (page 44).

The administration of R-Met or OMDM-2 significantly reduced the percentage of angiogenesis in the solid tumors by about 50% and 40%, respectively ***(Figure 5)***. This effect was antagonized in the R-Met-treated group but not in the OMDM-2-treated group by the pre-treatment with NIDA 41020 ***(Figure 5)***. Surprisingly NIDA 41020 also exerted a significant, albeit small, anti-angiogenic action *per se* ***(Figure 5)***.

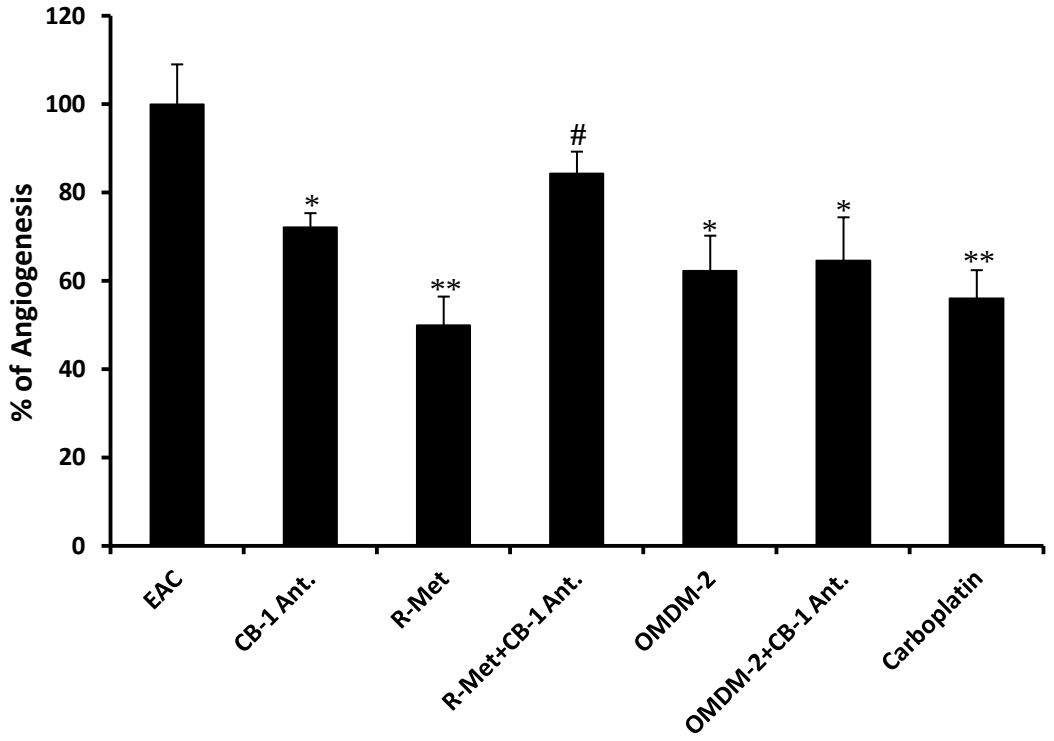

Figure (5): Effect of the systemic administration of R-Met or OMDM-2 with/without CB-1 blocker pretreatment on the percentage of angiogenesis in Ehrlich solid tumor.

Effect of i.p injection of R-Methanandamide (0.5 mg/kg) or OMDM-2 (5 mg/kg) either alone or in combination with NIDA 41020 (CB-1 antagonist) pretreatment (0.7 mg/kg) on the percentage of angiogenesis. Mice were inoculated intradermally (i.d) at 2 sites bilaterally on the lower ventral side with Ehrlich ascites carcinoma cells ($2.5x10^6$ cells/0.1 ml) on each site. The treatment was initiated 24 hours after tumor inoculation for a single dose. The degree of angiogenesis was assessed by measuring the tumor vascular volume on day 3 using Evans blue method. Each value represents the mean ± S.E of *n*= 10 mice. All data were analyzed using ANOVA followed by Bonferroni post-hoc test for multiple comparisons of means. Results are expressed as percentage of EAC control.

* Significantly different from EAC control group at $p \leq 0.05$. # Significantly different from the individual corresponding treatment (i.e. without CB-1 antagonist) at $p \leq 0.05$.

5.4 Role of TGF-β_1/CD-105 system

In the current study, the *in-vivo* effects of R-Met or OMDM-2 either alone or combined with NIDA 4120 (CB-1 blocker) pretreatment on the serum levels of TGF-β_1 and on the expression of endoglin (CD-105) receptor in tumor tissue were assessed as a time course on days 7, 14, and 21 post-inoculation.

5.4.1 Serum levels of TGF-β_1

EAC induced a significant and persistent increase in the serum concentrations of TGF-β_1 compared to the normal control group on days 7, 14, and 21 ***(Figure 6)***. On day 7, both R-Met and OMDM-2 significantly increased the serum concentrations of TGF-β_1 compared to the EAC-control group by about 47% ***(Figure 6)***.

Interestingly, a pre-treatment with NIDA 41020 significantly antagonized the enhancing effect of R-Met on the TGF-β_1 concentrations on day 7. The decrease was about 25% followed by a non-significant increase on day 21 compared to the R-Met-treated group. In case of OMDM-2, the CB1-blocker, NIDA 41020, significantly augmented the inducing effect of OMDM-2 on the TGF-β_1 concentrations on day 7 and increased it by about 26% compared to the OMDM-2-treated group. Interestingly at day 7 NIDA 41020 *per se* decreased the elevated level of TGF-β_1 in EAC-bearing mice ***(Figure 6)***.

On days 14 and 21 post-inoculation, individual treatments with R-Met, OMDM-2 or NIDA 41020 did not affect the elevated serum levels of TGF-β_1 compared to the EAC-control group ***(Figure 6)***. Carboplatin did not affect the elevated levels of TGF-β_1 at all time points compared to the EAC-control group ***(Figure 6)***.

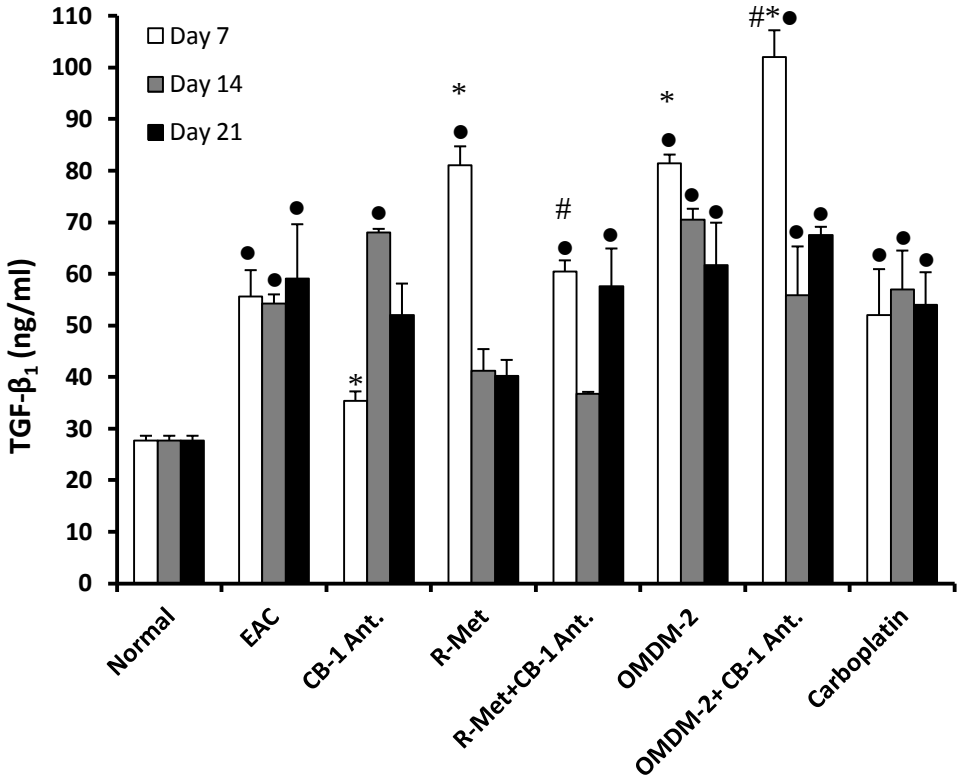

Figure (6): Effect of R-Met or OMDM-2 with/without CB-1 blocker pretreatment on the serum levels of TGF-β_1 in EAC-bearing mice.

Effect of i.p injection of R-Methanandamide (0.5 mg/kg) or OMDM-2 (5 mg/kg) either alone or in combination with CB-1 blocker pretreatment, NIDA 41020, (0.7 mg/kg) on serum levels of TGF-β_1. Mice were inoculated i.d. in the lower ventral side with EAC cells ($2.5x10^6$ cells/mouse). 24 hrs post-inoculation, mice bearing solid Ehrlich carcinomas were treated with the drugs twice a week for 1, 2 or 3 weeks (total 6 doses). The time course levels of TGF-β_1 were determined using ELISA. Each value represents the mean ± S.E of *n*= 6-7 mice. All data were analyzed using ANOVA followed by Bonferroni post hoc-test for multiple comparisons of means. • Significantly different from normal group at $p \leq 0.05$. * Significantly different from EAC control group at $p \leq 0.05$. # Significantly different from the individual corresponding treatment (without CB-1 antagonist) at $p \leq 0.05$.

5.4.2 Intra-tumoral expression of endoglin receptor (CD-105)

On day 7 post-inoculation; a significant difference in tissue CD-105 expression was observed among the 7 groups using Chi-square test; while, the evaluation of intra-tumoral CD-105 on days 14 and 21 post-inoculation showed a poor expression of the receptor in all groups including the EAC-control group ***(Table 4)***. Expression of tissue CD-105 was confirmed by the presence of brown stained cells in EAC tissue ***(Figure 7)***.

The tissue expression of CD-105 was up-regulated among all mice in EAC control group ***(Table 4, Figure 7)***. The systemic administration of R-Met (0.5 mg/kg) was able to reduce the percentage of high expression of CD-105 in EAC-bearing mice to reach 33% ***(Table 4, Figure 7)***. While, OMDM-2-treated group showed only 17% moderate expression and 83% poor expression of tissue CD-105 ***(Table 4, Figure 7)***. On the other hand, the systemic administration of CB-1 blocker *per se*, NIDA 41020, did not affect the up-regulated expression of CD-105 in EAC-bearing mice as the percentage of CD-105-rich tumors remained 100% ***(Table 4, Figure 7)***.

Meanwhile, the CB-1 blocker completely antagonized the down-regulating effect of R-Met; as this group showed 100% high expression ***(Table 4, Figure 7)***. On the other hand, the pretreatment with CB-1 blocker, NIDA41020 increased the percentage of poor expression to reach 100% in OMDM-2-treated group as efficaciously as carboplatin ***(Table 4, Figure 7)***.

Table (4): Effect of the systemic administration of R-Met or OMDM-2 with/without CB-1 blocker pretreatment on the number of animals exhibiting different grades of intratumoral CD-105 assessed immunohistochemically on day 7 post-inoculation of EAC cells in Swiss albino mice

Grades / Groups	Grade 0 ≤10%	Grade 1 11-30%	Grade 2 31-50%	Grade 3 >50%	%CD-105 rich tumors*
EAC-Control	0	0	0	6	100
R-Met	0	4	2	0	33*
OMDM-2	0	5	1	0	17*
CB-1 Ant.	0	0	0	6	100
R-Met+CB1 Ant.	0	0	0	6	100
OMDM-2+CB1 Ant.	0	6	0	0	0*
carboplatin	0	6	0	0	0*

* CD-105 rich tumors include specimens with moderate and strong expression of CD-105 (Grades 2 and 3, respectively). Chi-square test was performed to compare CD-105 immunohistochemical expressions

Figure (7): Representative samples of CD-105 immunostaining.

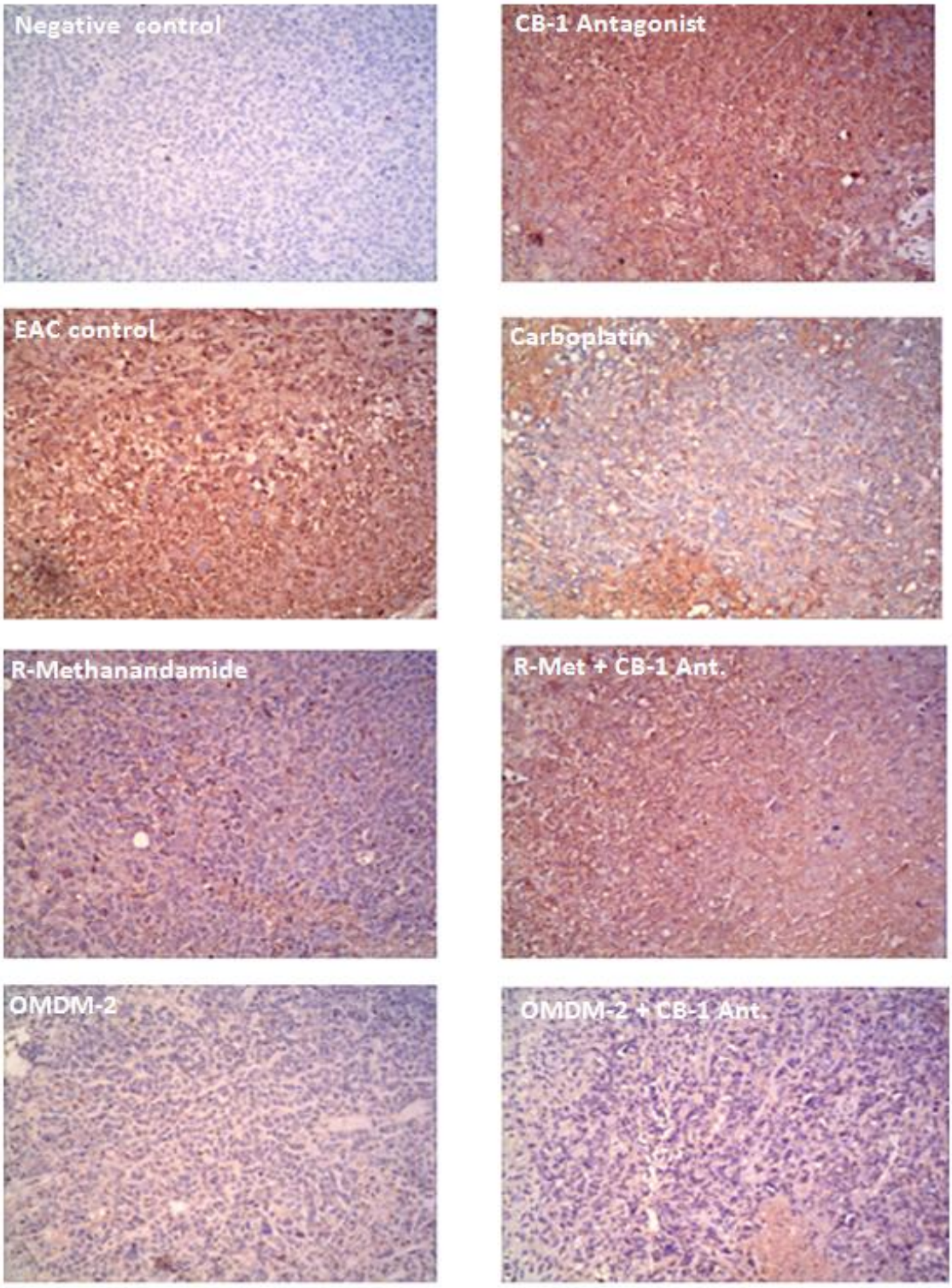

Effect of R-Met or OMDM-2 systemic administration with/without CB-1 blocker pretreatment, NIDA41020, on the cytoplasmic expression of CD-105 on day 7 post-inoculation of EAC cells in Swiss albino mice. CD-105 appears to be expressed with a ground glass pattern in the cytoplasm of breast tumor cells (brown stain). Meyer's hematoxylin counterstain (×250 original magnification)

5.5 Effect on the tumor weights

The systemic administration of either OMDM-2 or carboplatin led to a significant reduction in tumor weights on days 7, 14 and 21 post-inoculation as compared to the EAC-group ***(Figure 8)***. The R-Met-treated group showed similar results on days 7 and 21 post-inoculation while on day 14 results did not reach statistical significance ***(Figure 8)***. Blocking of CB-1 receptor significantly antagonized the tumor reducing ability of R-Met at both time points ***(Figure 8)***. In case of OMDM-2, the CB-1 blocker, NIDA41020, pre-treatment did not alter its tumor reducing activity on days 7 and 21.

However, on day 14 a pre-treatment with the CB-1 blocker, NIDA4102, decreased the antitumor activity of OMDM-2 without reaching statistical significance compared to the OMDM-2-treated group.

On the other hand, the treatment with NIDA41020 (0.7 mg/kg, i.p.) *per se* did not affect the tumor weights at all time points along the experiment period as compared to the EAC-control group ***(Figure 8)***.

5.6 Correlation between serum TGF-β_1 and tumor weights

The Pearson correlation coefficient was determined for the relationship between serum concentrations of TGF-β_1 and tumor weights in the EAC model. On day 7 post-inoculation a negative association was found (r_p = - 0.8), however, without reaching statistical significance (p=0.052) ***(Figure 9)***. The results indicated that on the progression of tumor (days 14 and 21) this association seems to be lost (r_p = - 0.5 and - 0.15, respectively) ***(Figure 9)***.

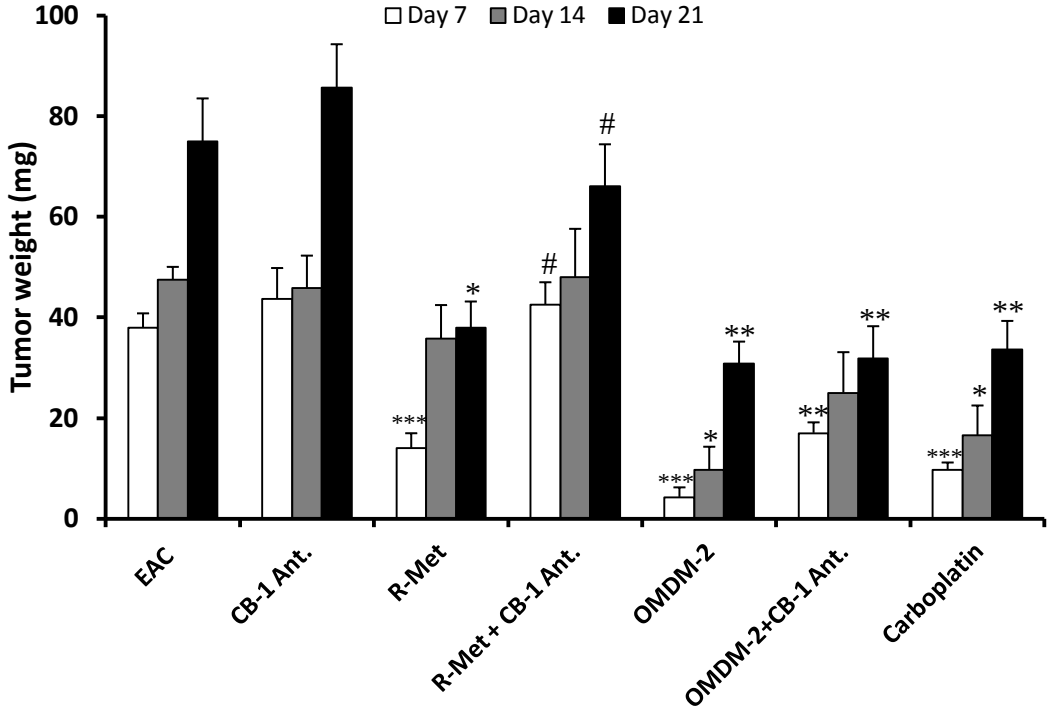

Figure (8): Effect of the systemic administration of R-Met or OMDM-2 with/without CB-1 blocker pretreatment on the tumor weight of EAC

Effect of i.p injection of R-Methanandamide (0.5 mg/kg) or OMDM-2 (5 mg/kg) either alone or in combination with CB-1 blocker pretreatment, NIDA 41020, (0.7 mg/kg) on tumor weight. Mice were inoculated in the lower ventral side with Ehrlich ascites carcinoma cells ($2.5x10^6$ cells/mouse). 24 hrs post-inoculation, mice bearing solid Ehrlich carcinomas were treated with the drugs twice a week for 1, 2, or 3 weeks and the change in tumor weights (mg) were determined. Each value represents the mean ± S.E of *n*= 7 mice. All data were analyzed using ANOVA followed by Bonferroni post-hoc test for multiple comparisons of means. * Significantly different from EAC control group at $p \leq 0.05$. ** Significantly different from EAC control group at $p \leq 0.01$. *** Significantly different from EAC control group at $p \leq 0.001$.$^{\#}$ Significantly different from individual corresponding treatment (without CB-1 antagonist) at $p \leq 0.05$.

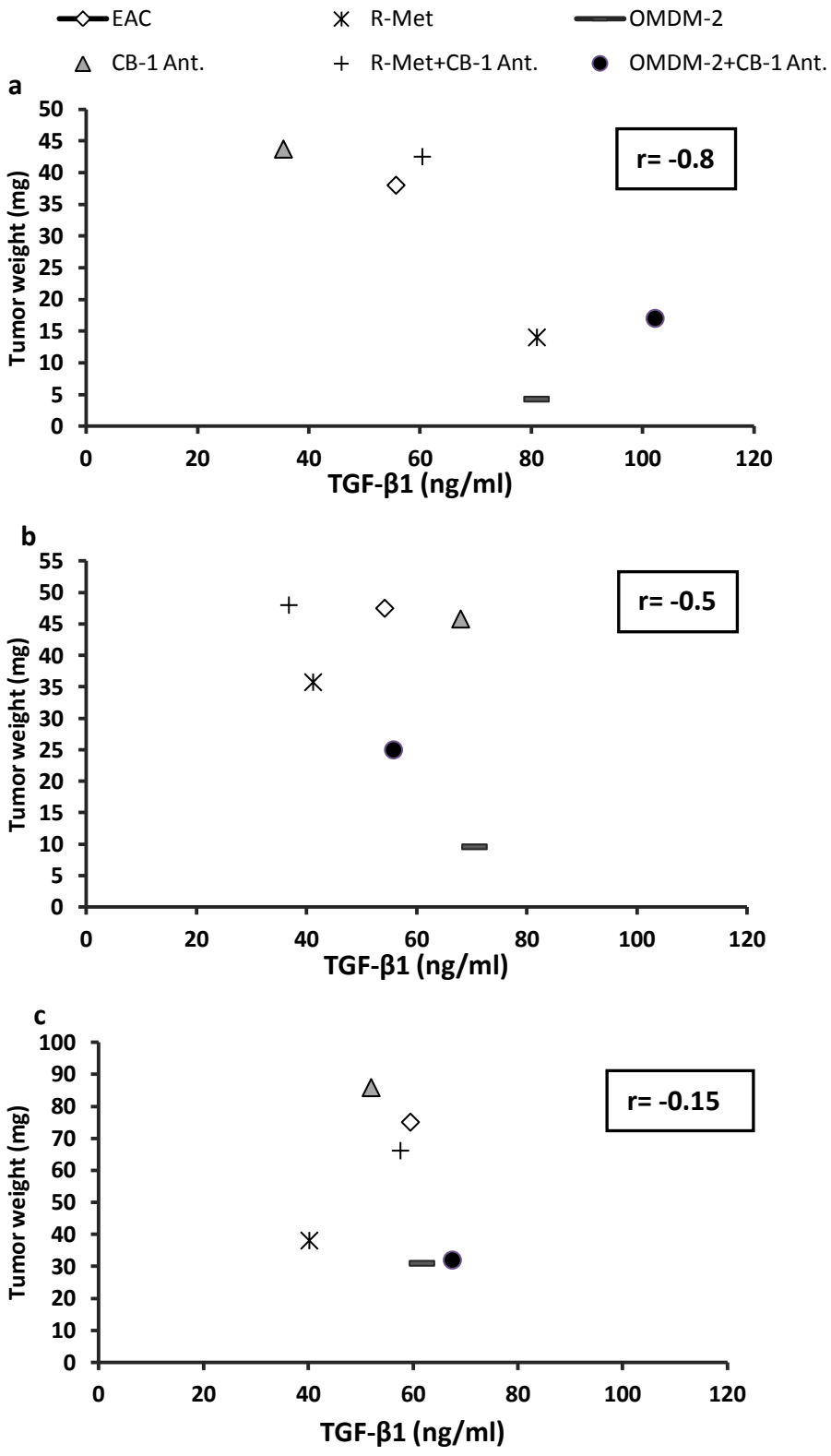

Figure (9): Correlation between the serum levels of TGF-β_1 and the tumor weights in EAC-bearing mice treated with R-Methanandamide (0.5 mg/kg, i.p.) or OMDM-2 (5 mg/kg, i.p.) and their combination with CB-1 blocker, NIDA 41020, (0.7 mg/kg, i.p.) on days 7, 14 and 21 (a, b and c, respectively) post-inoculation. r denotes the Pearson's correlation coefficient obtained for the linear regression line. r did not reach significance.

5.7 Effect on hematological status

The analysis of the hematological parameters showed minimum toxic effect in mice treated with OMDM-2 or R-Met after 14 days of transplantation. Both OMDM-2 and R-Met were able to reverse the changes observed in the hematological parameters consequent to tumor inoculation.

The hematological parameters of the tumor-bearing mice on day 14 showed significant changes when compared to the normal mice as shown in ***Table 5***. The total WBC count was found to be doubled ($P<0.01$) with a reduction in the hemoglobin content of RBC by about 63% as compared to normal group ($P<0.001$). The differential count of WBC showed that the percentage of neutrophils increased ($P<0.001$) while that of lymphocytes decreased ($P<0.05$). At the same time interval, OMDM-2 (5 mg/kg) or R-Met (0.5 mg/kg) treatment could change these altered parameters to near normal as shown in ***Table 5***.

Table (5): Effect of the systemic administration of OMDM-2 or R-Met on the hematological parameters of EAC-bearing mice

Parameter	Normal	EAC tumor	R-Met	OMDM-2
Hb (g/dl)	13.4±0.2	5±1.4$^{\bullet\bullet\bullet}$	10±0.3*	10±0.2*
RBC (million/mm^3)	8.27±0.1	3±0.3$^{\bullet}$	8±0.73*	7±0.64*
WBC (million/mm^3)	4.7±0.46	9±0.4$^{\bullet\bullet}$	5.8±0.2*	5.5±0.7*
Lymphocytes (%)	78.9±1.7	70±1.1$^{\bullet}$	71.8±2	71±1.78
Neutrophils (%)	10.1±1.5	19±2$^{\bullet\bullet\bullet}$	12.8±1.6	12±0.6*
Monocytes (%)	6.7±0.15	5.2±0.2	5±0.7	6.75±0.3

Each value represents the mean ± S.E of *n*= 6-7 mice per data. All data were analyzed using ANOVA followed by Bonferroni post-hoc test for multiple comparisons of means. $^{\bullet, \bullet\bullet, \bullet\bullet\bullet}$ significantly different from normal control at $p \leq 0.05$, 0.01, and 0.001, respectively. * Significantly different from EAC control group at $p \leq 0.05$.

5.8 *In-vitro* anti-proliferative activity

OMDM-2 was screened for its ability to reduce the cell proliferation on two different human cell lines, MCF-7 and U-87 cells. OMDM-2 significantly inhibited the MCF-7 and glioma cells proliferation in a dose dependent manner after 24 hrs of incubation **(*Figure 10)***. The concentrations of OMDM-2 reduced the proliferation of MCF-7 and U-87 cells to 50% (IC_{50}) were 4.9 µM and 2.7 µM, respectively **(*Figure 10).***

5.8.1 Role of CB-1 receptors in the OMDM-2 cytotoxicity

The pre-treatment with NIDA 41020 (selective CB-1 antagonist) at 0.2 µM did not substantially change the cytotoxicity profile of OMDM-2 against MCF-7 cells **(*Figure 11)***. The pre-treatment with NIDA 41020 antagonised the growth inhibitory effects of low concentrations of OMDM-2 in U-87 glioma cells. This was not the case with higher concentrations **(*Figure 11)***. Noteworthy, the used concentration of NIDA 41020 could block the CB-1 receptor without affecting the viability of both cells *per se* (data not shown).

5.8.2 Role of TRPV1 receptors in the OMDM-2 cytotoxicity

In U-87 glioma cells, the pre-treatment with capsazepine (selective TRPV1 antagonist) antagonised the growth inhibitory effects of low concentrations of OMDM-2 **(*Figure 11)***. While in case of MCF-7 cells, capsazepine did not change the cytotoxicity profile of OMDM-2. Remarkably, the selected dose of capsazepine (1 µM) reduced the viability of MCF-7 cells to a little extent (87% ± 2.3) (data not shown). On the other hand, it did not affect the viability of U-87 glioma cells.

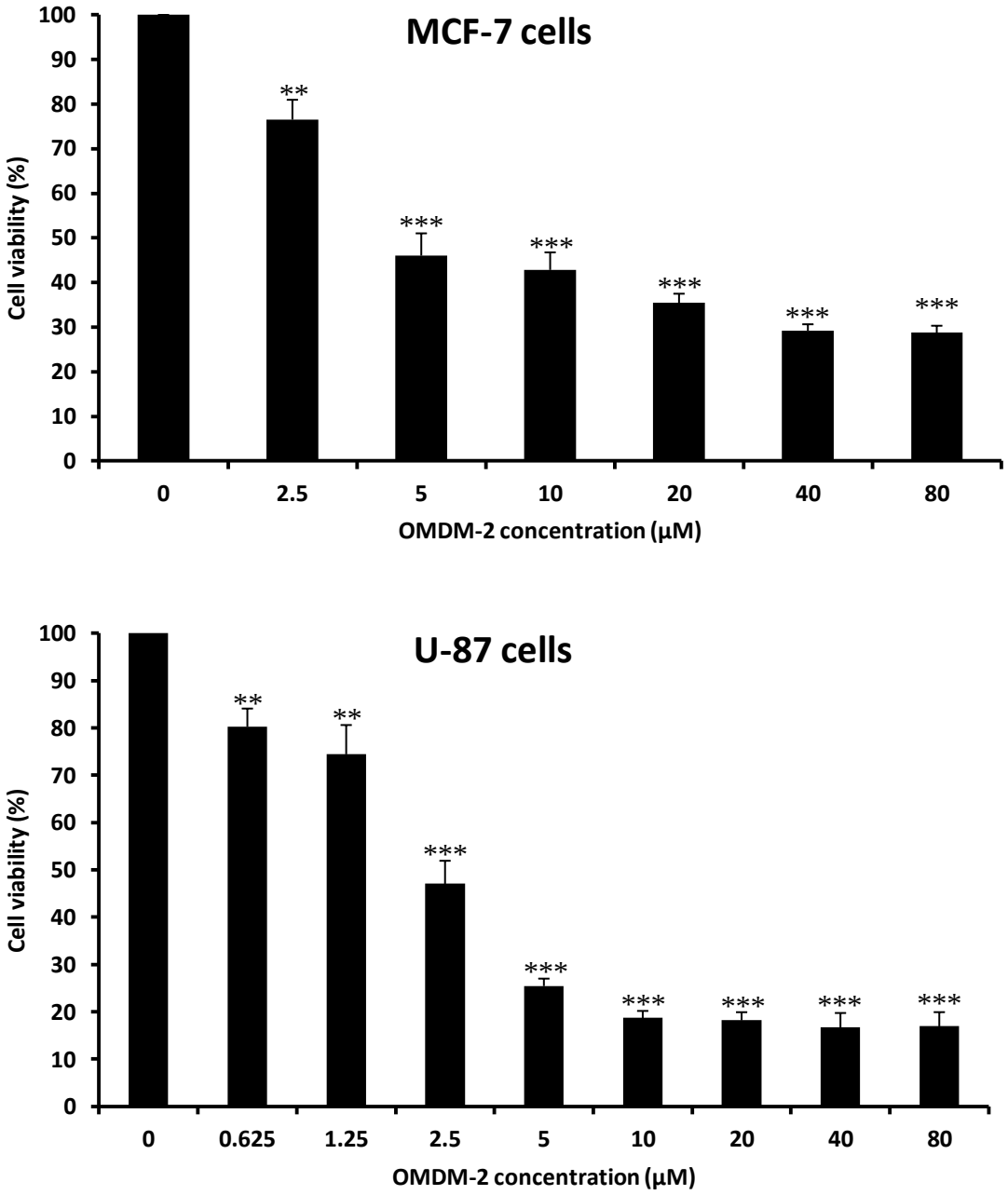

Figure (10): Concentration response curve of OMDM-2-induced cytotoxicity.

The effect of 24 hrs incubation with various concentrations of OMDM-2 on the proliferation of human breast carcinoma cells (MCF-7) [upper panel] and glioma cells (U-87) [lower panel] was determined fluorometrically using a Resazurin based assay. The IC_{50} were 4.9 µM and 2.7 µM for MCF-7 and U-87, respectively. Each data point represents the mean ± S.E of five independent experiments.

** Significantly different from control at $p \leq 0.01$. *** Significantly different from control at $p \leq 0.001$.

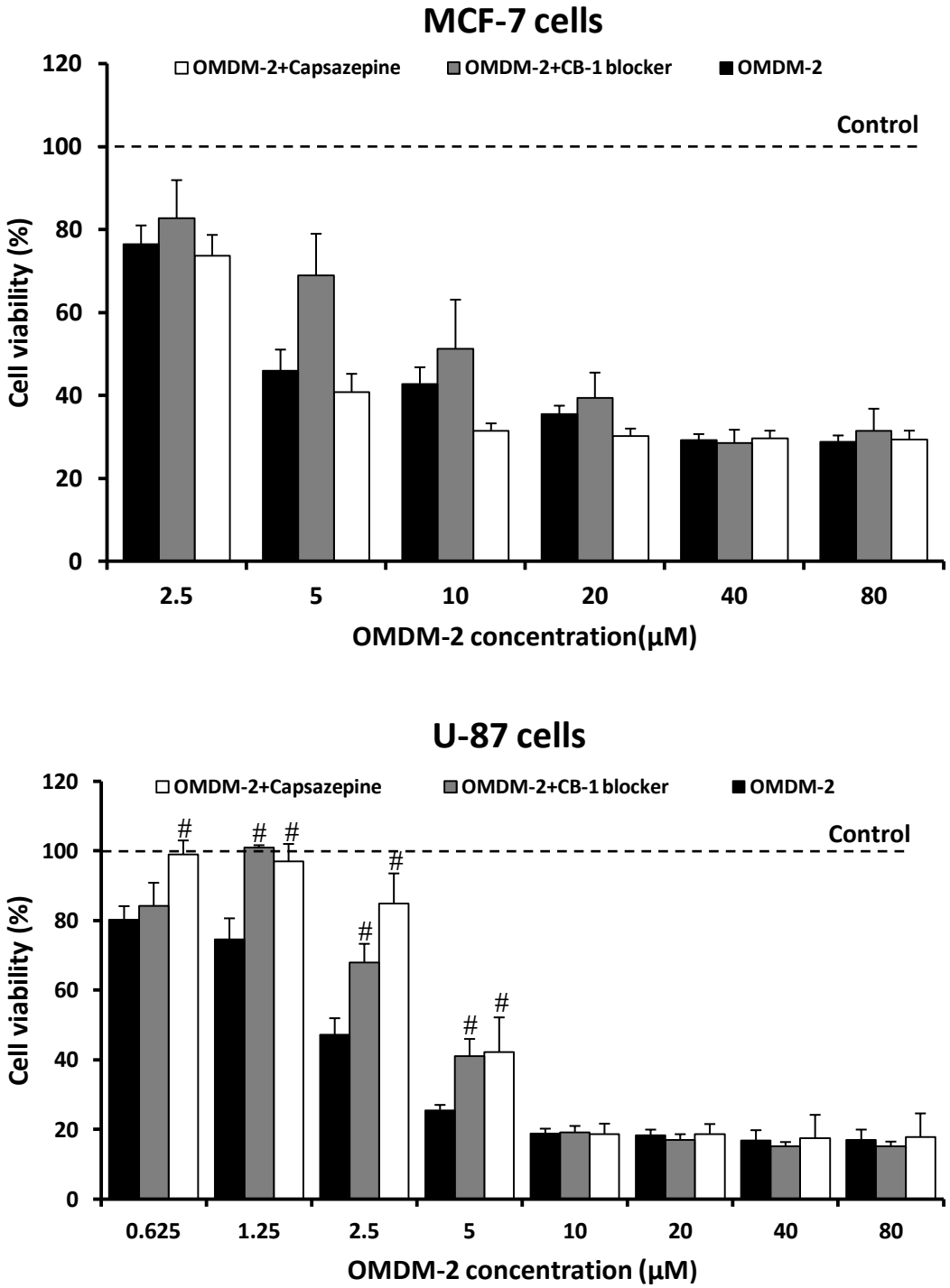

Figure (11): Modulatory effect of CB-1 or TRPV1 blockers pre-treatment on OMDM-2 induced cytotoxicity in MCF-7 and U-87 cells.

Effect of the pretreatment with CB-1 blocker, NIDA41020, (0.2 µM) or TRPV1 blocker, capsazepine (1 µM) on the anti-proliferative activity of different concentrations of OMDM-2 using human breast carcinoma cells (MCF-7) [upper panel] and glioma cells (U-87) [lower panel]. Each data point represents the mean ± S.E of five independent experiments. # Significantly different from the individual treatment without blocker at $p \leq 0.05$.

5.9 Effect of OMDM-2 on VEGF concentration

The concentration of VEGF, angiogenic marker, in the culture supernatants of MCF-7 cells treated with 7.2 µM of OMDM-2 (IC_{50}) was significantly reduced by 90% as compared to the MCF-7-control group ***(Figure 12)***. This experiment was conducted in Egypt and the IC_{50} was chosen according to the results of the *in-vitro* study carried out there under different culture conditions which included the addition of serum.

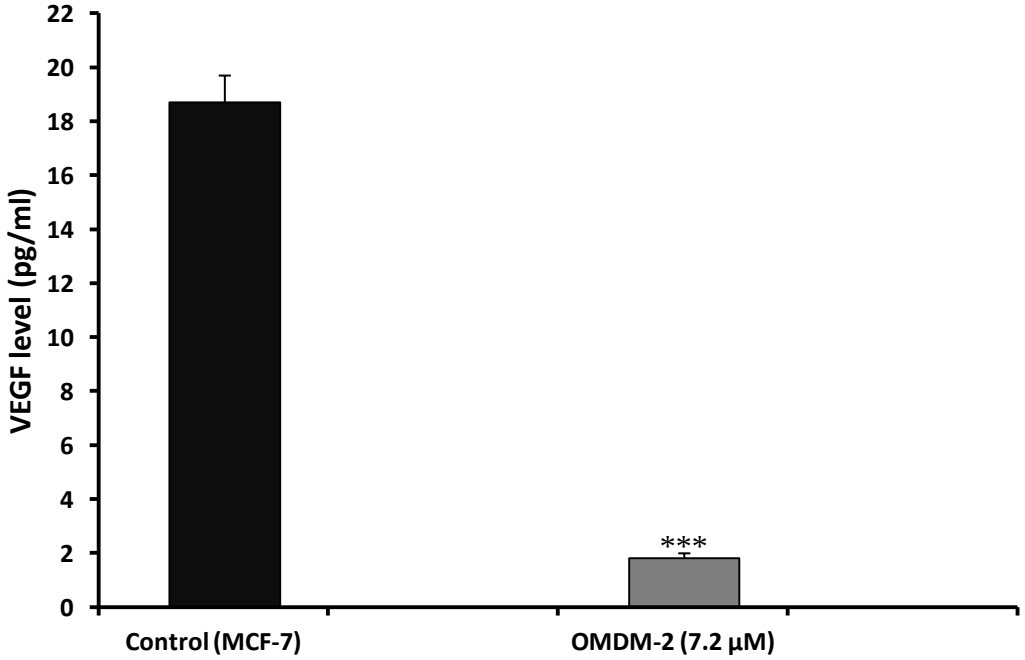

Figure (12): Effect of OMDM-2 on VEGF level in MCF-7 cells.

The VEGF concentrations in MCF-7 cells exposed to 7.2 µM of OMDM-2 for 24 hrs were evaluated using ELISA. Each point represents mean ± S.E of three independent experiments.
Means were compared using paired t-test. *** Significantly different from control group at $p \leq 0.001$.

5.10 Characteristics of cell death mediated by OMDM-2

Four different sets of experiments were used to evaluate the characteristics of cell death mediated by OMDM-2:

5.10.1 Quantification of oligonucleosomal DNA fragments (marker of apoptotic cell death)

By examining the U-87 cells after 8 hrs, 12 hrs or 24 hrs of incubation with increasing concentrations of OMDM-2, almost no quantitative differences in DNA fragmentation were observed between the control and the treated cells as shown in ***Figure 13***. Also, no apoptosis was shown in MCF-7 cells exposed to increasing concentration of OMDM-2 for 24 hrs **(*Figure 13)***.

5.10.2 Caspase-3 activity

OMDM-2 failed to increase the activity of caspase-3 in U-87 cells at different concentrations and time points **(*Figure 14)***. The caspase-3 activity was not measured in MCF-7 cells because they lack the caspase-3 gene.

5.10.3 DNA fragmentation (laddering)

To further confirm that apoptosis is not mediating the glioma cell death, we performed electrophoretic analysis of DNA laddering, a key feature of cell undergoing apoptosis. As shown in ***Figure 15***, cell death induced by OMDM-2 is not mediated by classical apoptosis or necrosis.

5.10.4 Morphological changes

As shown in ***Figure 16***, U-87 cells treated with different concentrations of OMDM-2 displayed marked morphological changes. The adherent cells appear round in shape, with extensive cytoplasmic vacuolation.

This type of cell death fits the criteria of paraptosis which includes: rounding of the cells, cytoplasmic vacuolation, lack of caspase activation, and lack of apoptotic morphology.

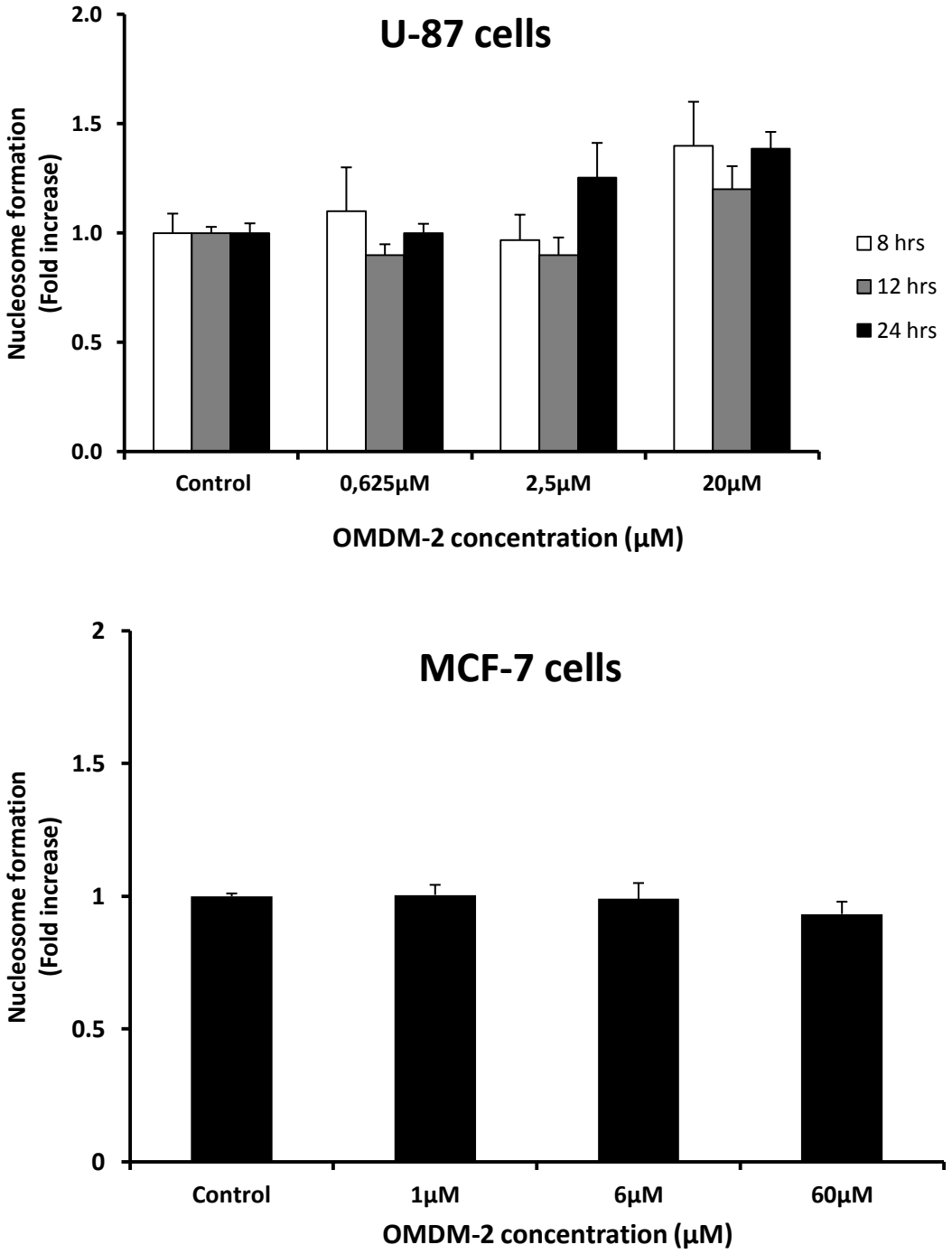

Figure (13): Role of apoptosis in OMDM-2 mediated cytotoxicity.

Detection of oligonucleosomes indicative of the process of apoptosis in U-87 glioma cells after 8, 12, and 24 hrs treatment with increasing concentrations of OMDM-2 [upper panel] and in MCF-7 cells after 24 hrs treatment [lower panel]. Cells were collected for apoptosis assay using cell death ELISA Kit. ELISA OD was normalized to protein content. Each point represents mean ± S.E of three independent experiments.

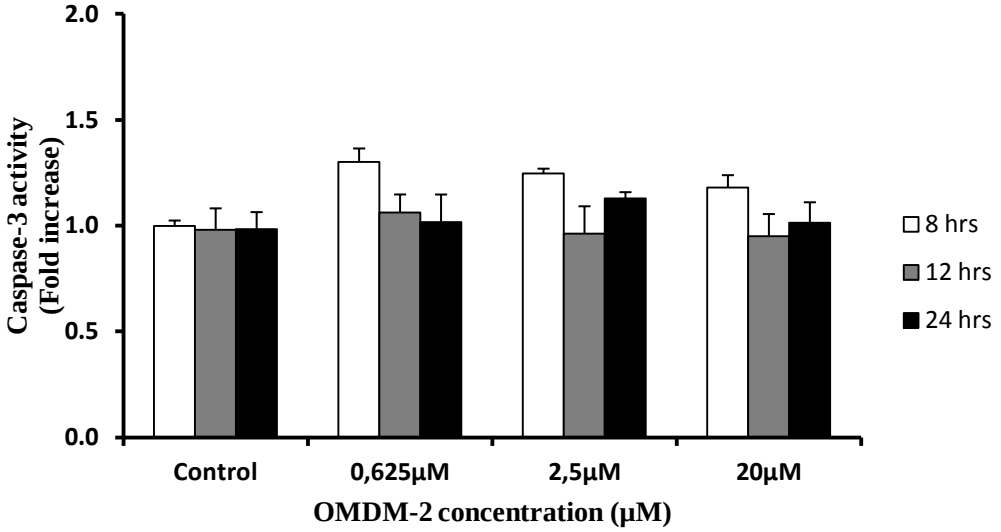

Figure (14): Caspase-3 activity

Spectrophotometric measurement of caspase-3 activities in U-87 glioma cells exposed to increasing concentrations of OMDM-2 for 8, 12, and 24 hrs. 150 µg proteins were used to measure the activity of caspase-3. Each point represents mean ± S.E of three independent experiments.

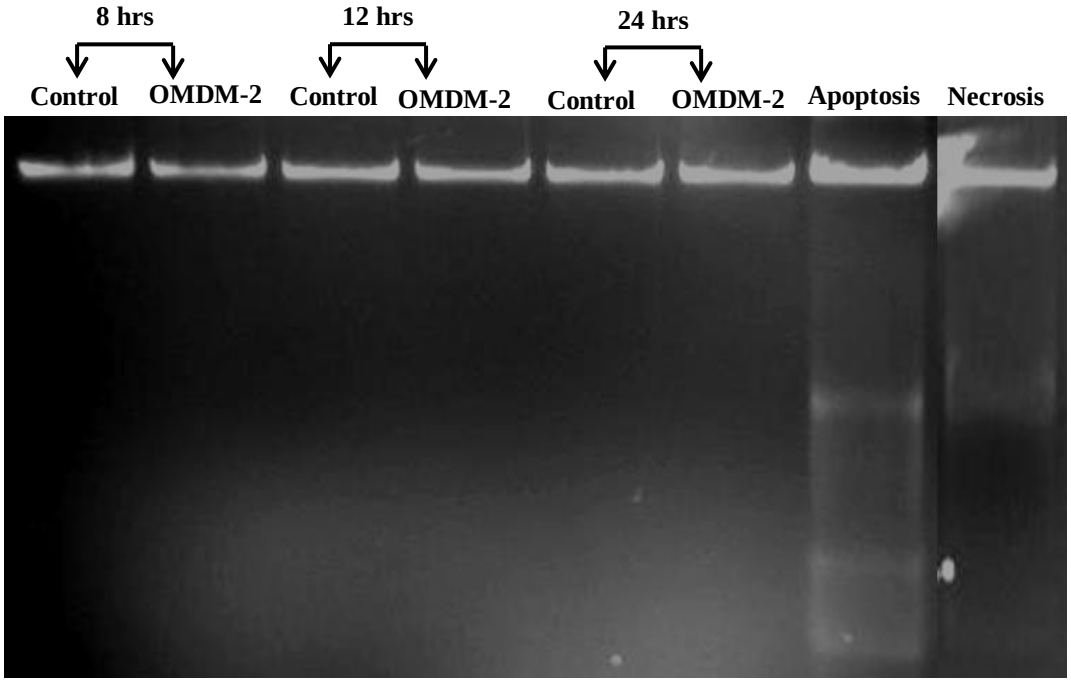

Figure (15): OMDM-2 induced cell death was neither apoptosis nor necrosis.

U-87 cells were treated for 8, 12, and 24 hours with either vehicle control (DMSO) or 20 µM OMDM-2. After the incubation period, the adherent and the floating cells were subjected to DNA extraction and qualitatively analyzed by DNA gel electrophoresis (1.5%). U-87 cells were also treated with 500 nM paclitaxel for 72 hours as a positive control for apoptosis or 32 mM H_2O_2 (incubated for 24 hrs followed by 3 cycles of freeze-thawing) as a positive control for necrosis. The pattern of DNA separation for OMDM-2 treated cells appears to be different from apoptosis and necrosis.

Figure (16): Representative samples of OMDM-2 induced morphological changes.

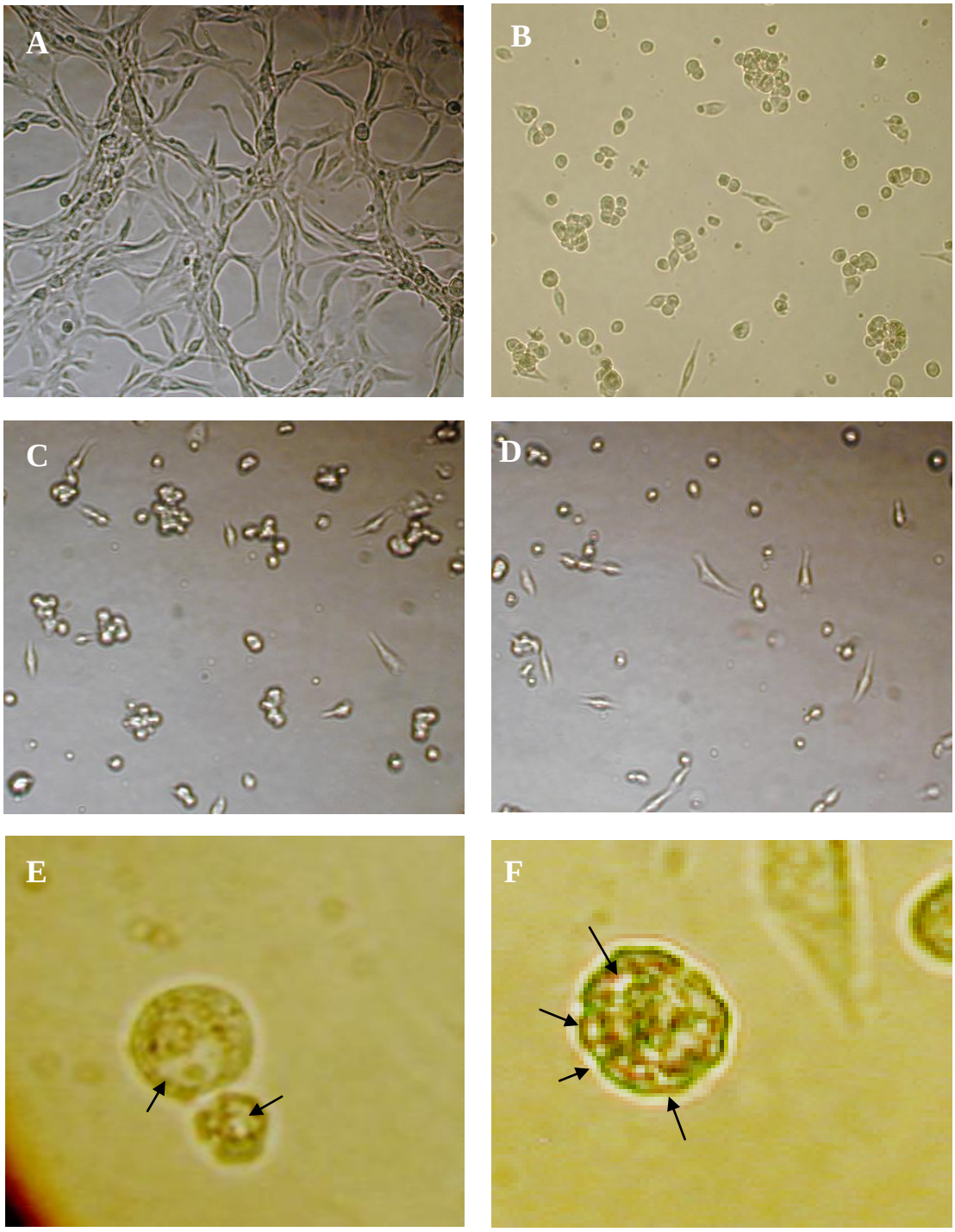

Photomicrograph observations in cultured U-87 glioblastoma cells, 20X magnification power except (E) and (F) 40X. Cells were treated with OMDM-2 at (A) 0 µM, (B) 0.625 µM , (C) 2.5 µM, (D) 20 µM (E) 2.5 µM (40 X), (F) 20 µM (40 X) for 24 hrs.

5.11 Effect of OMDM-2 on the phosphorylation status of ERK1/2 and AKT

To probe the involvement of ERK1/2 and AKT pathways in regulating the cell death mediated by OMDM-2, we assessed the effects of OMDM-2 on the level of phospho-ERK1/2 and AKT after 24 hrs of treatment. The U-87 cells exposed to different concentrations of OMDM-2 showed a tendency to increase the activity of ERK1/2 without reaching statistical significance **(*Figure 17)***. On the other hand, the MCF-7 cells exposed to low concentrations of OMDM-2 showed a significant increase in the ERK1/2 phosphorylation as compared to the control group **(*Figure 18)***. Importantly, the 24 hrs exposure of MCF-7 cells to a very high concentration of OMDM-2 (60 µM) resulted in a strong decrease in the expression of ERK1/2 and consequently in its phosphorylated form **(*Figure 18)***.

The exposure of both U-87 and MCF-7 cells to OMDM-2 did not affect the level of p-AKT as compared to the control groups **(*Figures 17&18, respectively)***. Interestingly, the MCF-7 cells exposed to 60 µM of OMDM-2 showed a dramatic decrease in the expression of AKT protein similar to that happens with ERK1/2 **(*Figure 18)***.

The U-87 and MCF-7 cells exposed to either NIDA 41020 or capsazepine, *per se*, did not show any significant changes in the expression of p-ERK1/2 and p-AKT (data not shown).

U-87 Glioma

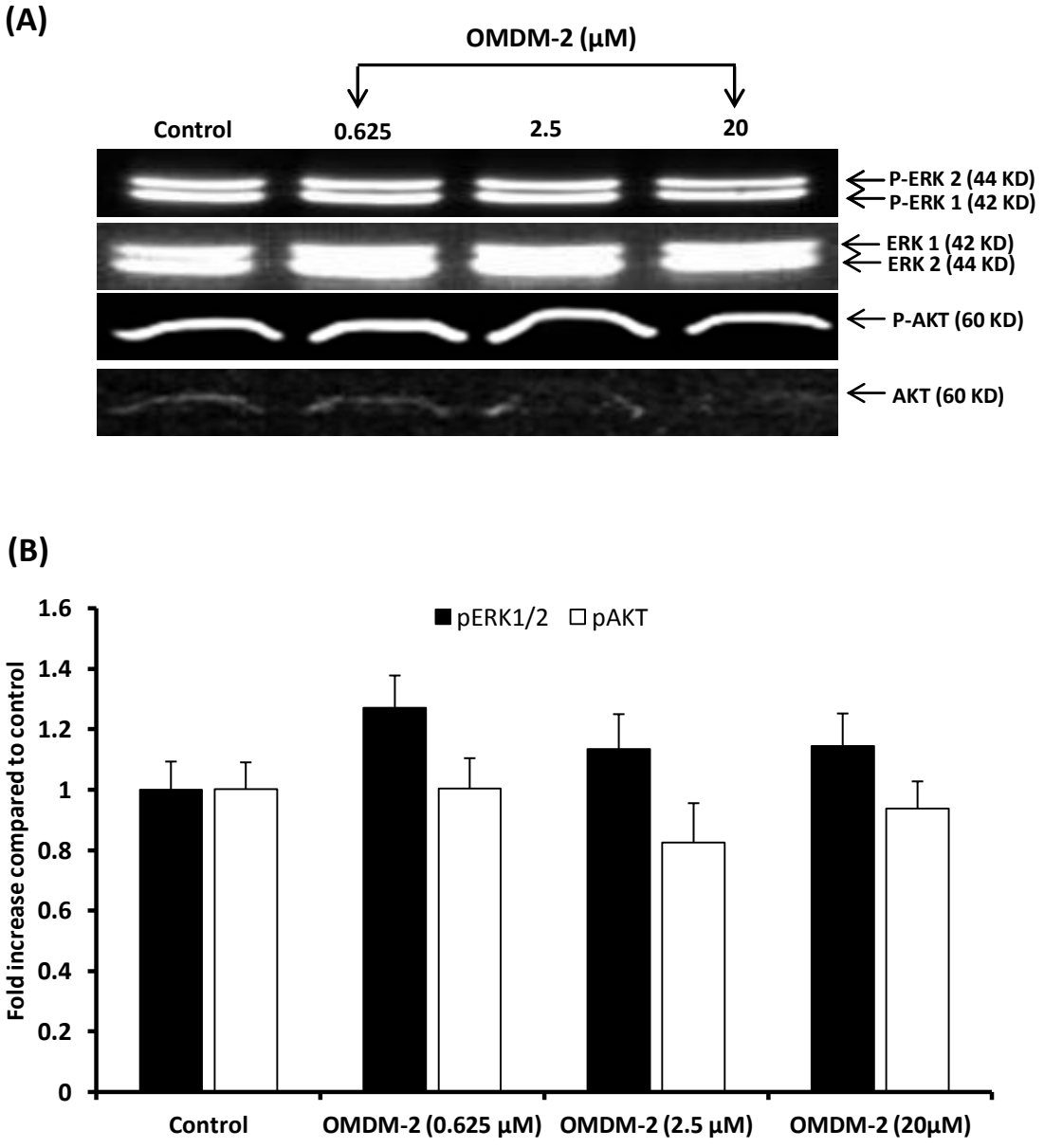

Figure (17): Effect of OMDM-2 on ERK1/2 and AKT phoshorylation in U-87 cells.

Control cells were cultured during the experiment in serum-free medium containing DMSO (0.5%). Western blot analysis was performed using antibodies recognising specific residues of pan, phosphorylated ERK1/2 and AKT. Pictures are representative of six independent experiments (A). Quantitative changes in ERK1/2 and AKT phosphorylation were determined by densitometric analysis of immunoblots. Data in values relative to total ERK1/2 or AKT level represent mean ± S.E of six independent experiments (B).

MCF-7 cells

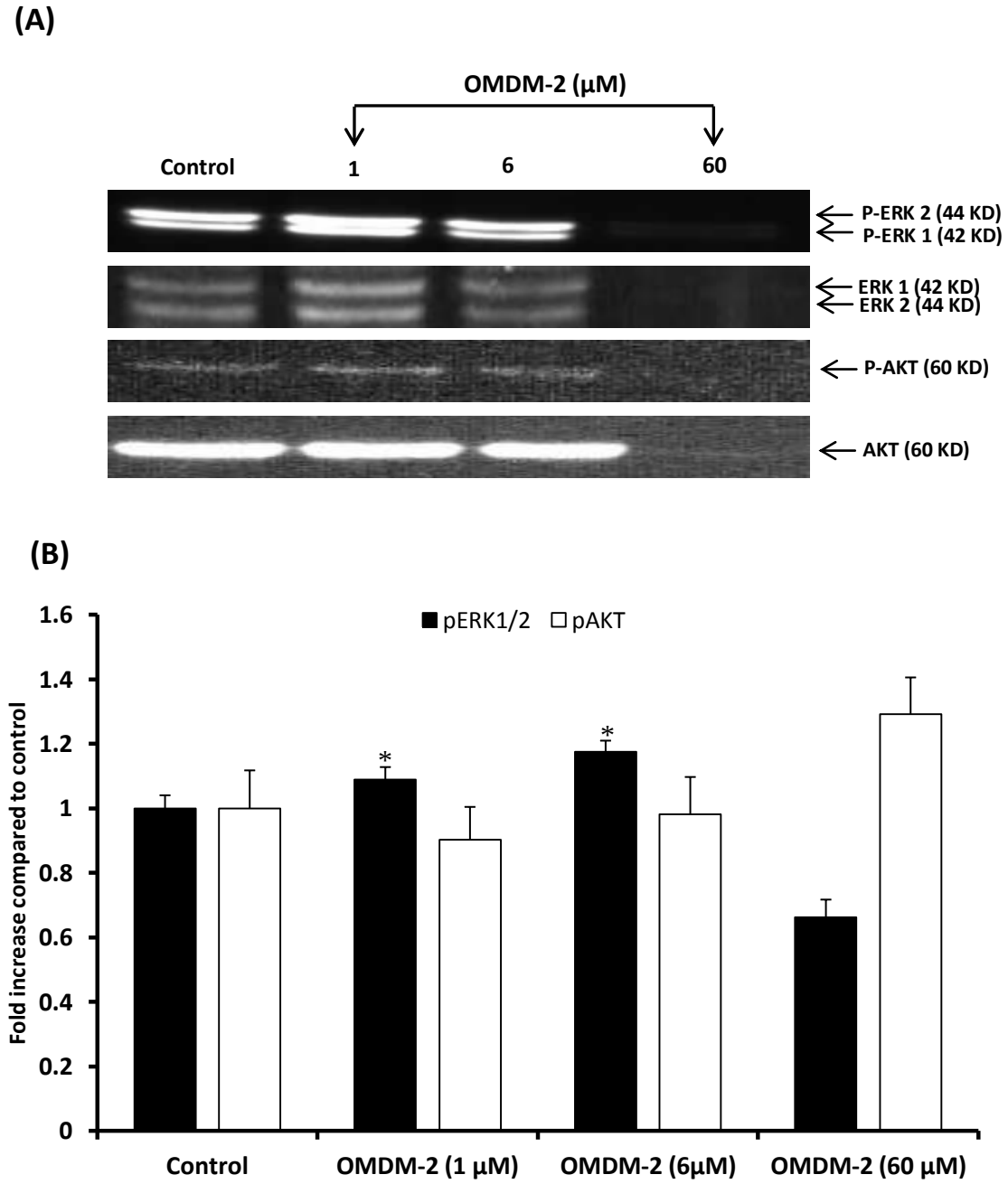

Figure (18): Effect of OMDM-2 on ERK1/2 and AKT phoshorylation in MCF-7 cells.

Control cells were cultured during the experiment in serum-free medium containing DMSO (0.5 %). Western blot analysis was performed using antibodies recognising specific residues of pan, phosphorylated ERK1/2 and AKT. Pictures are representative of six independent experiments (A). Quantitative changes in ERK1/2 and AKT phosphorylation were determined by densitometric analysis of immunoblots. Data in values relative to total ERK1/2 or AKT level represent mean ± S.E of six independent experiments (B). * Significantly different from control group at $p \leq 0.05$.

5.12 Optimization of OMDM-2 effect (combination therapy)

5.12.1 Sensitivity of MCF-7 cells to OMDM-2 in the presence of curcumin

The effects of 24 hrs co-exposure to different doses of curcumin on the sensitivity of the MCF-7 cells to OMDM-2 are shown in ***Table 6.*** Both IC_{50} and IC_{70} values were chosen in order to analyze the combination effect. In order to measure the increase in the sensitivity, a sensitization factor was determined by dividing both the IC_{50} and IC_{70} values for OMDM-2 alone by those in the presence of curcumin. Curcumin enhanced the growth inhibitory activity of OMDM-2 in a dose-dependent manner.

The type of interaction between OMDM-2 and curcumin was evaluated by performing a series of isobologram transformations of multiple dose-response analyses. Representative isobolograms are presented in ***Figures 19, 20***. These results indicate a strong synergistic interaction between OMDM-2 and curcumin for both IC_{70} and IC_{50}. Using the mutually non-exclusive assumption of the CI method of Chou and Talalay, the CI values ranged from 0.02 to $2E^{-5}$ for 50-95% cell death levels ***(Figure 21)***. These data were consistent with the results of the isobologram analysis.

5.12.2 Sensitivity of U-87 cells to OMDM-2 in the presence of curcumin

The effects of a 24 hrs co-exposure to different doses of curcumin on the sensitivity of the U-87 cells to OMDM-2 are shown in ***Table 7.*** Both IC_{50} and IC_{77} values were chosen in order to analyze the combination effect.

As shown in ***Figures 22, 23***, the type of interaction between OMDM-2 and curcumin against glioma cells differ at different dose ratios. These results indicate synergistic or additive interaction between certain ratios of OMDM-2 and curcumin while antagonistic interaction with others for both IC_{77} and IC_{50}. In addition, the combination was analyzed by the CI method as shown in ***Figure 24***.

The percentage of cells killed by drugs used in combination (fraction affected) and the dose reduction index (DRIs), which represent the order of magnitude (fold) of dose reduction obtained in combination setting compared with each drug alone, are shown in ***Table 8***.

Table (6): Effect of curcumin on the sensitivity of MCF-7 cells to OMDM-2

OMDM-2 : Curcumin	IC_{50}	Sensitization factor	IC_{70}	Sensitization factor
OMDM-2 alone	4.9	____	38	____
1:1	3.8	1.3	5.5	6.9
1:2	3	1.6	4.2	9
1:4	2.9	1.7	3.9	9.74
1:8	1.8	2.7	2.9	13.1

MCF-7 cells were incubated with serial dilutions of OMDM-2 in the absence or presence of curcumin for 24 hrs. IC_{50} and IC_{70} were calculated from the dose response curve. Results represent three independent experiments.

Table (7): Effect of curcumin on the sensitivity of U-87 cells to OMDM-2

OMDM-2 : Curcumin	IC_{50}	Sensitization factor	IC_{77}	Sensitization factor
OMDM-2 alone	2.7	____	6.4	____
1:1	3.2	0.8	5.2	1.2
1:2	3.8	0.7	4.2	1.5
1:8	1.9	1.4	3.5	1.8
1:16	1	2.7	2.5	2.6
1:32	0.3	9	1.1	5.8

U-87 cells were incubated with serial dilutions of OMDM-2 in the absence or presence of curcumin for 24 hrs. IC_{50} and IC_{77} were calculated from the dose response curve. Results represent three independent experiments.

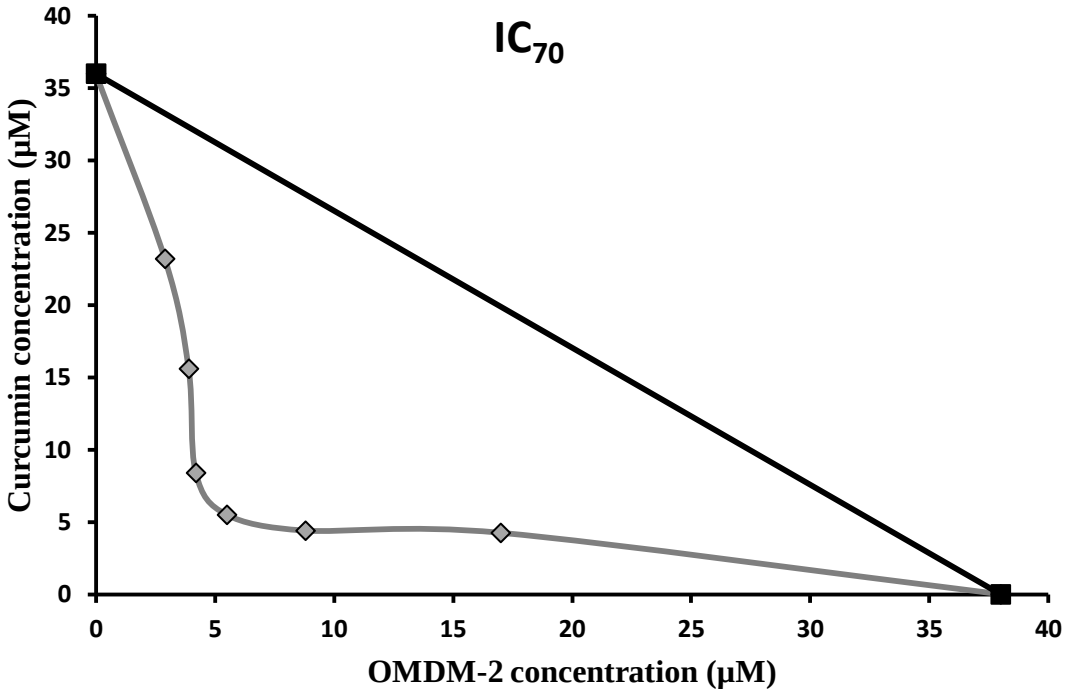

OMDM-2 : Curcumin	IC_{70} (µM)	OMDM-2 (µM)	Curcumin (µM)
1 : 8	26.1	2.9	23.2
1 : 4	19.5	3.9	15.6
1 : 2	12.6	4.2	8.4
1 : 1	11.0	5.5	5.5
2 : 1	13.2	8.8	4.4
4 : 1	21.3	17	4.25

Figure 19: Isobol curve for the 70% inhibition of OMDM-2 / Curcumin combination against MCF-7 proliferation; IC_{70} (µM) for various dose combinations. Results represent three independent experiments.

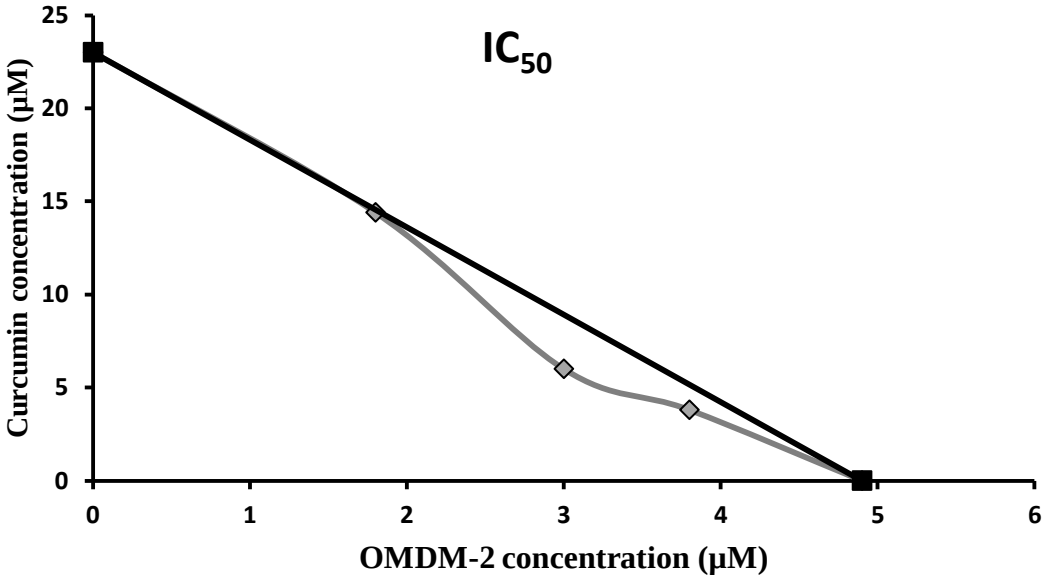

OMDM-2:Curcumin	IC_{50} (µM)	OMDM-2 (µM)	Curcumin (µM)
1 : 8	16.2	1.8	14.4
1 : 2	9	3	6
1 : 1	7.6	3.8	3.8

Figure 20: Isobol curve for the 50% inhibition of OMDM-2 / Curcumin combination against MCF-7 proliferation; IC_{50} (µM) for various dose combinations. Results represent three independent experiments.

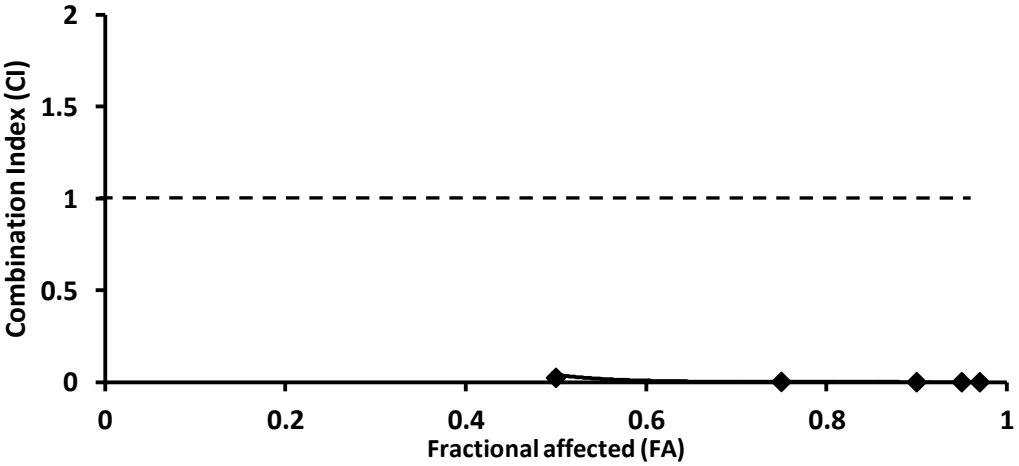

ED	ED50	ED75	ED90	ED95	ED97
CI	0.02371	0.00153	1.17E-4	2.09E-5	6.15E-6

Figure 21: Combinatory effect of OMDM-2 and curcumin in MCF-7 cells. CI/FA curve showed the CI *vs* the fraction of cells affected by OMDM-2 and curcumin in combination after 24 hrs of treatment. Combination analysis was done using the method described by Chou and Talalay (see materials and methods). Results represent three independent experiments.

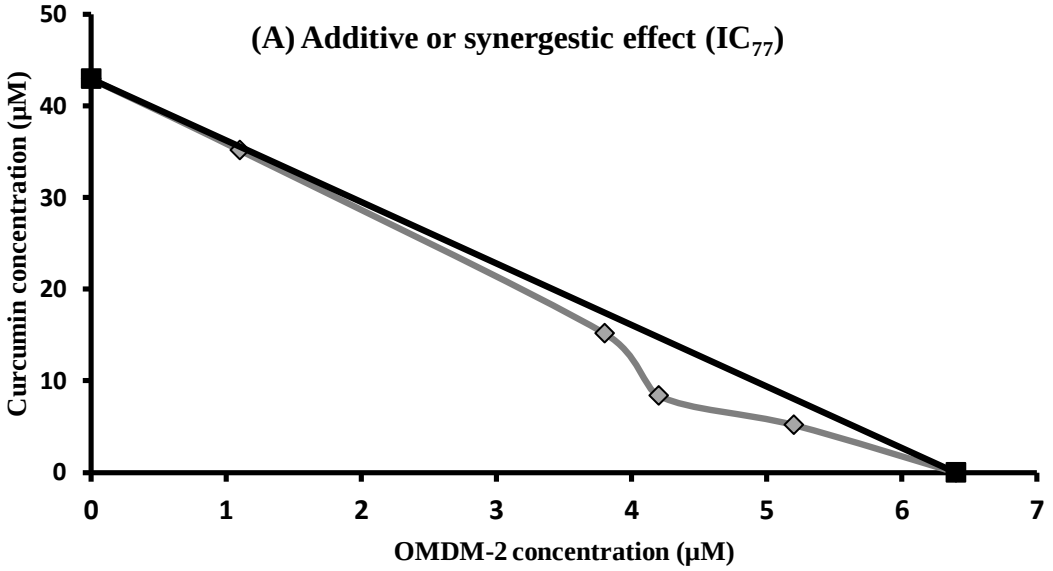

OMDM-2 : Curcumin	IC_{77} (µM)	OMDM-2 (µM)	Curcumin (µM)
1 : 32	36.3	1.1	35.2
1 : 4	19	3.8	15.2
1 : 2	12.6	4.2	8.4
1 : 1	10.4	5.2	5.2

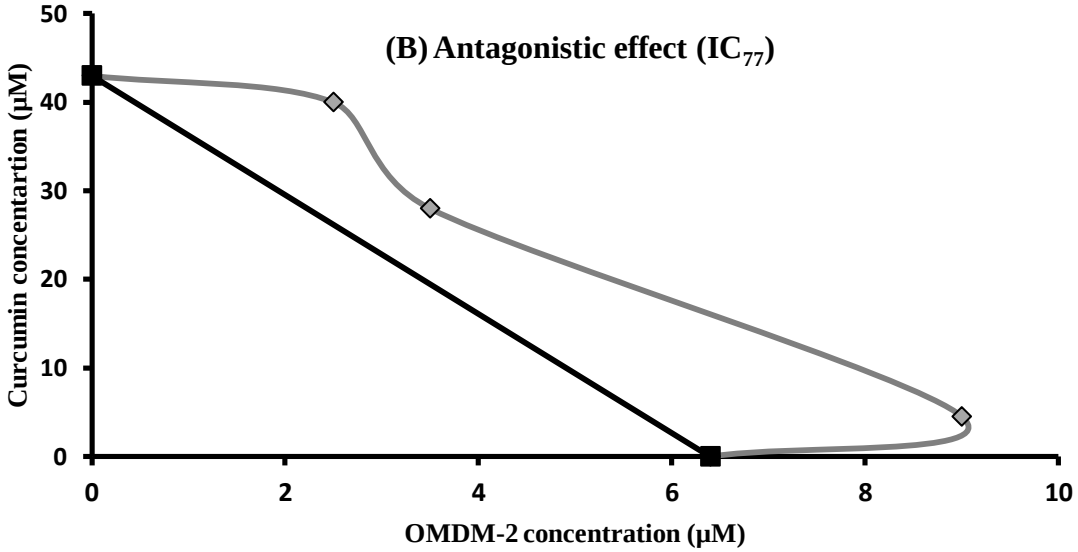

OMDM-2 : Curcumin	IC_{77} (µM)	OMDM-2 (µM)	Curcumin (µM)
1 : 16	42.5	2.5	40
1 : 8	31.5	3.5	28
2 : 1	13.5	9	4.5

Figure 22: Isobol curve for the 77% inhibition of OMDM-2 / Curcumin combination against U-87 proliferation. (A) IC_{77} (µM) for the dose combinations showed synergy or additive effect. (B) IC_{77} (µM) for the dose combinations showed antagonistic effect. Results represent three independent experiments.

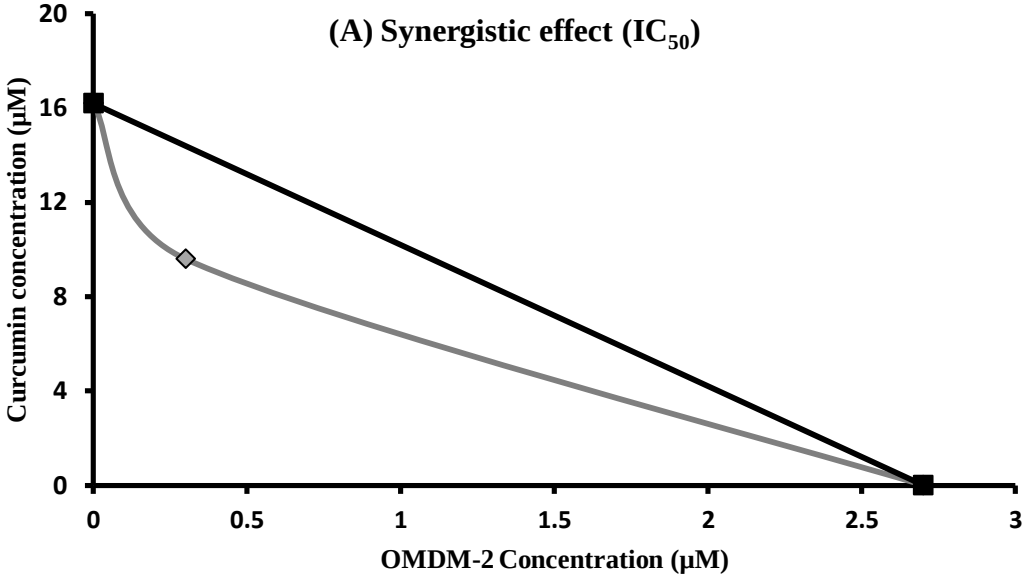

OMDM-2 : Curcumin	IC_{50} (µM)	OMDM-2 (µM)	Curcumin (µM)
1 : 32	9.9	0.3	9.6

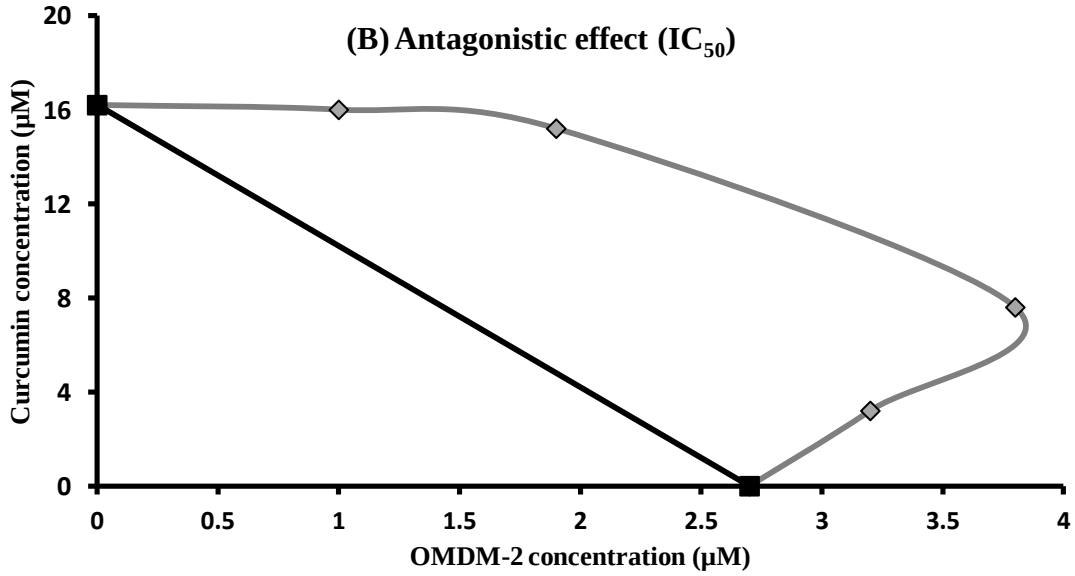

OMDM-2 : Curcumin	IC_{50} (µM)	OMDM-2 (µM)	Curcumin (µM)
1 : 16	17	1	16
1 : 8	17.1	1.9	15.2
1 : 2	11.4	3.8	7.6
1 : 1	6.4	3.2	3.2

Figure 23: Isobol curve for the 50% inhibition of OMDM-2 / Curcumin combination against U-87 proliferation. (A) IC_{50} (µM) for the dose combination (1:32) showed synergistic effect. (B) IC_{50} (µM) for the dose combinations showed antagonistic effect. Results represent three independent experiments.

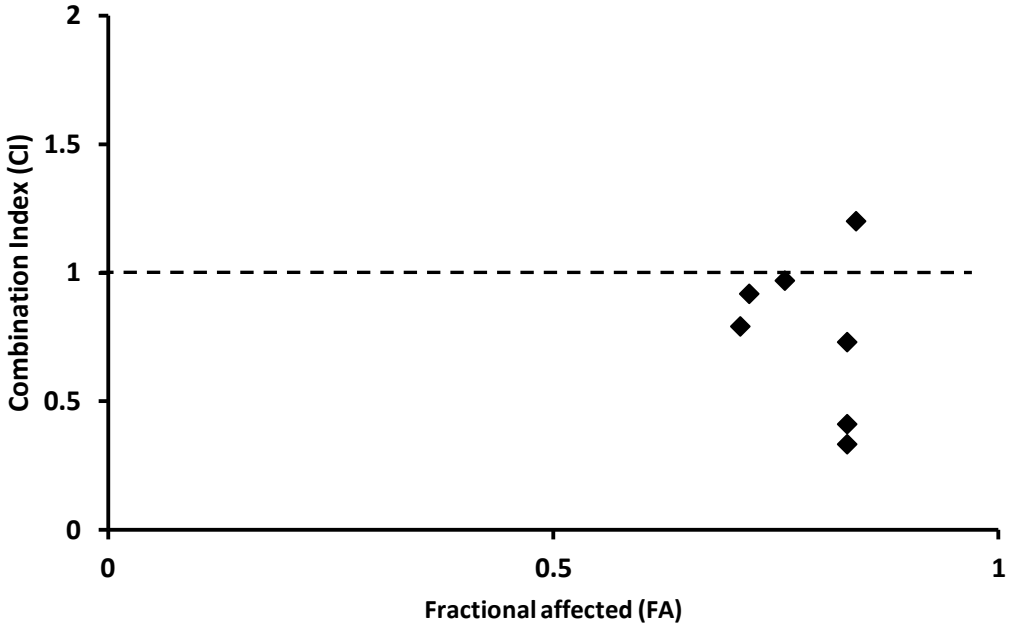

Figure 24: Combinatory effect of OMDM-2 and curcumin in U-87 glioma cells. CI/FA curve showed the CI *vs* the fraction of cells affected by OMDM-2 and curcumin in combination after 24 hrs of treatment. Combination analysis was done using the method described by Chou and Talalay (see materials and methods). Results represent three independent experiments.

Table (8): Fraction affected (FA) and dose reduction index (DRI) for OMDM-2 and curcumin combination against U-87 cells

FA	Dose (µM) OMDM-2	Dose (µM) Curcumin	DRI OMDM-2	DRI Curcumin
0.76	15.9323	43.0063	25.4917	1.07516
0.72	11.6286	37.0266	9.30289	1.23422
0.71	10.7968	35.7429	4.31872	1.78714
0.83	30.6637	58.7115	6.13275	5.87115
0.84	34.2221	61.8577	0.85555	12.3715

5.12.3 Sensitivity of U-87 cells to temozolomide in the presence of OMDM-2

The effects of 24 hrs co-exposure to different doses of OMDM-2 on the sensitivity of the U-87 cells to temozolomide are shown in ***Table 9*****.** The sensitization factor at IC_{50} level was chosen in order to analyze the combination effect. OMDM-2 enhanced the growth inhibitory activity of temozolomide in a dose-dependent manner.

Assessment of the drug interaction was performed calculating CI. CI/fractional effect curves represent the CI vs. the fraction of cells affected/ killed by OMDM-2 and temozolomide in combination ***(Figure 25)***. This result indicates that 24 hrs exposure of glioma cells to OMDM-2 and temozolomide combination produced very strong synergism at high level of cell death (CI= 0.13 at the IC_{95}).

The percentage of cells affected by the drugs used in combination (fraction affected) and the fold of dose reduction obtained in combination setting compared with each drug alone are shown in ***Table 10***.

5.12.4 Sensitivity of the MCF-7 cells to Paclitaxel in the presence of OMDM-2

The CI was calculated for paclitaxel and OMDM-2 combination as shown in ***Figure 26***. These results indicate strong synergistic activity at high levels of cell death. Also DRI was calculated for both drugs **(*Table 11)***.

Table (9): Effect of OMDM-2 on the sensitivity of U-87 cells to temozolomide

OMDM-2 : temozolomide	IC_{50}	Sensitization factor
Temozolomide alone	709	____
1:320	321	2.2
1:160	306	2.3
1:80	283.5	2.5
1:40	155.8	4.5
1:20	84	8.4
1:10	45.1	15.7
1:5	36	19.6
1:2.5	38.9	18.2

U-87 cells were incubated with serial dilutions of temozolomide in the absence or presence of OMDM-2 for 24 hrs. IC_{50} was calculated from the dose response curve. Results represent three independent experiments.

Table (10): Fraction affected (FA) and dose reduction index (DRI) for OMDM-2 and temozolomide combination

FA	Dose (µM) Temozolomide	Dose (µM) OMDM-2	DRI Temozolomide	DRI OMDM-2
0.5	709.366	2.78763	2.50311	0.78915
0.55	864.357	3.77598	2.79524	0.97689
0.6	1060.55	5.14674	3.12855	1.21460
0.65	1312.74	7.10887	3.51856	1.52433
0.7	1648.90	10.0395	3.98929	1.94314
0.75	2119.40	14.6815	4.58071	2.53851
0.8	2824.93	22.6835	5.36610	3.44708
0.85	4000.37	38.4119	6.49931	4.99257
0.9	6350.12	77.3219	8.38274	8.16576
0.95	13394.2	239.359	12.6442	18.0765
0.97	22779.6	534.843	16.9396	31.8179

Table (11): Fraction affected (FA) and dose reduction index (DRI) for OMDM-2 and paclitaxel combination

FA	Dose (µM) Paclitaxel	Dose (µM) OMDM-2	DRI Paclitaxel	DRI OMDM-2
0.17	0.013	0.55133	1.31867	0.22053
0.52	20	10.7039	23579.6	2.14078
0.6	250	19.1075	25043.8	1.91075
0.68	3140	35.5274	31406.9	1.77637
0.71	8780	45.7170	8781.62	1.14292

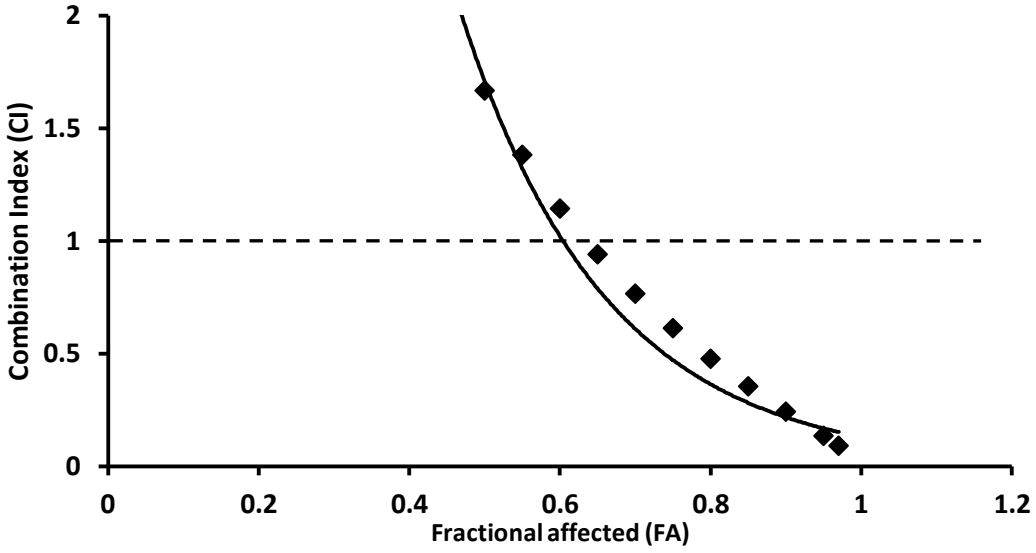

ED	ED95	ED90	ED75	ED50
CI	0.13	0.24	0.61	1.6

Figure 25: Combinatory effect of OMDM-2 and temozolomide in U-87 glioma cells. CI/FA curve showed the CI *vs* the fraction of cells affected by OMDM-2 and temozolomide in combination after 24 hrs of treatment. Combination analysis was done using the method described by Chou and Talalay (see materials and methods). Results represent three independent experiments.

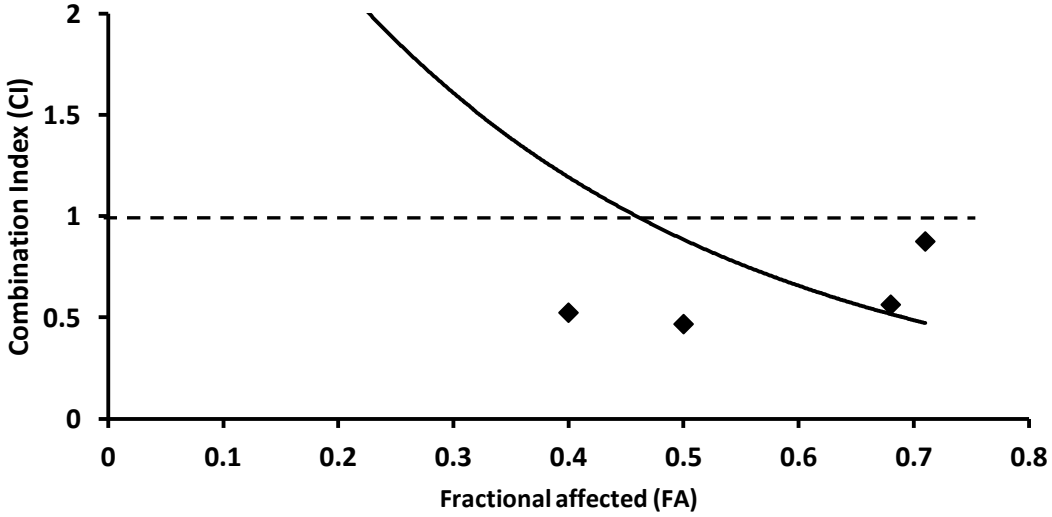

ED	ED50	ED60	ED68	ED71
CI	0.5	0.5	0.56	0.87

Figure 26: Combinatory effect of OMDM-2 and paclitaxel in MCF-7 cells. CI/FA curve showed the CI *vs* the fraction of cells affected by OMDM-2 and paclitaxel in combination after 24 hrs of treatment. Combination analysis was done using the method described by Chou and Talalay (see materials and methods). Results represent three independent experiments.

6. Discussion

Cannabinoid-based therapies are increasingly introduced into the palliative care of cancer ***(Pertwee, 2009)***. Δ^9-THC (dronabinol) and LY109514 (nabilone) are approved to be used as valuable adjunctive agents to treat nausea and vomiting, weight loss and lack of appetite associated with cancer chemotherapy ***(Pertwee, 2009)***.

But also cannabinoids themselves showed potential antitumor activity. They are reported to influence cancer cell growth and apoptosis ***(Guzmán et al., 2002)*** and suppress tumor neovascularization and metastasis ***(Blázquez et al., 2003)***. However, their clinical usage is severely restricted by their psychotropic nature. Thus novel approaches are required to benefit from the potential anticancer activity of cannaboinid based drugs. The rationale behind this study was provided by a simple consideration based on previous reports: if endocannabinoid concentrations are enhanced in some tumors ***(Schmid et al., 2002)*** and thereby exert a tonic inhibition of cancer cell proliferation ***(Ligresti et al., 2003)***, then substances that inhibit the reuptake of endocannaboids like OMDM-2 ***(Di Marzo et al., 2008)*** should be capable of inhibiting cancer growth. This assumption, if valid, would open the way to develop new cannabinoid related anti-cancer drugs that are potentially devoid of, or at least very low in, the psychotropic ***(Guzmán, 2003)*** or immunosuppressive ***(Bifulco et al 2004)*** side effects typical for direct agonists of cannabinoid receptors. Their site of action would be restricted to an ongoing metabolism of endocannbinoids i.e. at the site of cancer growth and thus more selective. Therefore, we investigated the *in-vivo* and *in-vitro* antitumor potential of OMDM-2. We further were interested in investigating the possible mechanism(s) of action involved in this activity.

We selected the solid Ehrlich tumor as an undifferentiated solid tumor derived from mouse breast adenocarcinoma which is an aggressive, virulent and rapidly growing tumor denoting high grade of malignancy ***(Nascimento et al., 2006; Silva et al., 2006; Sakai et al., 2010)***.

Utilizing this transplantable model of tumor has the advantage that there is a previous knowledge of the amount to be inoculated and the sites of injections to obtain different forms of cancer (liquid or solid) ***(Kabel et al., 2013)***. Also, rapid development of the tumor leads to a short study duration ***(Stewart, 1959)***. Ehrlich carcinoma resembles human tumors which are most sensitive to chemotherapy due to the fact that it is undifferentiated and has a rapid growth rate ***(Ozaslan et al., 2011; Kabel et al., 2013)***. It is commonly used as a tumor model to investigate the antitumor effects of new drugs ***(Silva et al., 2006; Sakai et al., 2010; Kabel et al., 2013)***.

Initial and basic criteria for judging the value of any new anticancer drug is the reduction of solid tumor volume, the prolongation of life span of tumor bearing animals, and the decrement of the elevated levels of WBC in their blood samples ***(Oberling and Guerin, 1954; Marklund et al., 1982)***.

Antitumor activity

The current study showed that the stable anandamide analog, R-Met (0.5 mg/kg, i.p.), an agonist for the CB-1 receptor (Ki 20 nM) and to a lower extent also an agonist for the TRPV1, administered every third day for 6 doses to EAC-bearing mice significantly reduced the tumor volume and impeded the tumor weight. These findings are in accordance with previous studies showing that anandamide was able to decrease the proliferation of breast cancer cells *in-vitro* by decreasing the levels of the long form of the prolactin receptor ***(De Petrocellis et al., 1998)*** and inhibited the nerve growth factor (NGF)-mediated proliferation by decreasing the expression of the Trk NGF receptor ***(Melck et al., 2000)***. Also, ***Eichele et al (2009)*** reported that R-Met, potently and selectively, inhibited the proliferation of human cervical carcinoma cells.

In the present study, the antitumor activity of R-Met was counteracted by a pre-treatment with the CB-1 blocker, NIDA 41020, thus suggesting that CB-1 receptors are uniquely involved in the *in-vivo* antitumor effect of this compound. This is augmented by ***Bifulco et al (2004)*** who reported that the CB-1 receptor antagonist SR141716A (0.2 μM) counteracted significantly the *in-vitro* effects of Met-F-AEA. In addition to other *in-vitro* ***(Khanolkar et al., 1996)*** and *in-vivo* reports ***(Burkey and Nation, 1997)*** which demonstrate that R-Met is more potent and selective for the CB-1 receptor than anandamide. Thus its anticancer mechanisms appear to be uniquely related to the CB-1 mediated pathways ***(Sarfaraz et al., 2008)***.

The endocannabinoid reuptake inhibitor, OMDM-2 is an inhibitor of the putative endocannabinoids membrane transporter and as such it inhibits their cellular reuptake ***(Ortar et al., 2003)***. This mode of action will potentiate the effect of extracellular AEA on the CB receptors ***(Ortar et al., 2003)***. Increasing the endocannabinoid tone by using OMDM-2 showed promising results in different models of diseases such as anorexia ***(Lewis and Brett, 2010)***, multiple sclerosis ***(Mestre et al., 2005)***, pain ***(De Lago et al., 2004)***, and sleep disorders ***(Murillo-Rodríguez et al., 2013)***.

Our study showed here for the first time that the systemic administration of OMDM-2 (5 mg/kg, i.p.) every third day for 6 doses was able to strongly and significantly reduce the tumor volume developed in the right flank of mice using s.c EAC cells. At the end of the experiment, the average size of the tumors treated with OMDM-2 was ~ 62% of those treated with the vehicle. The antitumor activity of OMDM-2 was further confirmed in our study by its ability to regress tumor weights developed in mice at all time points as efficaciously as the reference standard carboplatin. Especially at the early stage of the tumor development OMDM-2 reduced tumor weight by ~ 88%. These data indicate that endocannabinoids act as endogenous tumor suppressors and their administration would be more valuable at the first

stages of cancer development as reported by ***Pisanti and Bifulco (2009)***. Our results also support the finding that endocannabinoids can tonically control tumor cell proliferation *in-vivo* as shown by ***Bifulco et al (2004)*** who decreased the thyroid tumor volume in athymic mice by intratumoral administration of endocannabinoid degradation inhibitors. Our data indicate for the first time that the antitumor activity of the endocannabinoid reuptake inhibitors can be achieved by a systemic administration and is not limited to their local administration at the site of tumor growth ***(Bifulco et al., 2004)***. An approach which makes the shift to the clinical trials easier by avoiding the intratumoral administration as already done by ***Guzmán et al (2006)*** who administered the Δ^9-THC intrcranially to nine patients with recurrent glioblastoma multiforme.

We showed here also that the *in-vivo* antitumor effect of OMDM-2 in EAC bearing mice was not mediated by the CB-1 receptor. These data are in contrast to that obtained by ***Bifulco et al (2004)*** who reported that the antitumor activity of the transporter inhibitor VDM-11 which has a pharmacodynamic profile similar to OMDM-2, was mediated by the CB-1 receptor. This discrepancy suggests that other mechanisms might be also involved, possibly related to the pharmacokinetics and to the higher metabolic stability of OMDM-2 *in-vitro* ***(Ortar et al., 2003)*** and *in-vivo* ***(De Lago et al., 2004)*** as compared to VDM-11. Also, the discrepancy may be related to the difference in the type of cancer used in ***Bifulco et al (2004)*** study (thyroid cancer). It is well known that the receptors involved in mediating the antitumoral action of endocannabinoids differ according to the type of cancer ***(Pisanti and Bifulco, 2009)***.

Increased life span is a parameter that reflects the efficacy of anti-neoplastic agents. The systemic administration of OMDM-2 or R-Met was able to extend the life span of tumor bearing mice. In our study the effect of OMDM-2 on increasing the life span was, like the antitumor activity, not affected by blocking the CB-1 receptor. These results clearly

augmented the antitumor effect of OMDM-2 on EAC tumor cells and further support that its effect was not mediated by the CB-1 receptor.

In-vitro anti-proliferative activity

We next investigated the mechanism(s) of action of OMDM-2 by studying its anti-proliferative effect *in-vitro* on the human breast (MCF-7) and brain (U-87) cancer cell lines. OMDM-2 dose dependently inhibited the proliferation of both cell lines. The concentrations of OMDM-2 producing effects on cell proliferation in our study are in the range generally used for uptake inhibition experiments. The IC_{50} for OMDM-2 (for uptake inhibition) ranged from 3-17 µM depending upon cell type and experimental design ***(Ortar et al., 2003; De Lago et al., 2006)***. These findings augment a previous *in-vitro* study which showed that OMDM-2 produces a rapid loss of rat C6 glioma cell viability if used over the same concentration range required for the inhibition of the AEA uptake *in-vitro* ***(De Lago et al., 2006)***. Our results showed a significant decrease in U-87 glioma cells proliferation at the lowest concentrations of OMDM2 (lower than used for reuptake inhibition) similar to the results obtained by ***De Lago et al (2006)***.

Interestingly, our *in-vivo* results were supported by *in-vitro* data which showed that the anti-proliferative effect of OMDM-2 was not mediated by the CB-1 receptor expressed on MCF-7 human breast cancer ***(Di Marzo et al, 2001)***. This indicates that the CB-1 receptors are not likely to be involved in mediating the anticancer activity of OMDM-2 against both human and murine breast cancer.

The finding of inhibitory effects on cancer cell proliferation by the combination of OMDM-2 with the CB-1 receptor antagonist suggests that endocannabinoids might exert their tonic anti-proliferative effects also through non-CB-1 receptor-mediated mechanisms, particularly when CB-1 receptors are blocked. These mechanisms are not likely to involve the CB-2

receptors, because these receptors were previously shown not to be involved in the endocannabinoid anti-proliferative effects against colorectal ***(Ligresti et al., 2003)*** and thyroid ***(Bifulco et al., 2004)*** cancers.

Looking at the TRBV1, there is contradictory evidence on the involvement of TRBV1 in the action of reuptake inhibitors. Some studies showed that the reduction of intracellular AEA by reuptake inhibitors will reduce the effectiveness of accumulated AEA at the TRPV1 given that the binding site for AEA on these receptors is intracellular ***(De Petrocellis et al., 2001)***. However, other studies showed that the reuptake inhibitors may act by blocking the transport-mediated release of intracellular AEA from TRPV1-expressing cells ***(Cabranes et al., 2005)***, thereby potentiating AEA action at intracellular binding site on TRPV1 receptors.

We investigated the involvement of TRPV1 in OMDM-2 activity by using the TRPV1 blocker, capsazepine. Our results indicated that the TRPV1 receptors ,expressed on MCF-7 breast cancer cells ***(Barbero et al, 2006),*** are not responsible for mediating the anti-proliferative effect of OMDM-2.

Taken our *in-vitro* and *in-vivo* data together the findings indicate that the antitumor activity of OMDM-2 against breast cancer is independent on both cannabinoid (CB-1) and vanilloid (TRPV1) receptors. Several other membrane proteins and ion channels are being proposed as molecular targets for endocannabinoid under both physiological and pathological conditions ***(Di Marzo et al., 2002)***. The exact mechanism underlying the anti-cancer effect of OMDM-2 will clearly require further investigations.

Our results in glioma cells showed that the CB-1 and TPRV1 receptors ***(Contassot et al., 2004)*** mediated, at least in part, the anti-proliferative activity of low concentrations of OMDM-2 ($\leq$ 5μM) while these were not the case with higher concentrations ($\geq$ 10 μM). These results are in line with ***De Lago et al (2006)*** who showed that both receptors were not

involved in mediating the death of rat glioma cells using 10 µM of OMDM-2. These findings indicate that the low concentrations of OMDM-2 may mediate their activity through the effect of accumulated endocannabinoids on CB-1 and TRPV1 receptors. The CB-1 and TRPV1 independent effects of high concentrations of OMDM-2 could be attributed to a direct effect. Although described as an anandamide analogue and active as an anandamide reuptake inhibitor, OMDM-2 is structurally more similar to oleylethanolamide ***(Lewis and Brett, 2010)*** which acts as an agonist at the nuclear PPAR-α receptor ***(Fu et al., 2003)***. The activation of PPARα receptors could be useful for the prevention or the treatment of different cancers ***(Peters et al., 2012)***. Different PPARα agonists inhibited the growth of tumors that were derived from melanoma, Lewis lung carcinoma, glioblastoma and fibrosarcoma cell lines ***(Peters et al., 2012).*** There is little published information as yet on the pharmacological actions of OMDM-2 considering this aspect.

Hematological parameters

Pal et al (1993) reported that the growth of EAC in Swiss mice was accompanied by a decrease in the hemoglobin and the RBC values. Similar results were observed in the present study in the animals of the EAC tumor control group. The decrease in hemoglobin is a consequence of the reduction of RBC or a reduction in the hemoglobin production or both. This may occur either due to iron deficiency or to hemolytic or other myelopathic conditions ***(Hoagland, 1982)***.

The systemic administration of OMDM-2 was able to significantly increase the erythrocyte count and the hemoglobin level when compared to those of EAC control mice. These effects can be owed to the ability of accumulated AEA to promote the growth of hematopoietic cell as shown by ***Valk et al (1997)***. In addition, OMDM-2 was able to reduce the elevated level of WBC in EAC mice near to the normal level. These indicating parameters revealed that the systemic administration of OMDM-2 could restore the hematological profile of tumor

bearing mice nearly to the normal levels. An effect which may be particularly attractive if endocannabinoids-enhancing strategies were to be included in poly-chemotherapeutic protocols.

Role of TGF-β1/CD-105 system

TGF-β_1 behaves as a tumor suppressor at early stages of tumor development but promotes tumor progression at later stages ***(Pérez-Gómez et al., 2010)*** by promoting tumor cell migration, invasion and metastasis in a cell-autonomous manner, and by influencing the tumor microenvironment facilitating angiogenesis and evasion of the immune system ***(Derynck et al., 2001; Massagué, 2008)***. Most studies about the involvement of endoglin (TGF-β_1 receptor) in cancer have focused on its role as a pro-angiogenic molecule and its usefulness as a marker of microvessel density (MVD) in tumors. However, there is evidence that endoglin modulates cell proliferation, adhesion and migration of neoplastic cells suggesting a direct involvement of endoglin in cancer either by modulating the response of tumor cells to TGF-β or by as yet not completely understood TGF-β independent mechanisms ***(Pérez-Gómez et al., 2010)***.

To our knowledge, the time course expression of TGF-β_1 has not been previously evaluated in the EAC model, the untreated EAC-group showed higher serum concentrations of TGF-β_1 compared to the normal group on days 7, 14, and 21. We hypothesize that the high levels of TGF-β_1 may represent a compensatory response in order to suppress the initiation or expansion of a tumor but these higher concentrations, especially at an early stage of tumor development, were not able to suppress neither the tumor growth nor the angiogenesis. Our finding of a high intra-tumoral expression of CD-105 receptors in the EAC group on day 7 (early stage) support this hypothesis since high concentrations of CD-105 modulate the TGF-β_1 signaling and eventually lead to the loss of the growth inhibitory action of TGF-β_1

(Warrington et al., 2005). This could insulate tumor and endothelial cells from the negative control effects of TGF-β_1 and thus contribute to tumor growth and angiogenesis ***(Duff et al., 2003)***.

High levels of TGF-β_1 mediate autocrine production of other growth promoting factors suggesting an indirect mitogenic effect of TGF-β on the cell proliferation ***(Kay et al., 1998)***. The high serum concentrations of TGF-β_1 and the low expression of CD-105 combined with the high angiogenesis (%) and tumor weights as seen in our study in the EAC-group at days 14 and 21 support such a role for TGF-β_1. It further supports that the tumor growth during these late stages may be indirectly dependent on TGF-β_1/CD-105 as described by ***Nimeh et al (2001)*** who proposed that TGF-β_1 may be an indirect but necessary player in tumor angiogenesis and growth *in-vivo*.

In our study, the systemic administration of either OMDM-2 or R-Met resulted in a significant increase in the TGF-β_1 concentrations at an early stage of tumor development (day 7) paralleled by the down regulation of the expression of CD-105. In such a scenario high levels of TGF-β_1 can execute their tumor suppressing activity and inhibit tumor growth as shown in our study. Furthermore, the tumor expression levels of endocannabinoids can modulate the value of endoglin-positive vascular density as a prognostic marker as shown recently in prostate cancer patients ***(Fowler et al., 2013)***.

Interestingly the reference standard carboplatin did not affect the levels of TGF-β_1 but showed a significant anti-endoglin activity as shown recently by ***Ziebarth et al (2013)***.

The ability of OMDM-2 to continue its tumor suppressing activity at days 14 and 21 may be ascribed to the ability of accumulated AEA to inhibit other growth factors essential for tumor growth such as EGF ***(Guindon and Hohmann, 2011)***. On the other hand, the loss of the antitumor potential of R-Met on day 14 may be explained as a pharmakodynamic tolerance

with desensitization and down regulation of CB-1 as also recently shown by ***Falenski et al (2010)***.

With respect to the EAC model, our data showed a tendency for a negative correlation between serum TGF-β_1 levels and tumor weights in this model at early stage of tumor development. The presence of such a correlation is supported by ***Yamaguchi et al (1997)*** who showed a significant negative correlation between TGF-β_1 concentrations and the tumor size ($r = -0.327$, $p < 0.03$) in hepatocellular carcinoma.

Angiostatic activity

Considering that angiogenesis is essential for tumor growth, we investigated whether the antitumor effect of OMDM-2 may be correlated to its anti-angiogenic activity. The Evans Blue dye extravasation technique was used to measure the permeability of albumin for the capillaries in the tumor tissue as a reliable measure of angiogenesis ***(St-Pierre et al., 2006)***. This technique is based on the principle that all forms of pathological angiogenesis including neovascularization induced by tumors are characterized by vascular hyperpermeability ***(Dvorak, 2002)***. Evans Blue dye avidly binds to intravascular albumin, and is thus a reliable way to assess transvascular fluxes of macromolecules ***(Roghani et al., 2011)***.

Our study showed that the systemic administration of OMDM-2 significantly reduced the tumor vascular permeability. This also suggests that increasing the endocannabinoid tone by inhibiting their catabolism could be used as a tool to inhibit angiogenesis. This hypothesis is further supported by ***De Filippis et al (2010)*** who showed that the local administration of AA-5-HT, a FAAH inhibitor, significantly and dose-dependently reduced the new vessel formation in chronic granulomatous inflammation in rats.

The significant anti-angiogenic activity of R-Met seen in our study indicates that its tumor reducing ability may be in part mediated by anti-angiogenesis in accordance with ***Pisanti et***

al (2007) who demonstrated the anti-angiogenic activity of AEA *in-vitro* and *in-vivo* thereby supporting its tumor suppressing action.

Our finding that the anti-angiogenic effect of R-Met was mediated by CB-1 corresponds to previous reports showing that the activation of CB-1 by anandamide inhibited angiogenesis and thereby retarded skin cancer and glioma growth *in-vivo* ***(Pisanti et al., 2007)***. In our study the anti-angiogenic activity of OMDM-2 was, like the antitumor activity, not mediated by CB-1. Importantly, the CB-1 antagonist (NIDA 41020) also exerted a significant, albeit small, anti-angiogenic action *per se.* This supports earlier report that pharmacological and genetic inactivations of CB-1 inhibit angiogenesis ***(Pisanti et al., 2011)***.

The anti-angiogenic activity of NIDA 41020 may be explained by the ability of CB-1 antagonism to inhibit the proliferation, migration and differentiation of endothelial cells in response to angiogenic growth factors like basic fibroblast growth factor (bFGF) ***(Pisanti et al., 2011)***. Further, it should be considered that the presently available CB-1 antagonists, including NIDA 41020, act not only as antagonists but also as inverse agonists ***(Pisanti et al., 2011)***. They block the basal constitutive activity of CB-1 and thereby the transduction pathways downstream the tyrosine-kinase receptors (RTK) coupled to the CB-1 receptor including the ERK-MAPK cascade ***(Bouaboula et al., 1997)***. It is well known that angiogenic factors like bFGF stimulate their respective tyrosine-kinase receptors thereby inducing ERK-MAPK and Akt signaling pathways ***(Cross et al., 2001)***. Therefore inverse agonism could be a mechanism by which NIDA 41020 could switch off ERK and Akt activated by angiogenic factors as a consequence of a negative interference with particular RTK pathways. Regarding the anti-angiogenic activity of carboplatin, we hypothesize that this effect was indirectly obtained by decreasing the tumor size which in turn decreases the required blood supply.

We next sought to determine the mechanism by which OMDM-2 prevents vascular permeability. We evaluated the level of VEGF, also known as vascular permeability factor, because it is the most potent angiogenic and micro vascular permeability factor identified so far ***(Sheng et al., 2004)***. Our data showed that the level of VEGF was significantly reduced in MCF-7 cells exposed to OMDM-2. This is supported by a study with the prostate cancer cells LNCaP in which the cannabinoid receptor ligand WIN55,212-2 decreased the expression level of VEGF by 47% ***(Sarfaraz et al., 2007)***. These findings indicate that increasing the endocannabinoid tone in the tumor cells would result in a decreased secretion of the VEGF and hence its consequent angiogenesis and metastasis.

Type of cell death

Cell death has been classified into two main types: programmed cell death (PCD) and passive (necrotic) cell death. PCD is morphologically classified into three main types ***(Sperandio et al., 2004)***, including apoptosis, autophagy and non-lysosomal vacuolated degeneration, the latter of which includes oncosis and paraptosis. Previous reports indicated that endogenous cannabinoids inhibit the cell proliferation without inducing apoptosis as shown with human colon cancer cells ***(Linsalata et al., 2010)*** and cholangiocarcinoma ***(Demorrow et al., 2008)***. Also, AEA was able to induce non-apoptotic cell death in human breast cancer and rat thyroid epithelial cancer cell lines via a modulation of expression and activity of key S phase regulatory proteins ***(De Petrocellis et al., 1998; Bifulco et al., 2001; Laezza et al., 2006)***. However, AEA has also been described as being an apoptosis inducer in many cell types like colorectal cancer, gastric cancer, osteosarcoma, glioma or prostate cancer cell lines ***(Contassot et al., 2004; Hsu et al., 2007; Miyato et al., 2009; Patsos et al., 2010)***.

In the present study OMDM-2 did neither induce a coordinated internucleosomal degradation of DNA nor could the typical DNA-laddering be detected. Furthermore, we found that the

OMDM-2 mediated cell death was caspase-3 independent as OMDM-2 failed to increase the activity of caspase-3 in human glioma cells at all time points. The non-involvement of caspase-3 was further supported by the ability of OMDM-2 to induce cell death in MCF-7 strain used in our study which lacks the caspase-3 gene ***(Jänicke et al., 1998; Dumont et al., 2007; Ubol et al., 2007)***. Other strains of MCF-7 cells showed an expression for the caspase-3 gene and their deaths were mediated by its activation ***(Yang et al., 2006)***.

Collectively, these results suggest that the classical necrosis and the caspase driven apoptosis were not the major contributors to the cell death mediated by endogenous cannabinoids in our study. Our results are in line with previous reports using different cell lines, neuroblastoma ***(Hamtiaux et al., 2011)*** and colorectal carcinoma ***(Patsos et al., 2005)***. Interestingly, an unusual form of cell death has also been reported by ***Mimeault et al (2003)*** in response to anandamide in prostate carcinoma cells but was simply described as apoptotic/necrotic cell death. In a more recent study, using also anandamide, caspase-3 activation was found to be unnecessary to mediate the non-apoptotic and non-necrotic cell death in colorectal carcinoma ***(Patsos et al., 2010)***.

Induction of cell death other than apoptosis could be particularly beneficial for those tumor cells that have become resistant to the induction of apoptosis, and currently there is growing interest in the field of non-apoptotic forms of cell death ***(Tsujimoto, 2012)***.

Moreover, the microscopic images of U-87 cells treated with OMDM-2 for 24 hrs demonstrated gross morphological changes in support of a paraptosis like cell death. Paraptosis is a new type of PCD on which there are only a few reports until now, characterized by rounding of the cells, cytoplasmic vacuolation derived from endoplasmic reticulum and/or mitochondria swelling; it is caspase independent and lacks both DNA

fragmentation and the apoptosis morphological changes ***(Sperandio et al., 2004; Zhang et al., 2009)***.

A recent study showed that increasing the cannabinoid tone decreased the lymphoma cell viability in a caspase-3 independent manner ***(Wasik et al., 2011)***. Moreover, the cells responded to cannabinoid treatment through the formation of cytoplasmic vacuoles. The authors hypothesize that the observed features resemble paraptosis-like cell death, not previously described in response to cannabinoids ***(Wasik et al., 2011)***.

Based on our data we hypothesize that the OMDM-2 mediated cell death in glioma cells may also be paraptosis. This interpretation is supported by our findings that OMDM-2 treatment for 24 hrs did not affect the phosphorylated levels of both ERK1/2 and AKT proteins. Our findings further agree with other reports showing that MAPK and AKT pathways are not involved in mediating parapoptosis ***(Asare et al., 2008; Sun et al., 2010)***. Here the OMDM-2-induced paraptosis was different from the insulin-like growth factor I receptor (IGFIR)-induced paraptosis which requires the participation of the MAPK/ERK and JNK signalings ***(Sperandio et al., 2004; Asare et al., 2008)***.

Our data and previous findings indeed demand further investigations to characterize the molecular mechanisms mediate this rather new process of paraptosis. In addition to confirm that the paraptosis may be one of the possible types of cell death induced by endogenous cannabinoids.

Interestingly, our study showed that the exposure of MCF-7 to OMDM-2 for 24 hrs resulted in a significant increase in the phosphorylation of ERK1/2 which was not paralleled by any effect on the AKT signaling. The accumulated AEA may be responsible for the activity of ERK1/2 and hence the anti-proliferative activity. This interpretation is based on previous reports showing that AEA leads to an anti-proliferative activity in MCF-7 by inhibiting adenylyl cyclase and thus activating the Raf-1/ERK/MAPK cascade, which, upon sustained

activation, ultimately down-regulates prolactin and nerve growth factor Trk receptors ***(De Petrocellis et al., 1998; Melck et al., 2000; Caffarel et al., 2012).*** Collectively, these data indicate that the mechanism of action of endogenous canabinoids differ according to the type of cancer. Further investigations are required to investigate the type of cell death induced by OMDM-2 in MCF-7 cells.

Drug combination

In cancer therapy, the employment of combinations of drugs rather than a single drug represents a therapeutic strategy with distinct advantages. On one hand, the contemporaneous activation of different biochemical pathways can achieve synergistic effects; on the other hand, the combination can result in a reduction of the dose of each single drug thereby reducing side effects ***(Calvaruso et al., 2012)***.

Recent studies have demonstrated the ability of endo/cannabinoids to synergize with other molecules to trigger death pathways in cancer cells. In particular, ***Calvaruso et al (2012)*** demonstrated that the synthetic cannabinoid WIN55,212-2 sensitizes hepatocellular carcinoma cells to apoptosis, mediated by tumor necrosis-related apoptosis inducing ligand (TRAIL). Also, in pancreatic cancer cells the combination of cannabinoids with gemcitabine, a pyrimidine analog largely employed in anticancer therapy, induces synergistic effects via the activation of autophagy ***(Donadelli et al., 2011)***. Another example of synergistic effects of cannabinoids with other drugs has been reported by ***Gustafsson et al (2009)*** who demonstrated that the synthetic cannabinoid HU210, anandamide and its other derivatives induce synergistic effects when employed in combination with the classic pyrimidine antagonist 5-fluorouracil (5-FU) in the colorectal carcinoma cells.

Our combination studies investigated two different aspects. First we combined OMDM-2 with a natural anticancer drug with the question whether we could reduce the dose of OMDM-2. Second we combined OMDM-2 with benchmark chemotherapeutics to investigate

whether we could increase the sensitivity of the cancer cells to these drugs as well as to decrease their dose related side effects by the addition of OMDM-2.

In our study, co-incubation of MCF-7 cells with curcumin and OMDM-2 showed that 14.4 µM and 23.2 µM of curcumin sensitized MCF-7 cells to OMDM-2 by approximately 3-fold at the IC_{50} level and 13-fold at IC_{70} level, respectively. The isobologram technique showed that the two agents given concurrently demonstrate strong synergistic activity. Synergism was also assessed using the CI method which takes into account the potency of each drug alone, the potency of drug combination, the shape of their dose-effect curves and it quantitates the synergism or antagonism at different concentrations and at different effect levels. Exposure of MCF-7 cells to different ratios of OMDM-2 plus curcumin resulted in a consistent synergistic effect (CIs were less than 1 over all the range of cytotoxicity examined).

In our study MCF-7 cells showed a high resistance to paclitaxel. The deficiency of caspase-3 gene in MCF-7 cell line used in our study contributes to its chemotherapeutic resistance as shown by ***(Yang et al., 2001; Ubol et al., 2007; Yang et al., 2007)***. Furthermore, it is well known that paclitaxel mediates its anticancer activity in a caspase-3 dependent manner ***(Mollinedo and Gajate, 2003; Impens et al., 2008; McGrogan et al., 2008; Rensen et al., 2009)***. On the other hand, the addition of OMDM-2 increased significantly the sensitivity of MCF-7 cells to paclitaxel and induced a potent synergistic effect.

Glioblastoma multiforme (GBM) exhibits a high resistance to standard chemotherapy and radiotherapy ***(Franceschi et al., 2009)***. Current strategies for the treatment of GBM are only palliative and large numbers of chemotherapeutic agents [e.g., alkylating agents such as temozolomide and nitrosureas such as carmustine] have also been tested, but they display limited efficacy ***(Nieder et al., 2006; Wong et al., 2007)***. It is therefore essential to develop new therapeutic strategies for the management of GBM. Nowadays, it is believed that the

development of new combinational therapies may contribute to enhance the survival of patients suffering from GBM ***(Torres et al.,2011)***.

Our combination studies showed indeed promising results, the co-incubation of U-87 glioma cells with curcumin and OMDM-2 showed that 9.6 µM and 35.2 µM of curcumin sensitized U-87 cells to OMDM-2 by approximately 9-fold at the IC_{50} level and 6-fold at IC_{77} level, respectively. Our results also indicated that the previous combination could be synergistic depending on the ratio and the concentrations of the drugs. Importantly, our study showed that OMDM-2 was able to sensitize the glioma cells to temozolomide and to potentiate its cytotoxic ability. Interaction assessment using the combination index method revealed that the drug interaction was synergistic. Also we found that OMDM-2 was able to significantly reduce the dose of temozolomide required to achieve the IC_{50} against U-87 cells. These findings support the hypothesis of ***Torres et al (2011)*** that temozolomide/cannabinoid could be of potential clinical interest for the management of glioblastoma.

Additionally, GW Pharmaceuticals has recently announced that it has commenced a Phase 1b/2a clinical trial for the treatment of recurrent GBM. In this study 20 patients will participate and its objective is to assess the tolerability, safety and pharmacodynamics of a mixture of two principal cannabinoids, THC and cannabidiol (CBD) in a 1:1 allocation ratio, in combination with temozolomide in patients with recurrent GBM. Secondary endpoints include additional pharmacokinetic and biomarker analyses and additional measurable outcomes of tumor response.

In conclusion, this study indicates that modulating the endogenous levels of cannabinoids could be a promising strategy to benefit from the potential anticancer activity of direct cannabinoids, in particular the combination therapies with natural or benchmark chemotherapeutics.

7. Summary and conclusion

Summary

Direct cannabinoid agonists suppress the growth of cancer cells in several preclinical studies. However, their clinical application is hampered by the receptor mediated side effects. In order to avoid these side effects; we chose an indirect approach by using OMDM-2, a selective inhibitor of the cellular re-uptake of endocannabinoids. We investigated the antitumor activity and the possible mechanism(s) of action of OMDM-2 by using both *in-vivo* (Murine model of breast cancer) and *in-vitro* (Human glioma and breast cancer) studies. Furthermore, we evaluated the possibility of combining the endocannabinoid based drug, OMDM-2, with natural or benchmark chemotherapeutic agents. This would enhance its potential applicability in cancer therapy.

The main findings of the present work were as follows:

1- Anti-tumor potential of OMDM-2

- The systemic administration of OMDM-2 to EAC-bearing mice resulted in a significant antitumor activity comparable to the direct cannabinoid agonist, R-Met.
- OMDM-2 was able to increase the life span of the tumor bearing mice as compared to the tumor control group.
- The anti-proliferative activity of OMDM-2 was not specific to certain species or type of cancer as it inhibited the growth of both human and murine breast cancers and of human U-87 glioma cells.
- The systemic administration of OMDM-2 was able to restore the hematological profile of EAC bearing mice nearly to the normal levels.

2- Mechanisms of action

- **Involvement of CB-1 receptor**

  Breast cancer: Both *in-vivo* and *in-vitro* studies indicated that the effect of OMDM-2 was not mediated by the CB-1 receptor.

  Glioma: Our *in-vitro* studies indicated that the effects of low concentrations of OMDM-2 were mediated, at least in part, by the CB-1 receptor while these were not the case with high concentrations.

- **Involvement of TRPV1 receptor**

  Breast cancer: Both *in-vivo* and *in-vitro* studies indicated that the effect of OMDM-2 was not mediated by the TRPV1 receptor.

  Glioma: Our *in-vitro* studies indicated that the effects of low concentrations of OMDM-2 were mediated, at least in part, by the TRPV1 receptor while these were not the case with high concentrations.

- **Anti-angiogenic activity**

  OMDM-2 showed a significant anti-angiogenic activity using the Evans Blue method and this effect was, at least in part, mediated by decreasing the level of VEGF.

- **TGF-β_1/CD-105 system**

  This system appears to be involved in mediating the antitumor potential of OMDM-2 especially at early stages of tumor development by increasing the level of TGF-β_1 paralleled with down-regulating the expression of CD-105.

- **Caspase-3 involvement**

  Cell death mediated by OMDM-2 seems to be caspase-3 independent.

- **Morphology of cells**

  U-87 cells treated with different concentrations of OMDM-2 displayed marked morphological changes. The adherent cells appear round in shape, with extensive cytoplasmic vacuolation.

- **Type of cell death**

  Based on four different experimental set ups, it seems that the classical necrosis and caspase-3 dependent apoptosis are not the major contributors to the OMDM-2 mediated cell death. We suggest that paraptosis may be involved in glioma cell death.

- **Activity of ERK1/2 and AKT signalings**

  OMDM-2 showed an increase in the activity of ERK1/2 signaling in MCF-7 cells but did not have any effect on p-ERK1/2 in U-87 cells. The activity of AKT signaling was not affected by OMDM-2 in both cell lines.

3- Optimization of OMDM-2 treatment (combination studies)

The isobole, DRI and combination index methods were used to demonstrate whether there are synergistic, additive or antagonistic effects between OMDM-2 and curumin in both MCF-7 and U-87 glioma cells. The same analyses were used to evaluate the combination between OMDM-2 and Paclitaxel in MCF-7 cells as well as between OMDM-2 and temozolomide in U-87 glioma cells. The addition of curcumin to MCF-7 or glioma cells increased their sensitivity to OMDM-2 and induced potent synergistic effects. Also, our combination studies indicated that the addition of OMDM-2 to the chemotherapeutic resistant breast and glioma cancer cells not only increased their sensitivity but also decreased the required dose of benchmark chemotherapeutics.

Conclusion

This is the first report that the systemic administration of endocannabinoid reuptake inhibitor, OMDM-2, can impede the tumor growth and angiogenesis *in-vivo* indicating that the antitumor activity of this class of drugs is not limited to their local administration at the site of tumor growth. This makes the shift to clinical trials easier by the administration of the drugs systemically rather than intratumorally. Regardless the mechanism of the anticancer activity of endocannabinoids, our data suggest that a new and possibly safer strategy to block the tumor growth and angiogenesis could arise from substances that selectively delay endocannabinoid degradation. These compounds should be more specific than direct cannabinoid agonists since they primarily affect endocannabinoid levels and hence the state of activation of cannabinoid receptors not in all tissues expressing functionally active cannabinoid receptors but only in those where these compounds are produced on demand. So, by this strategy the psychotropic and immunosuppressive side effects which limit the use of cannabinoid based drugs could be reduced.

Combination therapies utilizing both - molecules targeting the endocannabinoid system and natural anticancer agents or benchmark chemotherapeutic agents- are a worthwhile option to be further systematically explored in the treatment of cancer.

8. References

Ahn K, McKinney MK, Cravatt BF (2008): Enzymatic pathways that regulate endocannabinoid signaling in the nervous system. *Chem Rev*, **108(5):** *1687-1707*.

Ammon HP, Wahl MA (1991): Pharmacology of Curcuma longa. *Planta Med*, **57(1):** *1-7*.

Asare N, Landvik NE, Lagadic-Gossmann D, et al (2008): 1-Nitropyrene (1-NP) induces apoptosis and apparently a non-apoptotic programmed cell death (paraptosis) in Hepa1c1c cells. *Toicol Appl Pharmacol*, **230(2):** *175-85*.

Attia MA, Weiss DW (1966): Immunology of spontaneous mammary carcinomas in mice. V. Acquired tumor resistance and enhancement in strain A mice infected with mammary tumor virus. *Cancer Res*, **26(8):** *1787-800*.

Bancher-Todesca D, Obermair A, Bilgi S, et al (1997): Angiogenesis in vulvar intraepithelial neoplasia. *Gynecol Oncol*, **64(3):** *496-500*.

Barbero R, Badino P, Cuniberti B, et al (2006): Identification of the VR-1 Vanilloid receptor in cell cultures. *Vet Res Commun*, **30(1):** *277-80*.

Barrio S, Gallardo M, Arenas A, et al (2013): Inhibition of related JAK/STAT pathways with molecular targeted drugs shows strong synergy with ruxolitinib in chronic myeloproliferative neoplasm. *Br J Haematol*, **161:** *667-76*.

Beltramo M, Stella N, Calignano A, Lin SY, Makriyannis A, Piomelli D (1997): Functional role of high-affinity anandamide transport, as revealed by selective inhibition. *Science*, **277(5329):** *1094-7*.

Bergers G, Benjamin LE (2003): Tumorigenesis and the angiogenic switch. *Nat Rev Cancer*, **3(6):** *401-10*.

Bertolino P, Deckers M, Lebrin F, ten Dijke P (2005): Transforming growth factor-β signal transduction in angiogenesis and vascular disorders. *Chest*, **128(6):** *585-90*.

Bifulco M, Laezza C, Pisanti S, Gazzerro P (2006): Cannabinoids and cancer: pros and cons of an antitumour strategy. *Br J Pharmacol,* **148(2):** *123-35*.

Bifulco M, Laezza C, Portella G, et al (2001): Control by the endogenous cannabinoid system of ras oncogene-dependent tumor growth. *FASEB J,* **15(14):** *2745-7*.

Bifulco M, Laezza C, Valenti M, Ligresti A, Portella G, Di Marzo V (2004): A new strategy to block tumor growth by inhibiting endocannabinoid inactivation. *FASEB J,* **18(13):** *1606-8*.

Bisogno T, Ligresti A, Di Marzo V (2005): The endocannabinoid signalling system: Biochemical aspects. *Pharmacol Biochem Behav,* **81(2):** *224-38*.

Blanco FJ, Santibanez JF, Guerrero-Esteo M, Langa C, Vary CP, Bernabeu C (2005): Interaction and functional interplay between endoglin and ALK-1, two components of the endothelial transforming growth factor-β receptor complex. *J Cell Physiol,* **204(2):** *574-84*.

Blankman JL, Simon GM, Cravatt BF (2007): A comprehensive profile of brain enzymes that hydrolyze the endocannabinoid 2-arachidonoylglycerol. *Chem Bio,* **14(12):** *1347-56*.

Blázquez C, Casanova ML, Planas A, et al (2003): Inhibition of tumor angiogenesis by cannabinoids. *FASEB J,* **17(3):** *529-31*.

Bobik A (2006): Transforming growth factor-βs and vascular disorders. *Arterioscler Thromb Vasc Biol,* **26(8):** *1712-20*.

Bock AJ, Tuft Stavnes H, Kærn J, Berner A, Staff AC, Davidson B (2011): Endoglin (CD105) expression in ovarian serous carcinoma effusions is related to chemotherapy status. *Tumour Biol,* **32(3):** *589-96*.

Bortolato M, Campolongo P, Mangieri RA, et al (2006): Anxiolytic-like properties of the anandamide transport inhibitor AM404. *Neuropsychopharmacology,* **31(12):** *2652-59*.

Bouaboula M, Perrachon S, Milligan L, et al (1997): A selective inverse agonist for central cannabinoid receptor inhibits mitogen-activated protein kinase activationn stimulated by insulin or insulin-like growth factor 1. Evidence for a new model of receptor/ligand interactions. *J Biol Chem*, **272(35):** *22330-9*.

Bric A, Miething C, Bialucha CU, et al (2009): Functional identification of tumor-suppressor genes through an in vivo RNA interference screen in a mouse lymphoma model. *Cancer Cell*, **16:** *324-35*.

Brown I, Cascio MG, Rotondo D, Pertwee RG, Heys SD, Wahle KW (2013): Cannabinoids and omega-3/6 endocannabinoids as cell death and anticancer modulators. *Prog Lipid Res*, **52(1):** *80-109*.

Burkey RT, Nation JR (1997): (R)-methanandamide, but not anandamide, substitutes for delta 9-THC in a drug discrimination procedure. *Exp Clin Psychopharmacol*, **5(3):** *195-202*.

Burnstock G (2009): Autonomic neurotransmission: 60 years since sir Henry Dale. *Annu Rev Pharmacol Toxicol*, **49:** *1-30*.

Cabranes A, Venderova K, De Lago E, et al (2005): Decreased endocannabinoid levels in the brain and beneficial effects of agents activating cannabinoid and/orvanilloid receptors in a rat model of multiple sclerosis. *Neurobiol Dis*, **20(2):** *207-17*.

Caffarel MM, Andradas C, Pérez-Gómez E, Guzmán M, Sánchez C (2012): Cannabinoids: a new hope for breast cancer therapy? *Cancer Treat Rev*, **38(7):** 911-8.

Caffarel MM, Sarrió D, Palacios J, Guzmán M, Sánchez C (2006): Delta9-tetrahydrocannabinol inhibits cell cycle progression in human breast cancer cells through Cdc2 regulation. *Cancer Res*, **66(13):** *6615-21*.

Calvaruso G, Pellerito O, Notaro A, Giuliano M (2012): Cannabinoid-associated cell death mechanisms in tumor models (review). *Int J Oncol*, **41(2):** *407-13*.

Carmeliet P (2003): Angiogenesis in health and disease. *Nat Med*, **9(6):** *653-60*.

Casanova ML, Blázquez C, Martínez-Palacio J, et al (2003): Inhibition of skin tumor growth and angiogenesis in vivo by activation of cannabinoid receptors. *J Clin Invest,* **111(1):** *43-50.*

Chakhachiro ZI, Zuo Z, Aladily TN, et al (2013): CD105 (endoglin) is highly overexpressed in a subset of cases of acute myeloid leukemias. *Am J Clin Pathol,* **140(3):** *370-8.*

Chen JL, Zhu JS, Hong J, et al (2007): Effect of 2-(8-hydroxy-6-methoxy-1-oxo-1H-2-benzopyran-3-yl) propionic acid in combination with carboplatin on gastric carcinoma growth in vivo. *World J Gastroenterol,* **13(4):** *509-14.*

Chen Y, Jian M, Lin C, et al (2008): The induction of orphan nuclear receptor Nur77 expression by n-butylenephthalide as pharmaceuticals on hepatocellular carcinoma cell therapy. *Mol Pharmacol,* **74(4):** *1046-58.*

Chou TC, Talalay P (1983): Analysis of combined drug effects: a new look at a very old problem. *Trends Pharmacol Sci,* **4:** *450-4.*

Chouchane L, Boussen H, Sastry KS (2013): Breast cancer in Arab population: molecular characteristics and disease management alterations. *Lancet Oncol,* **14(10):** *417-24.*

Contassot E, Wilmotte R, Tenan M, et al (2004): Arachidonylethanolamide induces apoptosis of human glioma cells through vanilloid receptor-1. *J Neuropathol Exp Neurol,* **63(9):** *956-63.*

Cravatt BF, Demarest K, Patricelli MP, et al (2001): Supersensitivity to anandamide and enhanced endogenous cannabinoid signaling in mice lacking fatty acid amide hydrolase. *Proc Natl Acad Sci U S A,* **98(16):** *9371-6.*

Crew JP, O'Brien T, Bradburn M (1997): Vascular endothelial growth factor is a predictor of relapse and stage progression in superficial bladder cancer. *Canc Res,* **57(23):** *5281-5.*

Cross MJ, Claesson-Welsh L (2001): FGF and VEGF function in angiogenesis: signalling pathways, biological responses and therapeutic inhibition. *Trends Pharmacol Sci*, **22(4):** *201-7*.

Davidoff AM, Leary MA, Ng CY, Vanin EF (2001): Gene therapy-mediated expression by tumor cells of the angiogenesis inhibitor flk-1 results in inhibition of neuroblastoma growth in vivo. *J Pediatr Surg*, **36(1):** *30-6.*

De Caestecker M (2004): The transforming growth factor-beta superfamily of receptors. *Cytokine Growth Factor Rev*, **15(1):** *1-11*.

De Filippis D, D'Amico A, Cipriano M (2010): Levels of endocannabinoids and palmitoylethanolamide and their pharmacological manipulation in chronic granulomatous inflammation in rats. *Pharmacol Res,* **61(4):** *321-8.*

De Lago E, Gustafsson SB, Fernández-Ruiz J, Nilsson J, Jacobsson SO, Fowler CJ (2006): Acyl-based anandamide uptake inhibitors cause rapid toxicity to C6 glioma cells at pharmacologically relevant concentrations. *J Neurochem*, **99(2):** *677-88.*

De Lago E, Ligresti A, Ortar G, et al (2004): In vivo pharmacological actions of two novel inhibitors of anandamide cellular uptake. *Eur J Pharmacol,* **484(2-3):** *249-57*.

De Petrocellis L, Bisogno T, Maccarrone M, Davis JB, Finazzi-Agro A, Di Marzo V (2001): The activity of anandamide at vanilloid VR1 receptors requires facilitated transport across the cell membrane and is limited by intracellular metabolism. *J Biol Chem*, **276(16):** *12856-63*.

De Petrocellis L, Melck D, Palmisano A, et al (1998): The endogenous cannabinoid anandamide inhibits human breast cancer cell proliferation. *Proc Natl Acad Sci U S A,* **95(14):** *8375-80*.

Demorrow S, Francis H, Gaudio E, et al (2008): The endocannabinoid anandamide inhibits cholangiocarcinoma growth via activation of the noncanonical Wnt signaling pathway. *Am J Physiol Gastrointest Liver Physiol,* **295(6):** *G1150-8.*

Derynck R, Akhurst RJ, Balmain A (2001): TGF-beta signaling in tumor suppression and cancer progression. *Nat Genet,* **29(2):** *117-29.*

DeSantis C, Siegel R, Bandi P, Jemal A (2011): Breast cancer statistics, 2011. *CA Cancer J Clin,* **61(6):** *409-18.*

Deschenes-Simard X, Gaumont-Leclerc MF, Bourdeau V, et al (2013): Tumor suppressor activity of the ERK/MAPK pathway by promoting selective protein degradation. Genes Dev, **27:** *900-15.*

Deschenes-Simard X, Kottakis F, Meloche S, Ferbeyre G (2014): ERKs in cancer: friends or foes? *Cancer Res,* **74(2):***412-9.*

Di Marzo V (2008): Targeting the endocannabinoid system: to enhance or reduce? Nat Rev *Drug Discov,* **7(5):** *438-55.*

Di Marzo V, De Petrocellis L, Fezza F, Ligresti A, Bisogno T (2002): Anandamide receptors. *Prostaglandins Leukot Essent Fatty Acids,* **66(2-3):** *377-91.*

Di Marzo V, Gobbi G, Szallasi A (2008): Brain TRPV1: a depressing TR(i)P down memory lane? *Trends Pharmacol Sci,* **29(12):** *594-600.*

Di Marzo V, Melck D, Orlando P, et al (2001): Palmitoylethanolamide inhibits the expression of fatty acid amide hydrolase and enhances the antiproliferative effect of anandamide in human breast cancer cells. *Biochem J,* **358(1):** *249-55.*

Dinh TP, Carpenter D, Leslie FM, et al (2002): Brain monoglyceride lipase participating in endocannabinoid inactivation. *Proc Natl Acad Sci U S A,* **99(16):** *10819-24.*

Donadelli M, Dando I, Zaniboni T, et al (2011): Gemcitabine/cannabinoid combination triggers autophagy in pancreatic cancer cells through a ROS-mediated mechanism. *Cell Death Dis,* **2:** *e152.*

Duff SE, Li C, Garland JM, Kumar S (2003): CD105 is important for angiogenesis: evidence and potential applications. *FASEB J,* **17(9):** *984-92*.

Duhamel S, Hebert J, Gaboury L, et al (2012): Sef downregulation by Ras causes MEK1/2 to become aberrantly nuclear localized leading to polyploidy and neoplastic transformation. *Cancer Res,* **72:** *626-35*.

Dumont P, Ingrassia L, Rouzeau S, et al (2007): The Amaryllidaceae isocarbostyril narciclasine induces apoptosis by activation of the death receptor and/or mitochondrial pathways in cancer cells but not in normal fibroblasts. *Neoplasia*, **9(9):** *766-76.*

Dvorak HF (2002): Vascular permeability factor/vascular endothelial growth factor: a critical cytokine in tumor angiogenesis and a potential target for diagnosis and therapy. *J Clin Oncol,* **20(21):** *4368-80*.

Dvorak HF, Nagy JA, Feng D, Brown LF, Dvorak AM (1999): Vascular permeability factor/vascular endothelial growth factor and the significance of microvascular hyperpermeability in angiogenesis. *Curr Top Microbiol Immunol,* **273:** *97-132*.

Eichele K, Ramer R, Hinz B (2009): R(+)-methanandamide-induced apoptosis of human cervical carcinoma cells involves a cyclooxygenase-2-dependent pathway. *Pharm Res*, **26(2):** *346-55***.**

El Saghir NS, Khalil MK, Eid T, et al (2007): Trends in epidemiology and management of breast cancer in developing Arab countries: a literature and registry analysis. *Int J Surg*, **5(4):** *225-33*.

Falenski KW, Thorpe AJ, Schlosburg JE, et al (2010): FAAH-/- mice display differential tolerance, dependence, and cannabinoid receptor adaptation after delta 9-tetrahydrocannabinol and anandamide administration. *Neuropsychopharmacology*, **35(8):** *1775-87*.

Ferlay J, Shin HR, Bray F, Forman D, Mathers C, Parkin DM (2010): Estimates of worldwide burden of cancer in 2008: GLOBOCAN 2008. *Int J Cancer,* **127(12):** *2893-917*.

Ferrara N, Chen H, Davis-Smyth T, et al (1998): Vascular endothelial growth factor is essential for corpus luteum angiogeneisis. *Nat Med,* **4(3):** *336-40.*

Flygare J, Sander B (2008): The endocannabinoid system in cancer-potential therapeutic target? *Semin Cancer Biol,* **18(3):** *176-89.*

Folkman J (1971): Tumor angiogenesis: therapeutic implications. *N Engl J Med,* **285(21):** *1182-6.*

Folkman J (1972): Anti-angiogenesis: new concept of therapy for solid tumors. *Ann Surg,* **175(3):** *409-16.*

Fonsatti E, Del Vecchio L, Altomonte M, et al (2001): Endoglin: an accessory component of the TGF-beta–binding receptor-complex with diagnostic, prognostic, and bioimmunotherapeutic potential in human malignancies. *J Cell Physiol,* **188(1):** *1-7.*

Fonsatti E, Nicolay HJ, Altomonte M, Covre A, Maio M (2010): Targeting cancer vasculature via endoglin/CD105: a novel antibody-based diagnostic and therapeutic strategy in solid tumours. *Cardiovasc Res,* **86(1):** *12-9.*

Fontanini G, Faviana P, Lucchi M, et al (2002): A high vascular count and overexpression of vascular endothelial growth factor are associated with unfavourable prognosis in operated small cell lung carcinoma. *Br J Cancer,* **86(4):** *558-63.*

Fowler CJ, Josefsson A, Thors L, et al (2013): Tumour epithelial expression levels of endocannabinoid markers modulate the value of endoglin-positive vascular density as a prognostic marker in prostate cancer. *Biochim Biophys Acta,* **1831(10):** *1579-87.*

Franceschi E, Tosoni A, Bartolini S, Mazzocchi V, Fioravanti A, Brandes AA (2009): Treatment options for recurrent glioblastoma: pitfalls and future trends. *Expert Rev Anticancer Ther,* **9(5):** *613-9.*

Fu J, Gaetani S, Oveisi F, et al (2003): Oleylethanolamide regulates feeding and body weight through activation of the nuclear receptor PPAR-alpha. *Nature,* **425(6953):** *90-3.*

Fujimoto J, Sakaguchi H, Hirose R, Ichigo S, Tamaya T (1998): Biologic implications of the expression of vascular endothelial growth factor subtypes in ovarian carcinoma. *Cancer,* **83(12):** *2528-33*.

Fukuda R, Hirota K, Fan F, Jung YD, Ellis LM, Semenza GL (2002): Insulin-like growth factor 1 induces hypoxia-inducible factor 1-mediated vascular endothelial growth factor expression, which is dependent on MAP kinase and phosphatidylinositol 3-kinase signaling in colon cancer cells. *J Biol Chem*, **277(41):** *38205-11*.

Gatley SJ, Gifford AN, Volkow ND, Lan R, Makriyannis A (1996): 123I-labeled AM251: a radioiodinated ligand which binds in vivo to mouse brain cannabinoid CB1 receptors. *Eur J Pharmacol,* **307(3):** *331-8*.

Gérard CM, Mollereau C, Vassart G, Parmentier M (1991): Molecular cloning of a human cannabinoid receptor which is also expressed in testis. *Biochem J,* **279(1):** *129-34*.

Giuffrida A, Beltramo M, Piomelli D (2001): Mechanism of endocannabinoid inactivation: biochemistry and pharmacology. *J Pharmacol Exp Ther,* **298(1):** *7-14.*

Glaser ST, Kaczocha M, Deutsch DG (2005): Anandamide transport: a critical review. *Life Sci,* **77(14):** *1584-604*.

Greenhough A, Patsos HA, Williams AC, Paraskeva C (2007): The cannabinoid delta(9)-tetrahydrocannabinol inhibits RAS-MAPK and PI3K-AKT survival signalling and induces BAD-mediated apoptosis in colorectal cancer cells. *Int J Cancer,* **121(10):** *2172-80.*

Guindon J, Hohmann AG (2011): The endocannabinoid system and cancer: therapeutic implication. *Br J Pharmacol*, **163(7):** *1447-63*.

Gustafsson SB, Lindgren T, Jonsson M, Jacobsson SO (2009): Cannabinoid receptor-independent cytotoxic effects of cannabinoids in human colorectal carcinoma cells: synergism with 5-fluorouracil. *Cancer Chemother Pharmacol,* **63(4):** *691-701*.

Guzmán M (2003): Cannabinoids: potential anticancer agents. *Nat Rev Cancer*, **3(10):** *745-55*.

Guzmán M, Duarte MJ, Blázquez C, et al (2006): A pilot clinical study of Delta9-tetrahydrocannabinol in patients with recurrent glioblastoma multiforme. *Br J Cancer*, **95(2):** *197-203*.

Guzmán M, Sánchez C, Galve-Roperh I (2001): Control of the cell survival/death decision by cannabinoids. *J Mol Med*, **78(11):** *613-25*.

Guzmán M, Sánchez C, Galve-Roperh I (2002): Cannabinoids and cell fate. *Pharmacol Ther*, **95(2):***175-84.*

Hamtiaux L, Hansoulle L, Dauguet N, Muccioli GG, Gallez B, Lambert DM (2011): Increasing antiproliferative properties of endocannabinoids in N1E-115 neuroblastoma cells through inhibition of their metabolism. *PLoS One*, **6(10):** *e26823*.

Hanahan D, Weinberg RA (2000): The hallmarks of cancer. *Cell*, **100(1):** *57-70.*

Hanahan D, Weinberg RA (2011): Hallmarks of cancer: the next generation. *Cell*, **144(5):** *646-74*.

Hasima N, Aggarwal BB (2012): Cancer-linked targets modulated by curcumin. *Int J Biochem Mol Biol*, **3(4):** *328-51*.

Hellwig-Bürgel T, Rutkowski K, Metzen E, Fandrey J, Jelkmann W (1999): Interleukin-1 beta and tumor necrosis factor-alpha stimulate DNA binding of hypoxia-inducible factor- 1. *Blood*, **94(5):** *1561-7*.

Hermanson DJ, Marnett LJ (2011): Cannabinoids, endocannabinoids, and cancer. *Cancer Metastasis Rev*, **30(3-4):** *599-612*.

Hoagland HC (1982): Hematologic complications of cancer chemotherapy. *Semin Oncol*, **9(1):** *95-102*.

Hsu SS, Huang CJ, Cheng HH, et al. (2007): Anandamide induced Ca2+ elevation leading to p38 MAPK phosphorylation and subsequent cell death via apoptosis in human osteosarcoma cells. *Toxicology,* **231(1):** *21-9.*

Impens F, Van Damme P, Demol H, Van Damme J, Vandekerckhove J, Gevaert K (2008): Mechanistic insight into taxol-induced cell death. *Oncogene*, **27(33):** *4580-91*.

Inoue M, Itoh H, Ueda M, et al (1998): Vascular endothelial growth factor (VEGF) expression in human coronary atherosclerotic lesions: possible pathophysiological significance of VEGF in progression of atherosclerosis. *Circulation,* **98(20):** *2108-16.*

Izzo AA, Aviello G, Petrosino S, et al (2008): Increased endocannabinoid levels reduce the development of precancerous lesions in the mouse colon. *J Mol Med (Berl),* **86(1):** *89-98.*

Jänicke RU, Sprengart ML, Wati MR, Porter AG (1998). Caspase-3 is required for DNA fragmentation and morphological changes associated with apoptosis. *J Biol Chem,* **273(16):** *9357-60.*

Jemal A, Siegel R, Ward E, Hao Y, Xu J, Thun MJ (2009): Cancer statistics, 2009. *CA Cancer J Clin,* **59(4):** *225-49.*

Jennings MT, Pietenpol JA (1998): The role of transforming growth factor beta in glioma progression. *J Neurooncol*, **36(2):** *123-40*.

Jiang BH, Jiang G, Zheng JZ, Lu Z, Hunter T, Vogt PK (2001): Phosphatidylinositol 3-kinase signaling controls levels of hypoxia-inducible factor-1. *Cell Growth Differ,* **12(7)**: *363-9.*

Jonsson KO, Holt S, Fowler CJ (2006): The endocannabinoid system: current pharmacological research and therapeutic possibilities. *Basic Clin Pharmacol Toxicol,* **98(2)**: *124-34.*

Joosten M, Valk PJ, Jordà MA, et al (2002): Leukemic predisposition of pSca-1/Cb2 transgenic mice. *Exp Hematol,* **30(2):** *142-9.*

Kabel AM, Abdel-Rahman MN, El-Sisi Ael-D, Haleem MS, Ezzat NM, El Rashidy MA (2013): Effect of atorvastatin and methotrexate on solid Ehrlich tumor. *Eur J Pharmacol,* **713(1-3):** *47-53.*

Kano M, Ohno-Shosaku T, Hashimotodani Y, Uchigashima M, Watanabe M (2009): Endocannabinoid-mediated control of synaptic transmission. *Physiol Rev,* **89(1):** *309-80*.

Karnoub AE, Weinberg RA (2008): Ras oncogenes: split personalities. *Nat Rev Mol Cell Biol*, **9:** *517-31*.

Kathuria S, Gaetani S, Fegley D, et al (2003): Modulation of anxiety through blockade of anandamide hydrolysis. *Nat Med,* **9(1):** *76-81*.

Katz LH, Li Y, Chen JS, Muñoz NM, Majumdar A, Chen J, Mishra L (2013): Targeting TGF-β signaling in cancer. *Expert Opin Ther Targets,* **17(7):** *743-60*.

Kay EP, Lee HK, Park KS, Lee SC (1998): Indirect mitogenic effect of transforming growth factor-beta on cell proliferation of subconjunctival fibroblasts. *Invest Ophthalmol Vis Sci,* **39(3):** *481-6*.

Khanolkar AD, Abadji V, Lin S, et al (1996): Head group analogs of arachidonylethanolamide, the endogenous cannabinoid ligand. *J Med Chem*, **39(22):** *4515-9*.

Klagsbrun M, Moses M (1999): Molecular Angiogenesis. *Chem Biol,* **6(8):** *217-24*.

Laezza C, Pisanti S, Crescenzi E, Bifulco M (2006): Anandamide inhibits Cdk2 and activates Chk1 leading to cell cycle arrest in human breast cancer cells. *FEBS Lett*, **580(26):** *6076-82*.

Lazarus H, Tegeler W, Mazzone HM, Leroy JG, Boone BA, Foley GE (1966): Determination of sensitivity of individual biopsy specimens to potential inhibitory agents: Evaluation of some explant culture methods as assay systems. *Cancer chemother Rep*, **50(8):** *543-55*.

Lebrin F, Deckers M, Bertolino P, ten Dijke P (2005): TGF-β receptor function in the endothelium. *Cardiovasc Res,* **65(3):** *599-608.*

Lebrin F, Goumans MJ, Jonker L, et al (2004): Endoglin promotes endothelial cell proliferation and TGF-β/ALK1 signal transduction. *Embo J,* **23(20):** *4018-28.*

Lee KE, Iwamura M, Cockett AT (1999): Cortisone inhibition of tumor angiogenesis measured by a quantitative colorimetric assay in mice. *Cancer Chemother Pharmacol,* **26(6):** *461-3.*

Levy L, Hill CS (2006): Alterations in components of the TGF-beta superfamily signalling pathways in human cancer. *Cytokine Growth Factor Rev,* **17(1-2):** *41-58.*

Lewis DY, Brett RR (2010): Activity-based anorexia in C57/BL6 mice: effects of the phytocannabinoid, Delta9-tetrahydrocannabinol (THC) and the anandamide analogue, OMDM-2. *Eur Neuropsychopharmacol,* **20(9):** *622-31.*

Li C, Hampson IN, Hampson L, Kumar P, Bernabeu C, Kumar S (2000): CD105 antagonizes the inhibitory signaling of transforming growth factor-β1 on human vascular endothelial cells. *FASEB J,* **14(1):** *55-64.*

Ligresti A, Bisogno T, Matias I, et al (2003): Possible endocannabinoid control of colorectal cancer growth. *Gastroenterology,* **125(3):** *677-87.*

Linderholm B, Grankvist K, Wilking N, Johansson M, Tavelin B, Henriksson R (2000): Correlation of vascular endothelial growth factor content with recurrences, survival, and first relapse site in primary node-positive breast carcinoma after adjuvant treatment. *J Clin Oncol,* **18(7):** *1423-31.*

Linsalata M, Notarnicola M, Tutino V, et al. (2010): Effects of anandamide on polyamine levels and cell growth in human colon cancer cells. *Anticancer Res,* **30(7):** *2583-9.*

Long JZ, Li W, Booker L, et al (2009): Selective blockade of 2-arachidonoylglycerol hydrolysis produces cannabinoid behavioural effects. *Nat Chem Biol,* **5(1):** *37-44.*

Louhimies S (2002): Directive 86/609/EEC on the protection of animals used for experimental and other scientific purposes. *Altern Lab Anim,* **30(2):** *217-9.*

Lutsenko SV, Kiselev SM, Severin SE (2003): Molecular mechanisms of tumor angiogenesis. *Biochemistry (Mosc),* **68(3):** *286-300*.

Mackie K (2006): Cannabinoid receptors as therapeutic targets. *Annu Rev Pharmacol Toxicol,* **46:** *101-22.*

Maheshwari RK, Singh AK, Gaddipati J, Srimal RC (2006): Multiple biological activities of curcumin: a short review. *Life Sci,* **78(18):** *2081-7.*

Malan TP Jr, Ibrahim MM, Lai J, Vanderah TW, Makriyannis A, Porreca F (2003): CB-2 cannabinoid receptor agonists: pain relief without psychoactive effects? *Curr Opin Pharmacol,* **3(1):** *62-7.*

Malfitano AM, Ciaglia E, Gangemi G, Gazzerro P, Laezza C, Bifulco M (2011): Update on the endocannabinoid system as an anticancer target. *Expert Opin Ther Targets,* **15(3):** *297-308.*

Mansouri Z, Sabetkasaei M, Moradi F, Masoudnia F, Ataie A (2012): Curcumin has neuroprotection effect on homocysteine rat model of Parkinson. *J Mol Neurosci*, **47(2):** *234-42*.

Marklund SL, Westman NG, Lundgren E, Roos G (1982): Copper- and zinc-containing superoxide dismutase, manganese-containing superoxide dismutase, catalase, and glutathione peroxidase in normal and neoplastic human cell lines and normal human tissues. *Cancer Res,* **42(5):** *1955-61*.

Massagué J (1998): TGF-beta Signal Transduction. *Annu Rev Biochem,* **67:** *753-91*.

Massagué J (2008): TGF beta in cancer. *Cell*, **134(2):** *215-30*.

Matas D, Juknat A, Pietr M, Klin Y, Vogel Z (2007): Anandamide protects from low serum-induced apoptosis via its degradation to ethanolamine. *J Biol Chem,* **282(11):** *7885-92*.

Matsuda LA, Lolait SJ, Brownstein MJ, Young AC, Bonner TI (1990): Structure of a cannabinoid receptor and functional expression of the cloned cDNA. *Nature,* **346(6284):** *561-4*.

Matsumoto T, Claesson-Welsh L (2001): VEGF signal transduction. *Sci STKE,* **112:** *21*.

Maurer G, Tarkowski B, Baccarini M (2011): Raf kinases in cancer-roles and therapeutic opportunities. *Oncogene*, **30:** *3477-88*.

Mazumdar UK, Gupta M, Maiti S, Mukherjee D (1997): Antitumor activity of Hygrophila spinosa on Ehrlich ascites carcinoma and sarcoma-180 induced mice. *Indian J Exp Biol*, **35(5):** *473-7*.

McGrogan BT, Gilmartin B, Carney DN, McCann A (2008): Taxanes, microtubules and chemoresistant breast cancer. *Biochim Biophys Acta,* **1785(2):** *96-132*.

Melck D, De Petrocellis L, Orlando P, et al (2000): Suppression of nerve growth factor Trk receptors and prolactin receptors by endocannabinoids leads to inhibition of human breast and prostate cancer cell proliferation. *Endocrinology*, **141(1):** *118-26*.

Menéndez JA, del Mar Barbacid M, Montero S, et al (2001): Effects of gamma-linolenic acid and oleic acid on paclitaxel cytotoxicity in human breast cancer cells. *Eur J Cancer*, **37(3):** *402-13*.

Mestre L, Correa F, Arévalo-Martín A, et al (2005): Pharmacological modulation of the endocannabinoid system in a viral model of multiple sclerosis. *J Neurochem,* **92(6):** *1327-39.*

Millauer B, Shawver LK, Plate KH, Risau W, Ullrich A (1994): Glioblastoma growth inhibited in vivo by a dominant-negative Flk-1 mutant. *Nature,* **367(6463):** *576-9.*

Mimeault M, Pommery N, Wattez N, Bailly C, Hénichart JP (2003): Anti-proliferative and apoptotic effects of anandamide in human prostatic cancer cell lines: Implication of epidermal growth factor receptor down-regulation and ceramide production. *Prostate*, **56(1):** *1-12*.

Miyato H, Kitayama J, Yamashita H, et al (2009): Pharmacological synergism between cannabinoids and paclitaxel in gastric cancer cell lines. *J Surg Res*, **155(1):** *40-7*.

Mollinedo F, Gajate C (2003): Microtubules, microtubule-interfering agents and apoptosis. *Apoptosis*, **8(5):** *413-50*.

Moreira FA, Aguiar DC, Campos AC, et al (2009): Antiaversive effects of cannabinoids: is the periaqueductal gray involved? *Neural Plast*, **2009:** *625469*.

Moreira FA, Wotjak CT (2009): Cannabinoids and Anxiety. In: Behavioral Neurobiology of Anxiety and Its Treatment, Current Topics in Behavioral Neurosciences (2nd ed). Stein MB, Steckler T (Eds.). Berlin Heidelberg: Springer-Verlag; pp. *429-50*.

Munro S, Thomas KL, Abu-Shaar M (1993): Molecular characterization of a peripheral receptor for cannabinoids. *Nature*, **365(6441):** *61-5*.

Murillo-Rodríguez E, Palomero-Rivero M, Millán-Aldaco D, Di Marzo V (2013): The administration of endocannabinoid uptake inhibitors OMDM-2 or VDM-11 promotes sleep and decreases extracellular levels of dopamine in rats. *Physiol Behav*, **109:** *88-95*.

Nascimento FR, Cruz GV, Pereira PV, et al (2006): Ascitic and solid Ehrlich tumor inhibition by Chenopodium ambrosioides L. treatment. *Life Sci*, **78(22):** *2650-3*.

Nicolussi S, Viveros-Paredes JM, Gachet MS, et al (2014): Guineensine is a novel inhibitor of endocannabinoid uptake showing cannabimimetic behavioral effects in BALB/c mice. *Pharmacol Res*, **80C:** *52-65*.

Nieder C, Adam M, Molls M, Grosu AL (2006): Therapeutic options for recurrent high-grade glioma in adult patients: recent advances. *Crit Rev Oncol Hematol,* **60(3):** *181-93.*

Nimeh T, Haghighat-Mortazavi R, Khiabani K, Malek N, Watters K, Philip A (2001): Ischemia Regulates Endoglin Expression in a Pig Skin Flap Model. *MJM,* **6:** *26-31*.

Nissen NN, Polverini PJ, Koch AE, Volin MV, Gamelli RL, DiPietro LA (1998): Vascular endothelial growth factor mediates angiogenic activity during the proliferative phase of wound healing. *Am J Pathol,* **152(6):** *1445-52*.

Nithipatikom K, Endsley MP, Isbell MA, et al (2004): 2-Arachidonoylglycerol: a novel inhibitor of androgen-independent prostate cancer cell invasion. *Cancer Res,* **64(24):** *8826-30.*

Nomura DK, Long JZ, Niessen S, Hoover HS, Ng SW, Cravatt BF (2010): Monoacylglycerol lipase regulates a fatty acid network that promotes cancer pathogenesis. *Cell,* **140(1):** *49-61*.

Oberling C, Guerin M (1954): The role of viruses in the production of cancer. *Adv Cancer Res,* **2:** *353-423.*

Ortar G, Ligresti A, De Petrocellis L, Morera E, Di Marzo V (2003): Novel selective and metabolically stable inhibitors of anandamide cellular uptake. *Biochem Pharmacol,* **65(9):** *1473-81*.

Oxmann D, Held-Feindt J, Stark AM, Hattermann K, Yoneda T, Mentlein R (2008): Endoglin expression in metastatic breast cancer cells enhances their invasive phenotype. *Oncogene,* **27(25):** *3567-75.*

Ozaslan M, Karagoz I, Kilic I, Guldur M (2011): Ehrlich ascites carcinoma. *Afr J Biotechnol,* **10:** *2375-8.*

Pacher P, Bátkai S, Kunos G (2006): The endocannabinoid system as an emerging target of pharmacotherapy. *Pharmacol Rev,* **58(3):** *389-462.*

Pagotto U, Marsicano G, Fezza F, et al (2001): Normal human pituitary gland and pituitary adenomas express cannabinoid receptor type 1 and synthesize endogenous cannabinoids: first evidence for a direct role of cannabinoids on hormone modulation at the human pituitary level. *J Clin Endocrinol Metab,* **86(6):** *2687-96.*

Pal S, Ray MR, Maity P (1993): Tumor inhibition and hematopoietic stimulation in mice by a synthetic copper-ATP complex. *Anticancer Drugs*, 4**(4):** *505-10.*

Parolaro D, Massi P (2008): Cannabinoids as potential new therapy for the treatment of gliomas. *Expert Rev Neurother,* **8(1):** *37-49*.

Patsos HA, Greenhough A, Hicks DJ, et al (2010): The endogenous cannabinoid, anandamide, induces COX-2-dependent cell death in apoptosis-resistant colon cancer cells. *Int J Oncol,* **37(1):** *187-93.*

Patsos HA, Hicks DJ, Dobson RR, et al (2005): The endogenous cannabinoid, anandamide, induces cell death in colorectal carcinoma cells: a possible role for cyclooxygenase 2. *Gut*, **54(12):** *1741-50*.

Pérez-Gómez E, Del Castillo G, Juan Francisco S, López-Novoa JM, Bernabéu C, Quintanilla M (2010): The role of the TGF-β coreceptor endoglin in cancer. ScientificWorldJournal, **10:** *2367-84*.

Pertwee RG (2005): Pharmacological actions of cannabinoids. *Handb Exp Pharmacol*, **168:** *1-51*.

Pertwee RG (2008): Ligands that target cannabinoid receptors in the brain: from THC to anandamide and beyond. *Addict Biol,* **13(2):** 147-59.

Pertwee RG (2009): Emerging strategies for exploiting cannabinoid receptor agonists as medicines. *Br J Pharmacol*, **156(3):** *397-411*.

Peters JM, Shah YM, Gonzalez FJ (2012): The role of peroxisome proliferator-activated receptors in carcinogenesis and chemoprevention. *Nat Rev Cancer,* **12(3):** *181-95*.

Petersen G, Moesgaard B, Schmid PC, et al (2005): Endocannabinoid metabolism in human glioblastomas and meningiomas compared to human non-tumour brain tissue. *J Neurochem,* **93(2):** *299-309.*

Piomelli D (2003): The molecular logic of endocannabinoid signalling. *Nature Rev Neurosci,* **4(11):** *873-84.*

Pisanti S, Bifulco M (2009): Endocannabinoid system modulation in cancer biology and therapy. *Pharmacol Res,* **60(2):** *107-16.*

Pisanti S, Borselli C, Oliviero O, Laezza C, Gazzerro P, Bifulco M (2007): Antiangiogenic activity of the endocannabinoid anandamide: correlation to its tumor-suppressor efficacy. *J Cell Physiol,* **211(2):** *495-503.*

Pisanti S, Picardi P, D'Alessandro A, Laezza C, Bifulco M (2013): The endocannabinoid signaling system in cancer. *Trends Pharmacol Sci,* **34(5):** *273-82.*

Pisanti S, Picardi P, Prota L, et al (2011): Genetic and pharmacologic inactivation of cannabinoid CB1 receptor inhibits angiogenesis. *Blood,* **117(20):** *5541-50.*

Postiglione L, Di Domenico G, Caraglia M, et al (2005): Differential expression and cytoplasm/membrane distribution of endoglin (CD105) in human tumour cell lines: Implications in the modulation of cell proliferation. *Int J Oncol,* **26(5):***1193-201.*

Pugh CW, Ratcliffe PJ (2003): Regulation of angiogenesis by hypoxia: role of the HIF system. *Nat Med,* **9(6):** *677-84.*

Reddy AC, Lokesh BR (1992): Studies on spice principles as antioxidants in the inhibition of lipid peroxidation of rat liver microsomes. *Mol Cell Biochem,* **111(1-2):** *117-24.*

Reddy AC, Lokesh BR (1994): Studies on the inhibitory effects of curcumin and eugenol on the formation of reactive oxygen species and the oxidation of ferrous iron. *Mol Cell Biochem,* **137(1):** *1-8.*

Rensen WM, Roscioli E, Tedeschi A, et al (2009): RanBP1 downregulation sensitizes cancer cells to taxol in a caspase-3-dependent manner. *Oncogene,* **28(15):** *1748-58.*

Rifkin DB (2005): Latent transforming growth factor-beta (TGF-beta) binding proteins: orchestrators of TGF-beta availability. *J Biol Chem,* **280(9):** *7409-12.*

Rinaldi-Carmona M, Barth F, Héaulme M, et al (1994): SR141716A, a potent and selective antagonist of the brain cannabinoid receptor. *FEBS Lett,* **350(2-3):** *240-4.*

Roghani M, Baluchnejadmojarad T, Dehkordi F (2011): The Sesame Lignan Sesamin Attenuates Vascular Permeability in Rats with Streptozotocin-Induced Diabetes: Involvement of Oxidative Stress. *Int J Endocrinol Metab,* **9(1):** *248-52.*

Rosen LS, Hurwitz HI, Wong MK, et al (2012): A phase I first-inhuman study of TRC105 (anti-endoglin antibody) in patients with advanced cancer. *Clin Cancer Res,* **18(17):** *4820-29.*

Saito VM, Wotjak CT, Moreira FA (2010): Pharmacological exploitation of the endocannabinoid system: new perspectives for the treatment of depression and anxiety disorders? *Rev Bras Psiquiatr,* **32(1):** *7-14.*

Sakai M, Ferraz-de-Paula V, Pinheiro M, et al (2010): Translocator protein (18kDa) mediates the pro-growth effects of diazepam on Ehrlich tumorcells in vivo. *Eur J Pharmacol,* **626(2-3):** *131-8.*

Samad TA, Rebbapragada A, Bell E, et al (2005): DRAGON, a bone morphogenetic protein co-receptor. *J Biol Chem,* **280(14):** *14122-9.*

Sánchez C, de Ceballos ML, Gomez del Pulgar T, et al (2001): Inhibition of glioma growth in vivo by selective activation of the CB2 cannabinoid receptor. *Cancer Res,* **61(15):** *5784-9.*

Santibanez JF, Letamendia A, Perez-Barriocanal F, et al (2007): Endoglin increases eNOS expression by modulating Smad2 protein levels and Smad2-dependent TGF-β signaling. *J Cell Physiol,* **210(2):** *456-68.*

Santos CR, Schulze A (2012): Lipid metabolism in cancer. *FEBS J,* **279(15):** *2610-23.*

Sarfaraz S, Adhami VM, Syed DN, Afaq F, Mukhtar H (2008): Cannabinoids for cancer treatment: progress and promise. *Cancer Res,* **68(2):** *339-42*.

Sarfaraz S, Afaq F, Adhami V, Malik A, Siddiqui I, Mukhtar H (2007): Cannabinoid receptors agonist WIN-55,212-2 inhibits angiogenesis, metastasis and tumor growth of androgen-sensitive prostate cancer cell CWR22Rv1 xenograft in athymic nude mice, in: Proceedings of the 98th Annual Meeting of the American Association for Cancer Research; 2007 Apr 14–18; Los Angeles, CA, USA, AACR, Philadelphia (PA), 2007 (Abstract nr 2195. Available online at (http://www.aacrmeetingabstracts.org/).

Schmid PC, Wold LE, Krebsbach RJ, Berdyshev EV, Schmid HH (2002): Anandamide and other N-acylethanolamines in human tumors. *Lipids,* **37(9):** *907-12*.

Schubbert S, Shannon K, Bollag G (2007): Hyperactive Ras in developmental disorders and cancer. *Nat Rev Cancer,* **7:** *295-308*.

Senger DR, Galli SJ, Dvorak AM, Perruzzi CA, Harvey VS, Dvorak HF (1983): Tumor cells secrete a vascular permeability factor that promotes accumulation of ascites fluid. *Science,* **219(4587):** *983-5*.

Seoane J (2006): Escaping from the TGFbeta anti-proliferative control. *Carcinogenesis*, **27(11)**: *2148-56*.

Sharma RA, Gescher AJ, Steward WP (2005): Curcumin: the story so far. *Eur J Cancer*, **41(13):** *1955-68*.

Sheng Y, Hua J, Pinney KG, et al (2004): Combretastatin family member OXI4503 induces tumor vascular collapse through the induction of endothelial apoptosis. *Int J Cancer,* **111(4):** *604-10*.

Silva A, Nascimento A, Maciel C, et al (2006): Sun flower seed oil-enriched product can inhibit Ehrlich solid tumor growth in mice. *Chemotherapy,* **52(2):** *91-4*.

Sperandio S, Poksay K, de Belle I, et al (2004): Paraptosis: mediation by MAP kinases and inhibition by AIP-1/Alix. *Cell Death Differ,* **11(10)**: *1066-75.*

Sreejayan, Rao MN (1994): Curcuminoids as potent inhibitors of lipid peroxidation. *J Pharm Pharmacol,* **46(12):** *1013-6.*

Sreejayan, Rao MN (1997): Nitric oxide scavenging by curcuminoids. *J Pharm Pharmacol,* **49(1):** *105-7.*

Stewart HL (1959): The cancer investigator. *Cancer Res,* **19:** *804-18.*

Stiehl DP, Jelkmann W, Wenger RH, Hellwig-Bürgel T (2002): Normoxic induction of the hypoxia-inducible factor-1 alpha by insulin and interleukin-1beta involves the phosphatidylinositol 3-kinase pathway. *FEBS Lett,* **512(1-3):** *157-62.*

Stover DG, Bierie B, Moses HL (2007): A delicate balance: TGF-beta and the tumor microenvironment. *J Cell Biochem,* **101(4):** *851-61.*

St-Pierre P, Bouffard L, Papirakis ME, Maheux P (2006): Increased extravasation of macromolecules in skeletal muscles of the Zucker rat model. *Obesity (Silver Spring),* **14(5):** *787-93.*

Sun Q, Chen T, Wang X, Wei X (2010): Taxol induces paraptosis independent of both protein synthesis and MAPK pathway. *J Cell Physiol,* **222(2):** *421-32.*

Thors L, Bergh A, Persson E, et al (2010): Fatty acid amide hydrolase in prostate cancer: association with disease severity and outcome, CB1 receptor expression and regulation by IL-4. *PLoS One,* **5(8):** *e12275.*

Tokunaga T, Oshika Y, Abe Y, et al (1998): Vascular endothelial growth factor (VEGF) mRNA isoform expression pattern is correlated with liver metastasis and poor prognosis in colon cancer. *Br J Cancer,* **77(6):** *998-1002.*

Torres S, Lorente M, Rodríguez-Fornés F, et al (2011): A combined preclinical therapy of cannabinoids and temozolomide against glioma. *Mol Cancer Ther,* **10(1):** *90-103.*

Tsujimoto Y (2012): Multiple ways to die: non-apoptotic forms of cell death. *Acta Oncol,* **51:** 293-300.

Ubol S, Kramyu J, Masrinoul P, et al (2007): A novel cycloheptapeptide exerts strong anticancer activity via stimulation of multiple apoptotic pathways in caspase-3 deficient cancer cells. *Anticancer Res,* **27(4B):** *2473-9.*

Ueda N, Tsuboi K, Uyama T (2010): Enzymological studies on the biosynthesis of N-acylethanolamines. *Biochim Biophys Acta,* **1801(12):** *1274-85*.

Valk P, Verbakel S, Vankan Y, et al (1997): Anandamide, a natural ligand for the peripheral cannabinoid receptor is a novel synergistic growth factor for hematopoietic cells. *Blood,* **90(4):** *1448-57*.

Van Sickle MD, Duncan M, Kingsley PJ, et al (2005): Identification and functional characterization of brainstem cannabinoid CB2 receptors. *Science,* **310(5746):** *329-32.*

Vaquero J, Zurita M, Morales C, Cincu R, Oya S (2000): Expression of vascular permeability factor in glioblastoma specimens: correlation with tumor vascular endothelial surface and peritumoral edema. *J NeuroOncol,* **49(1):** *49-55*.

Veikkola T, Alitalo K (1999): VEGFs, receptor and angiogenesis. *Semin Cancer Biol,* **9(3):** *211-20.*

Velasco G, Sánchez C, Guzmán M (2012): Towards the use of cannabinoids as antitumour agents. *Nat Rev Cancer,* **12(6):** *436-44*.

Vlachou S, Nomikos GG, Panagis G (2006): Effects of endocannabinoid neurotransmission modulators on brain stimulation reward. *Psychopharmacology,* **188(3):** *293-305.*

Vogelstein B, Kinzler KW (2004): Cancer genes and the pathways they control. *Nat Med,* **10(8):** *789-99.*

Wang D, Wang H, Ning W, Backlund MG, Dey SK, DuBois RN (2008): Loss of cannabinoid receptor 1 accelerates intestinal tumor growth. *Cancer Res,* **68(15):** *6468-76.*

Warrington K, Hillarby MC, Li C, Letarte M, Kumar S (2005): Functional role of CD105 inTGF-β1signalling in murine and human endothelial cells. *Anticancer Res,* **25(3B):** *1851-64.*

Wasik AM, Almestrand S, Wang X, et al (2011): WIN55,212-2 induces cytoplasmic vacuolation in apoptosis-resistant MCL cells. *Cell Death Dis,* **2:** *e225*.

Wilson RI, Nicoll RA (2002): Endocannabinoid signalling in the brain. *Science,* **296(5568):** *678-82*.

Wong ML, Kaye AH, Hovens CM (2007): Targeting malignant glioma survival signalling to improve clinical outcomes. *J Clin Neurosci*, **14(4):** *301-8*.

Yamaguchi M, Yu L, Hishikawa Y, Yamanoi A, Kubota H, Nagasue N (1997): Growth kinetic study of human hepatocellular carcinoma using proliferating cell nuclear antigen and Lewis Y antigen: their correlation with transforming growth factor-alpha and beta 1. *Oncology,* **54:** *245-51*.

Yang HL, Chen CS, Chang WH, et al (2006): Growth inhibition and induction of apoptosis in MCF-7 breast cancer cells by Antrodia camphorata. *Cancer Lett,* **231(2):** *215-27.*

Yang S, Zhou Q, Yang X (2007): Caspase-3 status is a determinant of the differential responses to genistein between MDA-MB-231 and MCF-7 breast cancer cells. *Biochim Biophys Acta,* **1773(6):** *903-11*.

Yang XH, Sladek TL, Liu X, Butler BR, Froelich CJ, Thor AD (2001): Reconstitution of caspase-3 sensitizes MCF-7 breast cancer cells to doxorubicin and etoposide-induced apoptosis. *Cancer Res,* **61(1):** *348-54.*

Zhang FJ, Yang JY, Mou YH, et al (2009): Inhibition of U-87 human glioblastoma cell proliferation and formyl peptide receptor function by oligomer procyanidins (F2) isolated from grape seeds. *Chem Biol Interact,* **179(2-3):** *419-29.*

Zheng D, Bode AM, Zhao Q, Cho YY, et al (2008): The cannabinoid receptors are required for ultraviolet-induced inflammation and skin cancer development. *Cancer Res,* **68(10):** *3992-8.*

Zhong H, Chiles K, Feldser D, et al (2000): Modulation of hypoxia-inducible factor 1 expression by the epidermal growth factor/phosphatidylinositol 3-kinase/PTEN/AKT/ FRAP pathway in human prostate cancer cells: implications for tumor angiogenesis and therapeutics. *Cancer Res,* **60(6):** *1541-5.*

Zhu Z, Witte L (1999): inhibition of tumor growth and metastasis by targeting tumor associated angiogenesis with antagonists to the receptors of vascular endothelial growth factor. *Inves New Drugs,* **17(3):** *195-212.*

Ziebarth AJ, Nowsheen S, Steg AD, et al (2013): Endoglin (CD105) contributes to platinum resistance and is a target for tumor-specific therapy in epithelial ovarian cancer. *Clin Cancer Res,* **19(1):** *170-82.*

9. Acknowledgements

First and foremost I would like to thank **"ALLAH"** for making completion of this work.

I would like to thank and express my gratitude to **PD. Dr. Gudrun Ulrich-Merzenich,** who welcomed me to her research group, for generous planning, expert supervision, correction of the thesis, and her undeniable help either scientifically or personally. Her broad knowledge and professional insight were of great importance to accomplish this work. I would like to deeply thank **DAAD**, **BONFOR, and Karl and Veronica Carstens Foundations** because this work would not have been possible without their financial support.

I am very grateful to **Prof. Dr. Ulrich Jaehde** who kindly accepted me as a PhD student and took over the responsibility of supervising this thesis in the division of Pharmacy, Faculty of Mathematics and Natural Sciences, Bonn University for his valuable supervision, and generous support throughout this work.

I would like to thank my Egyptian professors; **Prof. Dr. Medhat Ismail,** Professor of Pharmacology and Toxicology, Sinai University, Egypt, for his guiding and direct supervision during the practical work of the *in-vivo* experiments; **Dr. Mona El-Azab,** Assistant Professor of Pharmacology and Toxicology, Suez Canal University, Egypt, for teaching me the establishment of the Ehrlich model and for the statistical evaluation of the survival study; and **Prof. Dr. Yasser Moustafa,** Professor of Pharmacology and Toxicology, Suez Canal University, Egypt, for his continuous support.

I deeply appreciate the technical assistance I received from **Mr. Frederik Hartbrod** during the Western and DNA experiments.

I also express my gratitude to **Prof. Dr. Mohamed T. Khayyal,** Professor of Pharmacology, Faculty of Pharmacy, Cairo University, for his continuous support, encouragement and for offering valuable suggestions.

I am grateful and very thankful to **Dr. Heba Abdel-Aziz**, Head of scientific project management pre-clinical research, STEIGERWALD/Bayer Consumer Care. As my teacher and mentor, she has helped me to build up my scientific outlook, always seeking excellence and developing critical thinking. She has been a fantastic idol as a scientist, administrator and human being.

My parents encouraged me to achieve my goals and always stood behind me. Their life has been greatest source of inspiration to me. In no words I can express my deep gratitude, thanks and love towards my wife **Miasser** and my son **Ammar** for their love, compromises and support during all these years, really thank you so much.

Finally, I salute my motherland **EGYPT**.

Ramy Mohammed Ammar